
# The Longmenshan tectonic complex and adjacent tectonic units in the eastern margin of the Tibetan Plateau: A review

Dan-Ping Yan, Yu Zhou, Liang Qiu, Michael L. Wells, Hongxu Mu, Chen-Guang Xu

PII: S1367-9120(18)30240-2
DOI: https://doi.org/10.1016/j.jseaes.2018.06.017
Reference: JAES 3547

To appear in: *Journal of Asian Earth Sciences*

Received Date: 2 March 2018
Revised Date: 3 June 2018
Accepted Date: 4 June 2018

Please cite this article as: Yan, D-P., Zhou, Y., Qiu, L., Wells, M.L., Mu, H., Xu, C-G., The Longmenshan tectonic complex and adjacent tectonic units in the eastern margin of the Tibetan Plateau: A review, *Journal of Asian Earth Sciences* (2018), doi: https://doi.org/10.1016/j.jseaes.2018.06.017

# The Longmenshan tectonic complex and adjacent tectonic units in the eastern margin of the Tibetan Plateau: A review

Dan-Ping Yan[a*], Yu Zhou[a], Liang Qiu[a], Michael L. Wells[b], Hongxu Mu[a], Chen-Guang Xu[a]

a. The State Key Laboratory of Geological Processes and Mineral Resources, China University of Geosciences, Beijing 100083, China

b. Department of Geoscience, University of Nevada, Las Vegas, Las Vegas, Nevada 89154, USA

*. Corresponding author: Dr. Dan-Ping Yan

Prof. Dan-Ping Yan

Tectonic group

School of Earth Sciences and Resources

China University of Geosciences

Beijing 100083, China

Email address: yandp@cugb.edu.cn

**Abstract**

The Longmenshan Tectonic Complex (LSTC), along the eastern margin of the Tibetan Plateau, the site of devastating earthquakes such as the magnitude 8.0 (Wenchuan) earthquake on 12 May 2008, preserves an exceptionally complete history of the tectonic evolution of the Yangtze block and its relations to adjacent tectonic units. Due to sequential tectonic superposition and tectonic reactivation, the tectonic nature of the LSTC, and in particularly the older history, has been profoundly debated and many different tectonic models have been proposed. Herein we summarize the current understandings of the major tectonic events that have shaped this important tectonic complex, highlighting problems left to be solved by future work, including:

(1) The nature and constraints for at least 6 regional tectonic events, i.e., building of the metamorphic basement ($Ar_t$), the Columbia/Nuna supercontinent ($Pt_{1t}$), the Rodinia supercontinent ($Pt_{3t}$), the Paleozoic passive continental margin ($Pz_t$), the Paleotethys orogeny ($Mz_t$) and the Neotethys orogeny ($Kz_t$); (2) Metamorphic basement exposures and their tectonic implications, including rock types and geochronological constraints for the Archean, Paleoproterozoic and Neoproterozoic basements; (3) Nature of the present LSTC and its affinity with adjacent tectonic units; (4) Consideration of the NE-striking Longmenshan thrust belt and arcuate-shape Yanyuan-Muli thrust belt as parts of a single tectonic feature; (5) Mountain-basin coupled systems recording past tectonic eposides. We draw the following conclusions and tectonic models based on published research combined with our own recent studies: (1) The well preserved Archean Yudongzi gneiss group in the LSTC has a genetic affinity with the Kongling group, and thus belongs to the Yangtze block; (2) The Paleoproterozoic Hejiayan group, juxtaposed adjacent to the

Archean Yudongzi group, may represent a 2000-1800 Ma orogenic belt, which corresponds to the supercontinent Nuna/Columbia amalgamation event; (3) A Neoproterozoic trench-arc-basin system, which is reconstructed based on identification of a Neoproterozoic ophiolite complex, arc-type magmatic rock assemblages and volcaniclastic basinal deposits along the western margin of the Yangtze block and the LSTC, may represent the record of eastward subduction of the Neoproterozoic Mozambique oceanic lithosphere beneath the Yangtze block during the assembly of the Rodinia supercontinent; (4) A complete bidirectional Wilson cycle was reconstructed by the formation of the late Permian to the middle-late Triassic back-arc Ganze-Litang rift and ocean following the early Paleozoic Mianlue continental rift and ocean, and subsequent closure of the ocean basin by simultaneous bidirectional northward and southwestward subduction and later collision. This relatively uncommon bidirectional Wilson cycle might be attributed to the formation of the three-armed rift system in the eastern Paleotethys associated with the late Permian Eemeishan Large Igneous Province in the LSTC; (5) A three-stage tectonic sequence of, in-sequence imbricate thrust in the LSTC during India-Eurasian collisional orogeny at 55-15 Ma, extrusion from 15-5 Ma and the plateau uplift since ~5 Ma resulting from lower crustal channel flow, is proposed for the formation of the present LSTC.

**Key Words:** Longmenshan belt, Columbia/Nuna supercontinent, Rodinia supercontinent, three-armed rift system, bidirectional Wilson cycle

## 1. Introduction

The Longmenshan Tectonic Complex (LSTC) along the eastern margin of the Tibetan Plateau is composed of the NE-striking Longmenshan thrust belt in the north and the arcuate-shaped Yanyuan-Muli thrust belt in the south (Figs. 1 and 2). The LSTC, which is bounded by the Triassic south Qinling-Dabie orogenic belt to the north, the Cenozoic eastern Tibet Plateau and the Triassic Songpan-Ganze terrane to the west, and the Yangtze block (including the western Sichuan foreland basin) to the east, extends ~800 km from northeast to southwest (Figs. 1 and 2). Active tectonics within the LSTC has been widely documented and is characterized by SE to SSE vergent overthrusting with repeated thrusting and denudation since 20 Ma (Arne et al., 1997; Ali et al., 2004), manifests recently by the devastating magnitude 8.0 Ms (Wenchuan) earthquake on 12 May 2008, the 7.0 Ms Lushan earthquake on 20 April 2013, and the 7.0 Ms Jiuzhaigou earthquake on 8 August 2017 (Burchfiel et al., 2008; Lu et al., 2008; Parsons et al., 2008; Hubbard and Shaw, 2009; Jia et al., 2010; Jin et al., 2010; Xu et al., 2016). Marking the present eastern margin of the Tibetan Plateau, the LSTC includes both the pre-collisional Longmenshan orogenic belt with defined tectonic domains of the hinterland belt, the foreland thrust belt and western Sichuan foreland basin (Xu et al., 1992), and the Cenozoic orogenic belt produced by the on-going collision between the Indian and Eurasian continents and associated gravitational relaxation (c.f., Arne et al., 1997; Clark and Royden, 2000; Meng et al., 2005; Lai et al., 2007; Burchfiel et al., 2008; Parsons et al., 2008).

The LSTC has experienced a rich and protracted tectonic history and many aspects of the history continue to be debated. Multiple tectonic episodes have been identified, including: the formation of metamorphic basement, the assembly of supercontinent Rodinia, the breakup of Rodinia and the formation of the Sinian-Paleozoic passive continental margin, the Late Paleozoic continental rift and mantle plume, the Mesozoic Paleotethys orogenic cycle and the Cenozoic formation of the Tibetan Plateau during collision between the Indian and Eurasian continents, (e.g., SBGMR, 1991; Zhou et al., 2002; Yan et al., 2011; Li et al., 2016; Zheng et al., 2016). The superposition of younger deformation on older events (tectonic inheritance) has hindered interpretations of the older history. Nonetheless, efforts to look through the younger history have led to the development of new tectonic models for the LSTC (Yan et al., 2011, 2016). Moreover, new insights into the nature and superposition of these tectonic episodes has identified a number of scientific issues left to be answered:

1) Tectonic episodes: although at least six regional tectonic episodes have been identified, what characteristics define the major tectonic episodes and the deformational sequence? As is common in tectonic analysis, the superposition of younger events on the older ones has complicated studies of the older events.

2) Metamorphic basement: Are Archean rocks present within the LSTC? Metamorphic rocks of low metamorphic grade crop out along the margins of the South China Block, including the LSTC, have been determined to be of igneous origin with volcanic features and dated at 830-725 Ma (Li et al., 1995; Zhou et al., 2002; Zhao et al., 2011). However, the tectonic significance of these rocks has long been debated.

3) The LSTC: What is the importance of the Mesozoic shortening versus late Cenozoic shortening? Is the LSTC a foreland thrust belt of the Mesozoic Qinling-Dabie orogenic belt

and Songpan-Ganze terrane (Burchfiel et al., 1995; Chen and Wilson, 1996; Zhang et al., 2004; Jin et al., 2007)?

4) What are the differences and geological relationships between the NE-striking Longmenshan thrust belt in the north and the arcuate-shaped Yanyuan-Muli thrust belt in the south?

5) How do we establish the mountain belt-basin affinity between the LSTC and western Sichuan basin? Specifically, is the present LSTC, which couples with the western Sichuan foreland basin, inherited from the Paleo-Tethys domain?

In summary, great strides have been made in the past decades toward understanding the development of the LSTC, providing the basis for this review, in which we summarize results and consider possible interpretations. In this paper, we describe the main tectonic episodes, sequence, and their tectonic affinity with the adjacent terranes, and then reconstruct the tectonic evolution.

## 2. Tectonic division and geological setting

Here we describe six first-order tectonic units, identified based on their major tectonic boundaries, including sutures and regional faults, and their internal characteristics: (1) the South Qinling-Dabie orogenic belt and A’nyemaqen-Mianlue suture; (2) the Bikou terrane; (3) the Songpan-Ganze terrane; (4) the Yidun arc; (5) the Western Yangtze Block, and (6) the LSTC (Fig. 2 and Table 1).

The LSTC includes secondary-order tectonic units of the NE-striking Longmenshan thrust belt and arcuate Yanyuan-Muli thrust belt with several third-order tectonic units (Fig. 2; Table 1). The LSTC is separated from the Songpan-Ganze terrane by Maowen fault to the west, and from the Yangtze block by Guanxian-Anxian fault and Muli fault to the east. To the north of the LSTC, the triangular Bikou terrane, is between the Longmenshan thrust belt and south Qinling-Dabie orogenic belt and is bounded by Qinchuan-Pingwu fault to the south and Fuya-Xueshan fault to the west. The terrane has an eastward wedge type merging into A'nyemaqen-Mianlue suture (Figs. 1 and 2) (Dewey et al., 1988; Burchfiel et al., 1989; Chang, 2000; Yin and Harrison, 2000; Zhang et al., 2004; Li et al., 2007; Xu J.F. et al., 2008; Ji et al., 2016). To the southwest, the Yanyuan-Muli thrust belt stretches west from the Xianshuihe fault across the southern Ganze-Litang suture and southern Yidun arc and is separated from the Qiangtang block by Jinshajiang suture (Fig. 2) (Yang et al., 2012; Cao et al., 2015; Li et al., 2018) (Figs. 1 and 2).

### 2.1 The South Qinling-Dabie orogenic belt and A'nyemaqen-Mianlue suture

The South Qinling-Dabie orogenic belt has an Archean crystalline basement of amphibolites and granulites and the Mesoproterozoic to the Early Neoproterozoic folded basement of greenschist and amphibolite facies metabasites and metasedimentary rocks. The cover sequences overlying the basement include Sinian tillite and dolomite, Paleozoic to Middle Triassic platform carbonate and clastic rocks, and locally, Cretaceous to Cenozoic conglomerates (Meng and Zhang, 2000), which are similar to the cover sequences of the Yangtze Block. Early Mesozoic granitoid plutons and dykes (220–180 Ma) are common in this belt (Zhou and Graham, 1996; Zhang et al., 2007).

The 1-5 km wide A'nyemaqen-Mianlue suture extends ~160 km from west to east along the boundary between the south Qinling-Dabie orogenic belt and the Yangtze Block (Feng et al., 1996; Li et al., 1999; Meng and Zhang, 2000; Zhang et al., 2002, 2005;

Ratschbacher et al., 2003; Dong et al., 2004; Zhang et al., 2004; Li et al., 2007; Yan et al., 2007; Xu J.F. et al., 2008; Yang et al., 2013; Ji et al., 2016) (Fig. 1). This suture dips north with variable dip angles and is composed of tectonic slices or blocks of the Late Triassic-Early Jurassic mélange. These blocks strongly sheared, contain ophiolitic material, arc volcanic rocks, the Paleozoic sedimentary rocks and Precambrian metamorphic rocks (Meng and Zhang, 2000; Xu J.F. et al., 2008). Radiolarians separated from the cherts and limestones associated with the ophiolitic blocks have yielded Early Carboniferous ages (Meng and Zhang, 2000). Metamorphic minerals in the ophiolites yield metamorphic ages of 208-242 Ma, using whole rock Sm-Nd, zircon U-Pb and mica Ar-Ar methods (Meng and Zhang, 2000; Zhang et al., 2004; Dong et al., 2011; Dong and Santosh, 2016; Ji et al., 2016; Qian et al., 2016). Thus, the A'nyemaqen-Mianlue suture marks a branch of the Paleo-Tethys ocean that closed in the Late Triassic during collision of the North China and South China blocks (Zhao and Coe, 1987; Meng and Zhang, 2000; Zhang et al., 2004; Yan et al., 2011).

**2.2 Bikou terrane**

The Bikou terrane includes basement of the Archean Yudongzi group, the Paleoproterozoic Hejiayan group, the Neoproterozoic Bikou and Hengdan groups, and a cover sequence of the Sinian and Paleozoic sedimentary rocks (GBGMR, 1989; SBGMR, 1989; SBGMR, 1991). The basement and cover sequences of the Bikou terrane share many similarities with those of the Western Yangtze Block (GBGMR, 1989; SBGMR, 1989; SBGMR, 1991) (Fig. 4).

The Bikou terrane has a structural style of a thrust complex with a thick-skinned thrust ($Kz_t$) overprinting a cylindrical anticlinorium ($Mz_t$). This anticlinorium has a westward plunging axis represented by the Archean Yudongzi group ($Ar_t$) and the Paleoproterozoic Hejiayan group ($Pt_{1t}$) in the eastern core, with the Neoproterozoic Bikou and Hengdan groups ($Pt_{3t}$) and the Paleozoic ($Pz_t$) strata occupying the western core and the limbs (Fig. 1). The NE -striking Qingchuan-Pingwu fault forms the southern boundary for ~200 km (Fig. 1), and dips NNW with variable angles. The Qingchuan-Pingwu fault combines with the Fuya-Xueshan fault to forming an arcuate-shaped thrust fault, which produced SSE-ward thrusting of the Bikou thrust complex during the Cenozoic $Kz_t$ (Fig. 2). In summary, the Bikou terrane shows similarities of rock successions and history of tectonic episodes to the LSTC, with tectonic episodes $Ar_t$ to $Kz_t$ (Lu et al., 2010; Yan et al., 2011).

**2.3 Songpan-Ganze terrane and Xianshuihe fault**

The triangular shaped Songpan-Ganze terrane, which is covered by the Triassic flysch deposits in most of the regions, is different from most linear shaped orogenic belts on the Earth (Coney, 1970, 1972, 1980; Bruguier et al., 1997; Armstrong, 1982; Dewey, 1988; Andersen, 1998; Vanderhaeghe et al., 1999; Jolivet and Faccenna, 2000; Vanderhaeghe, 2012). Ages of more than one hundred silicic plutons in the Songpan-Ganze terrane range from the Permian to Cenozoic (GBGMR, 1989; SBGMR, 1991; Roger et al., 1995; Zhang, H.F. et al., 2006; Zhang, C.L., 2007; Yuan et al., 2010). These plutons are of variable composition and include calc-alkaline, alkaline, peralkaline and peraluminous rocks (Roger et al., 1995; Yuan et al., 2010).

The Xikang group in the Songpan-Ganze terrane has a ~7 km-thick Triassic flysch sequence that was intruded by a number of Mesozoic and Cenozoic granitic plutons (Fig. 1) (Rao et al., 1987; Mattauer et al., 1992; Nie et al., 1994; Zhou and Graham, 1996; Bruguier et al., 1997; Chang, 2000; Zhang et al., 2008; Zhou et al., 2008). This group is conformably underlain by the Paleozoic shallow marine sequences of the western passive continental margin of the Yangtze Block. The flysch sequence was mainly derived from the Qinling-Dabie orogenic belt, created by collision between the North China and South China blocks during the Triassic (Fig. 1) (SBGMR, 1991; Yin and Nie, 1993; Burchfiel, 1995; Zhou and Graham, 1996; Yan et al., 2003a, 2008a; Weislogel et al., 2006, 2010; Zhang et al., 2008). However, the flysch provenance has also been proposed from the Yidun arc in the west (Wang et al., 2013a, 2013b), and the Kunlun-Qiliang orogenic belt in the northwest (She et al., 2006).

The NW-striking Xianshuihe fault, a currently active, sinistral, strike-slip fault, cuts through the Songpan-Ganze terrane. The fault zone is composed of fault breccia, gouge and protomylonite, indicating brittle and brittle-ductile deformation (Wang et al., 1998; Wang and Burchfiel, 2000; Li et al., 2015; Shi et al., 2016). The 12-13 Ma Gonggashan granites intruded the fault zone during shearing, suggesting crustal channel flow initiated at the Miocene (Fig. 1) (Roger et al., 1995; Wang et al., 1998; Bai et al., 2010; Zhang et al., 2017).

**2.4 Yidun arc and bilateral sutures**

The Yidun arc is divided into Zhongza terrane (Zhongza micro-block) to the west and eastern arc on the basis of stratigraphy and lithology (Chen et al., 1987; Reid et al., 2005, 2007; Wang et al., 2011, 2013a, 2013b; Cao et al., 2015). The Zhongza micro-block, which is composed of Paleozoic carbonates, intercalated mafic volcanic rocks and younger intrusions, is a micro-continental fragment rifted from the Yangtze Block during the Late Permian opening of the Ganze-Litang Ocean (Chen et al., 1987; Chang, 1997; Zhang et al., 1998; Reid et al., 2005, 2007; Cao et al., 2015) (Figs. 2 and 5). The Permian basalts exposed in the Zhongza micro-block have a composition similar to the Emeishan basalts, suggesting an extensional setting associated with the Emeishan mantle plume (Song et al., 2004; Xiao et al., 2008).

The eastern Yidun arc is composed of mudstones, volcanic rocks and intrusions, which were interpreted as the products of the westward subduction of the Ganze-Litang ocean (Mo et al., 1993, 1994; Hou et al., 2003; Reid et al., 2005; Cao et al., 2015). The volcanic rocks are mostly calc-alkaline andesites with basalt-rhyolite and shoshonitic assemblages (Mo et al., 1994). Numerous plutons with zircon U-Pb ages of 215-225 Ma (Reid et al., 2007; Weislogel, 2008) crop out along the western side of the Ganze-Litang suture. Further to the west, the 94-104 Ma plutons that intrude the eastern Yidun Arc have been interpreted as products of intra-continental extension (Fig. 5) (Reid et al., 2007).

Integrated volcanic and sedimentary sequences, felsic intrusions, deformational and metamorphic series, new tectonic model of the Paleo-Tethys Yidun arc was suggested (Cao et al., 2015) (Fig. 5). The initial eastward subduction of the Paleo-Jinshajiang ocean during the Late Permian produced the Yidun volcanic arc and a back-arc rift, which evolved into the Ganze-Litang ocean and continued magmatism in the Yidun volcanic and plutonic arc complex during the Early-Middle Triassic (Hou et al., 2003; Reid et al., 2007; Zhu et al., 2011; Cao et al., 2015) (Fig. 5A-B). The onset of the Ganze-Litang back-arc rift was simultaneous with the formation of the Emeishan large igneous province (ELIP) (Song et al., 2004; Xiao et al., 2008). The collision of the Qiangtang Block with the Yidun arc during 241-224 Ma resulted in the Jinshanjiang orogen with ductile shear zones and Barrovian metamorphic belts, and the final closure of the Ganze-Litang ocean during 224-214 Ma, which probably produced the orogenic plateau and then transferred to extensional collapse (Fig. 5C-D) (Cao et al., 2015).

**2.5 Western Yangtze Block (western Sichuan basin and Kangding complex)**

The western Yangtze Block includes the western Sichuan foreland basin and the Kangding complex (Fig. 2), and comprises the Mesoproterozoic to Neoproterozoic basement rocks overlain by a late Neoproterozoic (the Nanhuan and Sinian) to Cenozoic cover sequence (Figs. 3 and 4). The basement rocks are exposed mainly along the Kangding complex, which are referred to as the Mesoproterozoic Hekou and Huili groups and the Neoproterozoic Yanbian group (Fig. 4) (Zhou et al., 2002a, 2006b; Zhao et al., 2007a, 2007b, 2008, 2009a, 2009b, 2010a, 2010b, 2013b; Sun et al., 2009). The Mesoproterozoic Hekou and Huili groups include marble, amphibolite, conglomerate, and schist, interbedded with basalt, with metamorphic grades of amphibolite to greenschist facies (SBGMR, 1991; Zhao et al., 2012). The Neoproterozoic Yanbian group of the Kangding complex consists of greywacke–slate succession and are included as part of the folded basement of the Yangtze Block (SBGMR, 1991; Sun et al., 2009). A thick (>10 km) cover sequence of the Nanhua, Sinian to middle Triassic include clastic, carbonate, and meta-volcanic rocks (SBGMR, 1991; Mattauer, 1992; Xu et al., 1992; Yan et al., 2003b, 2006, 2009). The Upper Triassic, Jurassic, Cretaceous and Cenozoic strata, which are entirely continental sequences, filled in the foreland basins during the Mesozoic and Cenozoic, respectively (HBGMR, 1990; SBGMR, 1991; Yan et al., 2011).

The western Sichuan basin, which is cut into two parts by the Xianshuihe sinistral strike-slip fault, is presently delimited between the foreland thrust belt to the west and the Longquanshan uplift to the east (Fig. 2). This basin has long been thought to represent the Cenozoic flexural basin corresponding to the SE-ward migration of the foreland thrust belt (Burchfiel et al., 1995; Yan et al., 2011). Recent results have revealed two phases of basin development for the western Sichuan Basin, i.e., a Late Triassic foreland basin overprinted and overlain by a Cenozoic foreland basin (Li et al., 2015a).

Striking north-south, the Kangding complex is a fault bounded block, 100 km long and 30 km wide (Figs. 1 and 2) (Zhou et al., 2002a). Numerous faults cut the complex and divide it into distinct rock slices. The eastern and western boundary faults are a series of the Mesozoic low-angle normal faults, whereas sinistral strike-slip faults present in the southwest and thrust faults in the west (Zhou et al., 2002a) (Fig. 2). Interaction of these faults were interpreted as a tranpressional restraining bend, giving rise to the rapid uplift and exhumation during the Cenozoic (Zhang et al., 2017).

### 2.6 Longmenshan tectonic complex

For purposes of clarity, we will divide the LSTC into the Longmenshan thrust belt to the north and Yanyuan-Muli thrust belt to the south (Table 1, Fig. 2). Both are separated by the Xianshuihe fault (Fig. 2).

#### 2.6.1 Longmenshan thrust belt

The NE-striking Longmenshan thrust belt extends ~500 km from the NW-striking Xianshuihe fault in the southwest to Hanzhong (basin) in the northeast (Fig. 1). Three main NE-striking faults define the thrust belt: from hinterland to foreland, these are the Maowen fault, the Beichuan-Yingxiu fault, and the Guanxian-Anxian fault (Fig. 2).

Both the Beichuan-Yingxiu and Maowen thrust faults show dextral strike-slip kinematics (Kirby et al., 2002; Xu Z.Q. et al., 2008; Yan et al., 2008a, 2011). The Maowen fault is ca. 275 km long and dips 30-50ºNW. This fault is marked by a major zone of mylonite and breccia, which yielded ages of ~220 Ma by matching stratigraphic sequence and has been reactivated probably since the Late Miocene (Dirks et al., 1994; Burchfiel et al., 1995; Chen et al., 1995; Worley and Wilson, 1996; Arne et al., 1997; Xu Z.Q. et al., 2008; Tian et al., 2013; Wang et al., 2014; Zheng et al., 2016).

The Beichuan-Yingxiu fault extends for more than 350 km along a NE direction and dips 40°-60º NW (Burchfiel et al., 2008; Parsons et al., 2008; Jin et al., 2010; Zheng et al., 2016). This fault is also marked by a zone of mylonite and breccia. It has been active since ~230 Ma using glass matrix zircon U-Pb and mica $^{40}Ar/^{39}Ar$ methods (Dirks et al., 1994; Burchfiel et al., 1995; Chen et al., 1995; Worley and Wilson, 1996; Arne et al., 1997; Xu Z.Q. et al., 2008; Zheng et al., 2016). A rupture along the Beichuan-Yingxiu fault caused the 8.0 Ms Wenchuan earthquake on May 12, 2008 (Burchfiel et al., 2008; De Michele et al., 2010). The Beichuan-Yingxiu fault divides the Longmenshan thrust belt into a hinterland belt to the northwest and a foreland thrust belt to the southeast (Chen and Wilson, 1996; Worley and Wilson, 1996; Arne et al., 1997; Meng et al., 2005; Jin et al., 2007; Yan et al., 2011). The hinterland and foreland thrust belts have remarkably different Mesozoic sequences and structural styles.

The Guanxian-Anxian thrust fault dips irregularly to the northwest with angles of 30-60º. This fault crosscuts the Late Triassic Xujiahe Formation through the Quaternary sediments, indicating the Cenozoic activity (SBGMR, 1991; Yong et al., 2003; Xu Z.Q. et al., 2008; Yan et al., 2008a, 2008b).

#### 2.6.1.1 Hinterland belt

The hinterland belt is bounded by the Maowen and Beichuan-Yingxiu faults (Fig. 2). This belt is characterized by a number of domal complexes of metamorphic rocks, including the Jiaoziding, Pengguan-Xuelongbao, Baoxin and Danba uplifts (Figs. 2 and 3). The domal complexes consist of Mesoproterozoic to Neoproterozoic paragneiss, mica schist, graphite-bearing sillimanite-garnet gneiss (khondalite), amphibolite, marble, and quartzite (Huangshuihe group and its equivalent Bikou group and Kangding group), which correspond to the Huili and Yanbian groups of the basement of Yangtze Block (Fig. 4D) (Zhou et al., 2002a, 2002b, 2006a; Yan et al., 2003a, 2008a, 2008b; Sun et al., 2009).

Unconformably overlying the basement rocks along the domal complexes are the Sinian metaclastic rocks, dolomite and tillite. The Sinian is unconformably overlain by Cambrian-Ordovician volcanic rocks, carbonates, and cherts, Silurian phyllonite (known as the Maoxian group), Devonian quartzite (known as the Weiguan group), and the Carboniferous to the Permian carbonate rocks and basalts (SBGMR, 1991; *Yan et al*., 2008a, 2008b). Triassic strata, referred to as the Xikang group and composed mainly of a low-grade metamorphic flysch sequence, tectonically overlie the Paleozoic sequences (SBGMR, 1991; Yan et al., 2011) (Fig. 4D).

A detachment fault in the hinterland belt separates the Sinian and Paleozoic strata of greenschist facies in the hanging wall from footwall amphibolite facies rocks of the domal complexes (Figs. 1 and 2). Significant tectonic removal of the strata across the detachment indicates the presence of a large-magnitude low-angle normal fault that records SE-directed extension (Figs. 4D). This extension occurred during the Early to Middle Jurassic, which has been constrained by zircon U-Pb and $^{40}Ar/^{39}Ar$ ages of 160-198 Ma (Zhou et al., 2002a, 2008; Yan et al., 2003a, 2008a, 2008b, 2011; Liu et al., 2008).

Alternative interpretations, however, have been presented for the formation and exhumation of the domal complexes based on variable geological data. The typical Danba domal complex in the southern Longmenshan thrust belt (Figs. 1 and 3) is interpreted as a regional scale antiform of the Neoproterozoic basement, overlain depositionally by the Paleozoic metasedimentary and metavolcanic rocks and Triassic turbidites (Xikang group) (Mattauer et al. 1992; Huang et al. 2003a, 2003b; Harrowfield and Wilson 2005; Zhou et al. 2008). Structurally above the domal complexes, the Triassic Xikang group and the Paleozoic sequence are generally affected by tight upright to close folds and related thrust faults coeval with the development of an E-W trending and steeply dipping axial planar foliation (Huang et al., 2003a, Harrowfield and Wilson, 2005, Weller et al., 2013, Jolivet et al. 2015; Billerot et al., 2017). This axial planar foliation is folded and replaced by a composite foliation that is common in the Danba domal complex (Harrowfield and Wilson, 2005). This complex is characterized by roughly concentric metamorphic isograds (biotite, garnet, staurolite, kyanite, sillimanite) delineating a Barrovian-type metamorphic gradient reaching partial melting as indicated by the presence of migmatites (Billerot et al., 2017). Most authors have proposed that the formation and exhumation of the domal complexes occur dominantly in a context of transpression as a result of Lower Mesozoic collision between the South China and North China blocks (Mattauer et al., 1992; Huang et al. 2003a; Roger et al., 2004; Harrowfield and Wilson, 2005; Weller et al., 2013; Jolivet et al., 2015).

#### 2.6.1.2 Foreland thrust belt

The foreland thrust belt between the Beichuan-Yingxiu fault and Guanxian-Anxian fault is represented by thrust-related structures and assemblages, including nappes, tectonic windows, fault-related folds and imbricate thrusts and duplexes (Fig. 6). The foreland thrust belt is sub-divided into the northern and southern segments. The northern segment is adjacent to the South Qinling-Dabie orogenic belt, whereas the southern segment is adjacent to the Xianshuihe strike-slip fault (Fig. 1). There is no clear geological boundary between them but rather a gradual transition of geological characteristics from north to south.

Metamorphic complexes, which are equivalent to the Huangshuihe group in the hinterland belt and the basement of the Yangtze Block, only crop out in the southern segment (Figs. 1 and 3). The cover sequences overlying the metamorphic complexes include the Sinian, Paleozoic and Triassic similar to that in the Western Yangtze Block (SBGMR, 1991; Yan et al., 2008a, 2008b; Yan et al., 2011) (Fig. 4F). The Triassic strata known as the Xujiahe Formation ($T_{3x}$) are variably unconformably or structurally overlain by Jurassic to Cretaceous clastic rocks (Yong et al., 2003; Yan et al., 2011) (Fig. 4F).

### 2.6.2 Yanyuan-Muli thrust belt

The arcuate-shaped Yanyuan-Muli thrust belt in the south LSTC extends ~400 km from the NS-striking Jinshajiang suture in the southwest to the Xianshuihe fault in the northeast (Figs. 1 and 2). This belt shares a similar tectonic framework to that of the Longmenshan thrust belt (Fig. 2). The Muli thrust fault has a sinuous trace for more than 400 km with a major salient and reentrant, and mainly dips 20°-65º NW (SBGMR, 1991; Yan et al., 2003a, Burchfiel et al., 2008; Parsons et al., 2008; Burchfiel et al., 2012; Zheng et al., 2016). This fault zone is marked by breccia and mylonite and has been estimated to have been active since the late Triassic (Xu Z.Q. et al., 1992; 2008; Yan et al., 1997, 2003a). The Muli fault divides the Yanyuan-Muli thrust belt into a hinterland belt to the northwest and a foreland thrust belt to the southeast (Fig. 2) (SBGMR, 1991; Xu et al., 1992; Yan et al., 1997, 2003a, 2011; Jin et al., 2007; Cao et al., 2015).

The hinterland belt is marked by a number of domal complexes, including the Taka, Jianglang, Changqiang and Qiasi domal complexes, which is similar to the hinterland belt of the Longmenshan thrust belt (Yan et al., 1997, 2003a) (Figs. 1 and 2). These domal complexes, which have rocks of the Liwu and Qiasi groups, are composed of mica schist, graphite-bearing sillimanite-garnet gneiss (khondalite), amphibolite, marble, and quartzite with Meso- to Neo-proterozoic ages; these rocks have been interpreted to represent the Yangtze basement (SBGMR, 1991; Yan et al., 2003a, 1997). A basement detachment fault with phyllonite and micro-breccia fault rocks was identified, separating the domal complexes from the Paleozoic sequence, that resulted in variable tectonic removal of the cover sequences (Yan et al., 2003a).

The cover sequences of both in the hinterland and foreland thrust belts have similar lithological compositions and include the Sinian, unconformity overlain by Cambrian-Ordovician volcanic rocks, carbonates, and cherts, Silurian phyllonite and basalt, Devonian quartzite, carbonate interlayered with basalt, and Carboniferous to Permian carbonates and basalts (SBGMR, 1991; Xu et al., 1992; Yan et al., 2003a, 2008a, 2008b; Song et al., 2004) (Fig. 4E). The Triassic strata disconformity overlie the Paleozoic strata and consist of carbonate and clastic rocks, unconformably or structurally overlain by Jurassic to Cretaceous clastic rocks (SBGMR, 1991; Yong et al., 2003; Wang et al., 2013a) (Fig. 4E). The Paleogene and Neogene sporadically crop out within the intermountain and piedmont basins and are mainly coarse clastic rocks, including loosely cemented conglomerates and coarse sandstones with thin layers of black mudstone (Fig. 4E) (Zhang Y.X., 2013).

## 3. Archean meta-volcanic and intrusive rocks ($Ar_t$)

The Archean metamorphic rocks have only been reported in the northernmost LSTC, represented by the Yudongzi group (Ary) (Figs. 1 and 7). The Yudongzi group ($Ar_t$), located in the northwestern of the Yangtze Block and northeastern margin of Bikou terrane, is composed of the Yudongzi gneiss group, the Longwanggou gneissic intrusion (Arl) and the Huangniping gneissic intrusion (Arh) (Fig. 7). The group consists of amphibolites, leptite, quartzite, banded iron formation (BIF), greenschist and schist in association with TTG gneiss and leucogranite (Qin et al., 1990, 1994; Zhang et al., 2001). The Yudongzi group, together with the Proterozoic to the Devonian rocks, was sliced and extruded along the A'nyemaqen-Mianlue tectonic melange and cut by ductile shear zones with NWW-SEE striking penetrative foliations (Fig. 7). The Yudongzi group experienced greenschist facies to epidote-amphibolite facies metamorphism with prograde metamorphic mineral assemblage of amphibole + biotite + muscovite, indicating temperatures of ~500℃ to ~800℃ (Zhou et al., in preparation).

The Yudongzi gneiss group was intruded by the coeval Longwanggou and Huangniping gneissic intrusions, which yielded zircon rim U-Pb age of ~2600 Ma (Zhou et al., 2018, in preparation). This age result is consistent with that of a whole-rock Sm–Nd isochron age of 2688±100 Ma for 13 amphibolite samples (meta-volcanic rocks) and a zircon upper intercept age of 2693 ±9 Ma for the gneissic leucogranite that intruded the Yudongzi group (Zhang et al., 2001). Although further isotopic dating is still needed (Zhao and Cawood, 2012), the Yudongzi group belongs to the Neoarchean, which defines the Archean tectonic event ($Ar_t$).

## 4. Paleoproterozoic and Columbia tectonic event ($Pt_{1t}$)

The Paleoproterozoic metamorphic Hejiayan group crops out southeast of the Yudongzi group in the northernmost LSTC (Fig. 7). The Hejiayan group contains schist series of chlorite-albite schist, epidote-chlorite-albite schist, actinolite epidote schist and sercite-quartz schist, and Heimulin foliated ultrabasic rocks. All these rocks experienced greenschist-facies metamorphism. The protolith assemblages are probably island-arc basaltic volcanic rocks and ultrabasic intrusions, which have yielded a zircon core U-Pb age of ~1933 Ma (GRT-SBGMR, 1996; Zhou et al., in preparation). This rock assemblage, which are blocks in a melange matrix with components of siliceous, pillow basalts, peridotite and serpentinite, indicates a Precambrian ophiolite melange (GRT-SBGMR, 1996; Zhang et al., 2001) (Fig. 7). Thus the ~1933 Ma Hejiayan volcanic rocks imply a tectonic episode of volcanic arc construction in the Paleoproterozoic ($Pt_{1t}$).

The supercontinent Nuna shares a common configuration with the core elements of Laurentia and Siberia (Zhao et al., 2002, 2011; Evans and Mitchell, 2011; Zhang et al., 2012; Pisarevsky et al., 2014) (Fig. 8). The exotic Yangtze Block accreted to the Rae Craton at 2400–2300 Ma and was involved in the assembly of Nuna, along with Laurentia and Siberia (Wang et al., 2016). These events of amalgamation in the interval 2320-1800 Ma, identified in the southwestern Yangtze Block and northern Vietnam, include metamorphic events at 2030–1950 Ma and 1850-1800 Ma in the Thelon and Akitkan orogens of northwest Laurentia and Siberia, respectively (Wang et al., 2016).

The Hejiayan group in the northmost of the LSTC has composition of volcanic arcs and ophiolitic melange is probably associated with orogenesis at continental collisional margins during the $Pt_{1t}$. The age at ~1933 Ma is synchronous with the Nuna assemblage orogens occurred in the southwestern Yangtze Block. Although geochemistry and age constraints are still under research, the spatial and temporal link between the southwestern Yangtze Block and the northern LSTC probably define the $Pt_{1t}$ of the Nuna assemblage orogen along the western Yangtze Block (Fig. 8).

## 5. Neoproterozoic metamorphic basement and Rodinia tectonic event ($Pt_{3t}$)

The Neoproterozoic basement is well exposed in the LSTC and its adjacent western Yangtze Block (Fig. 3). The basement is exposed along the domal metamorphic complexes, including Bikou terrane, Jiaoziding, Penguan-Xuelongbao, Baoxin, Danba, Jianglang (Taka), Changqiang and Qiasi domal complexes in the hinterland belt of the LSTC, and the Kangding complex in the western Yangtze Block (Zhao et al., 1994; Zhou et al., 2002a; Yan et al., 2003a, 2008a, 2008b) (Fig. 3).

During the past few decades, many studies have focused on the geology, petrology, geochemistry and geochronology of the intrusions, as well as the metamorphic, volcanic and sedimentary rocks within the domal complexes in the LSTC and western Yangtze Block (Pei et al., 2007, 2009; Zhou et al., 2002a, 2006a; Druschke et al., 2006; Xiao et al., 2007; Zhao et al., 2007, 2008, 2009a, 2009b, 2013a, 2013b; Yan et al., 2008a, 2008b; Sun et al., 2009). Although a variety of tectonic settings and genesis of these rocks represented due to the divergence of views, some commonalities are reached including tectonic settings ($Pt_{3t}$) of ophiolite complexes, magmatic arcs, backarc and forearc basins (Fig. 9).

**5.1 Ophiolite complex**

Tens of small-scale bodies of hornblende gabbros and olivine gabbros have been distinguished within the metamorphic complexes (SBGMR, 1991; Zhao et al., 2017) (Fig. 1). For example, the recently reported Shimian ophiolite, including gabbro and serpentinized peridotite intruded by mafic dikes within the Kangding complex has characteristics of a supra-subduction zone ophiolite complex (Sun and Vuagnat, 1992; Li et al., 1997; Zhao et al., 2017). The peridotite has low REE and trace element contents, suggesting a source of depleted mantle. Chromites from the peridotite have low contents of $TiO_2$ and $Fe_2O_3$, with moderate Cr/(Cr+Al) and Mg/(Mg+$Fe^{2+}$) ratios (Zhao et al., 2017). These spinel compositions associated with strong melt depletions are similar to those of supra-subduction zone peridotites. The mafic dikes and gabbros are chemically similar to MORB-affinity tholeiitic basalts and boninite-series volcanic rocks in the Izu-Bonin-Mariana arc system, and are dated at ~800 Ma by zircon U-Pb (Dilek et al., 2008; Kusky et al., 2011; Whattam and Stern, 2011; Zhao et al., 2017). Although a number of similar mafic rock assemblages exposed along the LSTC have yet to receive detailed study, the serpentinized peridotite, mafic dikes and gabbros, together with their geochemistry, define a supra-subduction zone ophiolite complex, and record the accretion of oceanic lithosphere along a trench to the western Yangtze Block (Zhao et al., 2017) (Fig. 10A-D).

**5.2 Arc magmatic signatures**

The Neoproterozoic granitoid intrusions in the LSTC, from northeast to southwest, are represented by the intrusions within the domal complexes of the Bikou terrane, Jiaoziding, Xuelongbao-Pengguan, Baoxing and Kangding (Fig. 3) (Zhou et al., 2002a, 2002b, 2006a; Druschke et al., 2006; Xiao et al., 2007; Zhao et al., 2007, 2009a, 2009b; Yan et al., 2008b; Liu et al., 2009a; Pei et al., 2009; Sun et al., 2009). Three rock types, adakites, mafic intrusions and granitic intrusions, have been identified.

Adakitic plutons include the ones within the Xuelongbao complex, Datian of the Danba complex, and the Huatan and Mopanshan plutons of the Kangding complex (insert in Fig. 3). Pluton within the Xuelongbao domal complex in the middle of the Longmenshan thrust belt are composed of tonalite and granodiorite with adakitic affinity, and display high Sr contents and Sr/Y ratios, depletion in HREE, variable enrichment in LREE, and positive Sr and negative Nb and Ti anomalies in the primitive mantle-normalized trace element spider diagram (Zhou et al., 2002a, 2006a; Zhao et al., 2017). These geochemical characteristics suggest derivation from adakite-like magmas (Zhou et al., 2006b; Zhao and Zhou, 2007a) (Fig. 9A). The pluton has been dated at 748 ± 7 Ma using SHRIMP zircon U–Pb (Zhou et al., 2006b). In the Mianning–Xichang area, south of the Kangding complex, the Mopanshan adakite is characterized by low MgO, Cr and Ni contents, high Rb/Sr and Sr/Y ratios and negative $\varepsilon_{Nd(t)}$ values, and was dated at 782 ± 6 Ma using LA-ICPMS zircon methods (Huang et al., 2009).

Taking together the geochemical and isotopic characteristics, the presence of relict zircons (1.16–0.83 Ga) and the Mesoproterozoic zircon Hf model ages (1.06–1.27 Ga), the adakites could be interpreted as derived from melting of a thickened continental lower crust (Huang et al., 2009) or melting of a subducted oceanic slab. Both possibilities are compatible with a compressional tectonic setting, ruling out an intra-continental extensional setting. Considering that the adakites exposed within Xuelongbao, Danba and Kangding complexes occur roughly along the trend of the LSTC in the western margin of the Yangtze Block (Zhou et al., 2006b; Zhao and Zhou, 2007a) (Fig. 3 and insert), we consider that these adakitic rocks are most likely the melting products of a subducted oceanic slab, together with evidences of arc-sedimentary sequences, normal-arc granites and arc-related mafic-ultramafic intrusions, suggesting an eastward supra-subduction tectonics along the western margin of the Yangtze Block (Zhao and Zhou, 2007b) (Fig. 9A).

The mafic intrusions are generally exposed and mixed cropout with granitic plutons (Fig. 3). The Baoxing domal complex is located in the south segment of the Longmenshan thrust belt and consists mainly of metamorphic gabbroic, dioritic gneisses, tonalitic and granodioritic gneisses, and massive monzogranites. The gabbros and gabbrodiorites are characterized by low $SiO_2$ contents, high Mg# values and Cr, Co, and Ni contents, significant enrichment in LREE and LILE, depletion in HFSE (e.g., Nb, Ta, Zr, and Hf) and positive zircon $\varepsilon_{Hf}$ values (Zhao et al., 2007a; Meng et al., 2015). These gabbroic rocks were proposed to derive from partial melting of depleted lithospheric mantle that had been metasomatized by subduction-derived fluids or melts (Zhao and Zhou, 2007a; Meng et al., 2015) (Fig. 9B). The tonalite, granodiorite and monzogranite exhibit enrichment in Rb, Ba, Th, and Pb and depletion in Nb, Ta, and Ti, and have low Sr/Y and $(La/Yb)_N$ ratios and high Y and Yb contents, and positive $\varepsilon_{Hf}$ values, indicating a juvenile crust source derived from partial melting of metamorphic basalts or metagreywacks in the lower crust (Meng et al., 2015). The Baoxing plutonic complex were dated at 848 ± 4 Ma for gabbro, 799 ± 5 Ma and 802 ± 6 Ma for gabbrodiorite, and 773 ± 5 Ma and 769 ± 5 Ma for granite, using LA-ICPMS zircon U–Pb method (Meng et al., 2015).

In the Yanbian region of the south Kangding complex, the Tongde plutonic complex intruded into the Kangding metamorphic complex, and consists of diorite, quartz diorite and minor gabbro, showing arc-type geochemistry and calc-alkaline affinities. The Tongde pluton was dated at 825 ± 7 Ma and 820-810 Ma by the SHRIMP U–Pb zircon method (Li Z.X. et al., 2003; Munteanu et al., 2010). Both the Gaojiacun and Lengshuiqing mafic intrusions, which intrude the Tongde pluton, show pronounced negative Nb–Ta and Zr–Hf anomalies, high $\varepsilon_{Nd(T)}$ values (+1.5 to +6.0), and initial $^{87}Sr/^{86}Sr$ ratios of 0.705–0.706, suggesting a typical arc assemblage formed on the western edge of the Yangtze Block (Zhou et al., 2006b; Zhao and Zhou, 2007a). Both mafic intrusions were dated at 812 ± 3 and 806 ± 4 Ma, respectively, by the SHRIMP zircon U–Pb method (Zhou et al., 2006b). Additionally, some mafic dykes in the Yanbian area of the south Kangding complex show OIB and MORB-like geochemical affinities, which were dated at 792 ± 13 and 761 ± 14Ma, respectively, by the SHRIMP zircon U–Pb method (Zhu W.G. et al., 2008).

In addition, the hornblende and olivine gabbroic intrusions that crop out in the southern the Kangding complex have tholeiitic and arc-like geochemical compositions, and show obvious depletion of Nb, Ta and Ti, and relatively low $\varepsilon_{Nd(T)}$ values (−0.12 to −1.73) with variable $^{87}Sr/^{86}Sr$ ratios (0.7045–0.7075) (Zhao and Zhou, 2007a). These small-scale intrusions were dated at 738 ± 23 and 746 ± 10 Ma, respectively, using SHRIMP zircon U-Pb geochronology (Zhao and Zhou, 2007a).

Large scale granitic plutons include the Jiaoziding of the northern segment and the Pengguan in the southern segment of the LSTC, and the Kangding pluton in the western Yangtze Block (Fig. 3). The intrusion within the Jiaoziding domal complex shows enrichment in LREE, depletion in Ta, Nb and Ti, and enrichment in Rb, Ba and Sr, which are compatible with peraluminous and S-type granite (Pei et al., 2009). Using SHRIMP zircon U–Pb methods, the foliated granite and massive granite within this pluton were dated at 793 ± 11 Ma and 792 ± 11 Ma, respectively (Pei et al., 2009). These rocks were thought to be the result of crustal thickening caused by active continental margin subduction or arc–continent collisional orogeny during the Neoproterozoic in the western margin of the Yangtze Block (Pei et al., 2009).

Plutons within the Pengguan domal complex, which are located in the southern segment of the LSTC (Fig. 3), are dominantly composed of monzonitic granite, granodiorite, tonalite and diorite showing calc-alkaline affinity and metaluminous to weakly peraluminous geochemical compositions. These plutons have a relative low abundance of REE, enrichment of Rb, Sr, Ba and K, and depletion of Nb, Ta, P and Y, suggesting formation through mixing of underplated mantle-derived magma and the melting of lower crust in a subducted-related volcanic arc environment (Yan et al., 2008b; Zhang et al., 2008) (Fig. 9C). The granites were dated at 809 ± 3 and 844 ± 6 Ma using LA-ICP-MS zircon U-Pb geochronology (Yan et al., 2008b).

The Kangding metamorphic complex, as well as the Danba domal complex with its associated granitoids, has traditionally been considered as a part of the Archean basement of the Yangtze Block (SBGMR, 1991). The gneissic granitoids within the Kangding and Danba complexes are dominantly tonalite, granodiorite and monzogranite, and are enriched in LREE with positive $\varepsilon_{Nd(t)}$ values, and significantly depleted in Nb, Ta, P and Ti, suggesting a subduction-related setting (Zhou et al., 2002a, 2002b). The Kangding gneissic granites were dated at 797 ± 10, 795 ± 13 Ma, 796 ± 14 Ma and 764 ± 9 Ma, whereas the protolith of the Danba gneissic complex was dated at 824 ± 14 Ma, and the monzogranite within the Danba complex was dated at 826 ± 29 and 767 ± 24 Ma, respectively, by SHRIMP U–Pb zircon (Zhou et al., 2002a, 2002b; Liu S.W. et al., 2009b).

Integrating the elemental and isotopic geochemistry and the age results, the hornblende gabbros, and mafic intrusions were probably derived from a source strongly modified by subducted slab fluids, whereas the olivine gabbros came from a mantle source modified by subducted slab melts during the Neoproterozoic (Zhao and Zhou, 2007a) (Fig. 9B). Geochemical data and isotopic results reveal the granitic plutons have a TTG composition (insert in Fig. 3) with magmatic arc signatures. The similar ages for the deformed granite and massive granite suggest that the granitoids in the Longmenshan tectonic complex and Kangding region were formed in a compressional tectonic setting, which most likely was a magmatic arc above a subduction zone during the Neoproterozoic (830 to 760 Ma) (Zhou et al., 2002a, 2002b; Zhou et al., 2006b; Zhu W.G. et al., 2008) (Fig. 9C).

**5.3 Fore-arc and back-arc deposits**

The Bikou terrane in the northern LSTC consists of a volcanic assemblage of the Bikou group, and a correlative volcanic clastic turbidite sequence of the Hengdan group with lower amphibolite to middle greenschist facies metamorphism (Figs 1 and 2). Detrital zircon studies of the Hengdan group have found euhedral, volcanic grains varying from ca. 850 to 700 Ma with a peak near 770 Ma (Druschke et al., 2006). The Hengdan group contains a thick succession of coarsening-upward volcaniclastic marine sediments, which has provenance from the volcanic Bikou group to the south, and has been interpreted to represent a fore-arc basin during the Neoproterozoic southward subduction beneath the Yangtze Block (Druschke et al., 2006).

The Yanbian group in the south Kangding complex is a well-preserved Neoproterozoic volcanic-sedimentary sequence (SBGMR, 1991). This group consists of a lower sequence of basaltic lavas with a thickness of ~1500 m, and an upper sequence of flysch deposits wih a thickness of ~3500 m. The flysch sequence contains typical deep marine turbidites consisting mainly of fine-grained volcaniclastic sandstones and mudstones, indicating a submarine fan depositional system (Sun et al., 2008a, 2008b, 2009). The lavas have variable bulk-rock compositions with $SiO_2$ ranges from 45.3 to 50.7 wt%, $Al_2O_3$ from 12.8 to 16.8 wt%, and $TiO_2$ from 1.3 to 2.9 wt%. Although the incompatible trace elements, including Nb, Ta, Zr, Hf, Ti, and HREE, are similar to those of MORB, the lavas show features of island-arc tholeiites with pronounced enrichments in Rb, Ba, U, Sr, and Pb. These lavas are characterized by low initial $^{87}Sr/^{86}Sr$ ratios (0.7030 to 0.7040) and strongly depleted $\varepsilon_{Nd(t)}$ values (+3.8 to +8.0) (Sun et al., 2008a, 2008b, 2009). The sandstones contain abundant feldspar, lithic fragments of andesitic and felsic volcanic rock, minor amount of quartz and have an average composition of Q (16%) F (35%) and L (49%), suggesting a proximal source and an undissected to arc setting. The sandstones and mudstones have intermediate $SiO_2/Al_2O_3$ (typically 3-6), high $Fe_2O_3$ + MgO contents (5-12 wt%), and moderate to high $K_2O/Na_2O$ ratios (generally 0.1-1 and 1-10 for sandstones and mudstones, respectively) (Sun et al., 2007, 2008a, 2009). These rocks have strong negative Nb-Ta anomalies, slight depletion of Zr-Hf, La and Th, but moderate enrichment of V, Cr, Ni, and Sc. They show LREE enrichment (La/Yb-N = 5.3-7.4) with flat HREE, and pronounced negative Eu anomalies (Eu/Eu-center dot = 0.6-0.74) in chondrite-normalized REE patterns, similar to post-Archean shales (Sun et al., 2008a, 2008b).

The age of the Yanbian group is constrained by detrital zircon geochronology and the age of a cross cutting pluton. The Yanbian group has detrital zircon ages from ca. 865 Ma to 1000 Ma with two peaks at ca. 900 Ma and 920 Ma, and is intruded by the 860 Ma Guandaoshan dioritic pluton, constraining its youngest depositional age at ca. 865 Ma. Geochemical data of the group suggests an back-arc basin setting and intermediate-felsic volcanic source, which is consistent with a back-arc basin scenario for the basaltic lavas in the lower Yanbian group (Sun et al., 2007, 2008a, 2009).

Integrating the characteristics of the ophiolite, adakitic rocks, mafic rocks, granitic intrusions and deposits within the metamorphic complexes (Fig. 3), a tectonic configuration of the Neoproterozoic trench-arc-basin system can be established (Fig. 9B). The trench is revealed by the newly distinguished Shimian ophiolitic melange, and a magmatic arc including mafic, adakitic and granitic rocks might extend more than 500 km from Hannan in the north LSTC to the south of Kangding complex on the western margin of the Yangtze block; and local preserved deposits support the presence of back- and fore-arc basins (Fig. 9D).

The Proterozoic trench-arc-basin system along the LSTC and western margin of the Yangtze block suggests that the western margin of the Yangtze block was an active margin in the Rodinia reconstruction (Yan et al., 2002; Zheng et al., 2006). This system has geochemical, isotopic and geochronological similarities to the northeastern Madagascar, Seychelles island and Malani in India (Tucker et al., 2001), which probably represent a native Andean-type margin on the edge of Rodinia (Yan et al., 2002; Zhou et al., 2002b; Zhao et al., 2017). We therefore correlate the western margin of the Yangtze block with the northeastern margin of the India Plate which had an active arc above an eastward subduction zone in the Neoproterozoic time (Yan et al., 2003a; Zheng Y.F., 2006) (Fig. 9E).

The dawn of 725-750 Ma rift, which corresponds to the formation of Nanhua basin within the Yangtze block, might represent initial break up of the Rodinia supercontinent (Fig. 9E). However, the Nanhua sequences were previously distinguished only within the Yangtze block (Fig. 4G). The equivalent strata in the LSTC have not been identified.

## 6 Sinian to Paleozoic passive continental margin ($Pz_t$)

The Sinian (Late Neoproterozoic, 630-542 Ma) to Paleozoic sedimentary sequences represent a well recognized passive continental margin $Pz_t^1$ (SBGMR, 1991; Mattauer et al., 1992; Xu et al., 1992;). This margin was stable until the development of a super-plume, effusive basaltic volcanism of the Emeishan basalt, and localized extension $Pz_t^2$ during the late Permian.

**Sinian to Carboniferous passive continental margin and formation of the Mianlue ocean ($Pz_t^1$)**

The Sinian rock record includes the Doushantuo and Dengying formations, which unconformably cover the metamorphic basement (metamorphic complex). The

Doushantuo formation is well exposed in the LSTC and its adjacent regions but has not been documented in the Songpan-Ganze terrane (Fig. 4). This formation includes black shale, mudstone, marlstone and sandstone with local phosphorite (SBGMR, 1991; Huang et al., 2003b; Roger et al., 2010; Zhang et al., 2017). In general, clastic grains in Sinian rocks of the LSTC and the western Yangtze block are coarser than those in the South Qinling-Dabie orogenic belt and Bikou terrane (comparing Fig. 4D-G with Fig. 4A-B), indicating littoral to shallow sea clastic assemblage with westward deepening of the sea water (SBGMR, 1991).

The Dengying formation comformably covers the Doushantuo formation, with widespread outcrops in the LSTC and western Yangtze block. This formation is composed of dolomite and dolomitic limestone with bedded chert bands and locally phosphorite (SBGMR, 1991; Huang et al., 2003b; Roger et al., 2010) (Fig. 4). The rock assemblage represents a transition from carbonate platform marginal facies to restricted platform facies (SBGMR, 1991).

Cambrian-Ordovician strata unconformably overlie Sinian rocks in the LSTC and its adjacent South Qinling-Dabie orogenic belt and western Yangtze block. The Cambrian-Ordovician strata include interlayers of carbonite and clastic rocks (i.e., sandstones, siltstones and shales), indicating shallow sea facies. Sedimentary or tectonic omission of most of the Cambrian-Ordovician strata around the domal complexes was interpreted as a north-south striking paleohigh belt, i.e., the Xikang-Yunnan axis from the LSTC to Kangding complex belt (Huang, 1947; SBGMR, 1991) (Fig. 4).

The Silurian is represented by muddy and sandy flysch with limestone known as the Maoxian group in the Bikou terrane, Songpan-Ganze terrane and hinterland belt of the

LSTC (Fig. 4B-D), and shallow marine lime-mud flat in the South Qinling-Dabie orogenic belt, foreland belt of the LSTC and western Yangtze block (Fig. 4A, F-G). The rock assemblages indicate a westward deepening from stable shallow marine platform facies to relative deep-water deposits, perhaps indicating the initial development of the Songpan-Ganze ocean (SBGMR, 1991) (Fig. 4).

Throughout the LSTC and its adjacent regions, Devonian and Carboniferous strata are well exposed with carbonates dominant, except where covered by the Triassic flysch in most of the the Songpan-Ganze terrane (Fig. 4). Lithofacies and sedimentary sequence reveal a westward deepening of marine facies, from lime-mud flat and algal flat facies in the foreland thrust belt to shallow sea or slope facies in the hinterland belt of the LSTC, to deep sea facies in the Songpan-Ganze terrane (SBGMR, 1991) (Fig. 4).

To the northmost of the LSTC, the Paleozoic Mianlue ocean is represented by a number of ophiolite suites, ophiolitic melange and oceanic island-arc volcanic rocks identified along the Mianlue suture (Fig. 1). These rock assemblages, which are distributed in the Nanping-Kangxian-Lueyang-Mianxian, have been widely investigated (Li et al., 1996; Lai and Yang, 1997; Lai et al., 2000, 2004; Xu et al., 2000a, b; Zhang et al., 2004; Dong et al., 2011). Details for the rock assemblage are available in Zhang et al. (2004) and Dong et al. (2011).

The initial spreading of the Mianlue ocean is represented by bimodal volcanic rocks that consist of meta-basalts, dacites and rhyolites with enrichment of LREE, Th, U, Sr and Zr and minor Ti negative anomalies in the west of Lueyang along the Mianlue suture (Li et al., 1996; Lai et al., 1998; Xu et al., 2000a, b; Zhang et al., 2004) (Fig. 2). Petrological and geochemical features indicate the rocks were derived either in a rift (Li et al., 1996) or in a transitional setting where an initial continent rift was expanding into a mature oceanic basin (Zhang et al., 2004). Based on a summary of the petrological, geochemical and geochronological results, initial rifting and formation of the juvenile ocean may have occured in the Devonian to the Carboniferous (Dong et al., 2011) (Fig. 4).

Intergrated the above results of sedimentary facies and rock assemblages, the shallow sea deposits along the LSTC imply a stable passive continental margin from the Sinian to the Carboniferous. To the northmost of the LSTC the development of the Mianlue ocean initiated in the Devonian to Carboniferous (Roger et al., 2010) (Fig. 4). We then define this tectonic event as the Paleozoic tectonic event $Pz_t^1$.

**6.2 Permian rift, Emeishan basalt and mature Mianlue ocean ($Pz_t^2$)**

Permian rocks are widespread in the LSTC and its adjacent regions, with carbonate strata roughly equivalent to that in the western Yangtze block. These rocks include carbonates of the Liangshan, Qixia, Maokou, Wujiaping and Changxing fomations, from lower to upper (Fig. 4). The Emeishan basalt occurs between the Maokou and Wujiaping formations and is exposed in the southern Sonpan-Ganze terrane and Yidun arc, south of the LSTC and western Yangtze block (SBGMR, 1991; Song et al., 2004). The Emeishan basalts, previously named as the Emeishan Large Igneous Province (ELIP), have been interpreted as products of a mantle plume (e.g. Zhou et al., 2000; Xu et al., 2001; Lo et al., 2002; Li et al., 2015b; Deng et al., 2016). Basalt assemblages of the ELIP have been dated at 260-250 Ma using LA-ICPMS and SHRIMP zircon U-Pb methods (Xu et al., 2001; Lo et al., 2002; Song et al., 2004; Shellnutt and Zhou, 2007; Jian et al., 2009; Wang et al., 2014; Li et al., 2015b; Li et al., 2016).

The center of the mantle plume has been determined by the recognition of a 1 km-scale domal uplift during initial Emeishan eruptions (He et al., 2003a, 2003b, 2006, 2009, 2010). The overall radiating patterns of mafic dyke swarms of the ELIP in the Yongren area, Yunnan province, was thought to coincide with the maximum pre-eruptive domal uplift and close to the high-temperature picrites (Li et al., 2015).

Basalts within the ELIP are geochemically divided into low-Ti and high-Ti types (Xu et al., 2001). The parent magmas of the low-Ti basalts, which were generated by higher degrees of partial melting (16%) of a distinct mantle source ($\varepsilon_{Nd}(t)$=+2, $^{87}Sr/^{86}Sr$ ($t$)=0.705) around the spinel–garnet transition zone, record the main episode of flood basalt emplacement (Xu et al., 2001). The eruption of low-Ti type magmas is concentrated in the lower part of the basalt column. The association of the eruption of the low-Ti basalts within incipient extensional features, which are lacking in the higher parts of the basalt succession, along the southern LSTC might imply an aulacogen along the LSTC (Meng et al., 2005) (Fig. 10).

The less abundant high-Ti basalts overlying the low-Ti basalts were generated by low degrees of partial melting (1.5%) of a mantle source that has $\varepsilon_{Nd}(t)$ of ~+5 and $^{87}Sr/^{86}Sr$ ($t$) of ~0.704 in the garnet stability field (Xu et al., 2001). The evolution from low-Ti basalts of higher degrees of partial melting of the mantle to high-Ti lavas with lower degrees of partial melting imply that it starts out with a thicker lithosphere and lower geotherm, and then evolves with thinner lithosphere and higher geotherm (Xu et al., 2001).

At least three geochemical types of A-type granites are spatially and temporally associated with the ELIP basalts: the Panzhihua and Taihe peralkalines granites, the Woshui metaluminous syenites and the Ailanghe peraluminous granite. These granitoids have found along the NS-striking Panzhihua rift (Shellnut and Zhou, 2007). The 260 Ma peralkalines granites in Panzhihua and Taihe have ASI of 0.76–1.12, Na+K/Al of 0.78–1.2 and high Fe* values (0.92–0.99) with negative Eu anomalies (Eu/Eu*=0.22–0.98). The 260 Ma metaluminous syenites in Woshui have ASI of 0.84–1.0, Na+K/Al of 0.91–1.01 and moderately high Fe* (0.79–0.81) and positive Eu anomalies (Eu/Eu*=0.82–1.91). Both the peralkaline and metaluminous rocks have mantle isotopic signatures (εNd(T)=+1.3–+3.2) and were probably derived from the ELIP mantle plume source. The 251 Ma peraluminous granites in Ailanghe have ASI of 0.97–1.29, high Fe* values (0.82–0.91) and negative Eu anomalies (Eu/Eu*=0.10–0.37) with crustal isotopic signature (εNd(T)=−5.7–−6.7), indicating possible derivation from melting of Yangtze block basement rocks by basaltic underplating (Shellnut and Zhou, 2007). Therefore, the association of high-Ti and low-Ti basalts and A-type granites, and their geochemistry, suggest a continental rift tectonic setting for the Panxi belt, for at least ~9 m.y. from 260 Ma to 251 Ma (Wang et al., 2014) (Fig. 10).

Late Permian mafic igneous rocks are also present in the Songpan-Ganze terrane and Yidun arc, covered in turn by early Triassic calc-alkaline volcanic rocks (SBGMR, 1991; Yang et al., 2011; Wang et al., 2013a, 2013b Cao et al., 2015). The late Permian basalts and metagabbros, which have geochemical characteristics of LREE enrichment (La/Sm=3.4-4.3), HREE depletion (Gd/Yb=2.4-4.3), variable trace elements of Zr/Nb=4.3-11.3, La/Nb=0.7-1.7, Ba/Nb=4.3-41.6, Th/La=0.1-0.2, and $\varepsilon_{Nd}(t)$ values of 0.3-4.8, are virtually identical to the basalts of the ELIP (Song et al., 2004). The similar geochemical characteristics indicate that parental melts of the basalts in the Songpan–Ganze terrane and Yidun arc were derived from the same source regions as the ELIP (Song et al. 2004), suggesting a tectonic setting of continental rift.

The early Triassic volcanic rocks are enriched in LREE ($La_N/Yb_N$ = 3–24), have mostly negative Eu anomalies (Eu* = 0.2–0.9), and exhibit negative Nb and Ta anomalies with $(Nb/La)_N$ of 0.21–0.91 and $(Nb/Th)_N$ of 0.05–0.49. Fractionation of the HREE is limited ($Gd_N/Yb_N$ = 1.0–2.5) (Wang et al., 2013a, 2013b; Yang et al., 2011). The early Triassic volcanic rocks and their coeval intrusions along the Yidun arc defines an oceanic affinity volcanic arc (Yang et al., 2014). Therefore, the Yidun arc and Songpan-Ganze terrane experienced a similar evolution of continental rifting leading to development of an ocean basin from the late Permian to the early Triassic (Fig. 10), followed by subduction along the Yidun arc.

In summary, the location of initial impingement of the Late Permian Emeishan mantle plume is recognized in the Yongren area, Yunnan province. A continental rift developed during plume-lithosphere interaction, within the Panxi region (Kangding complex), with one rift arm developing from a continental rift to an oceanic rift along the Yidun arc and Ganze-Litang suture, and a possible second arm, an aulacogen, developing along the LSTC seems, and the third one continental rift roughly along the Kangding complex (Panxi rift) to define a late Permian three-armed rift system (Fig. 10). The implication of this hypothesis is that LSTC may represent Triassic tectonic inversion of a late Permian aulacogen. This hypothesis can be tested by futher studies in the LSTC.

North of the LSTC, the late Permian development of the Mianlue ocean is represented by typical oceanic ophiolite suites with peridotitic compositions, as represented in the Wenjiagou-Zhuangke to the west of Lueyang and in the Anzishan to the west of Mianxian (Fig. 2). Basalts from Wenjiagou-Zhuangke and Anzishan ophiolites – characterized by strong depletion of LREE in the chondrite-normalized REE patterns, low concentrations of HFSE of Nb, Ta, La, Ce, Pr, P, Nd, Zr, Sm, Eu and Ti and flat HFSE distribution patterns in the primitive mantle-normalized trace element distribution diagrams – display typical N-MORB chemical compositions (Dong et al., 2011). The geochemistry of these ophiolitic basalts indicates a derivation from a depleted mantle source, and the integrated petrological and geochemical characteristics suggest development of mature spreading within the Mianlue ocean (Lai and Yang, 1997). These ophiolitic rocks, which were deformed and metamorphosed during the middle to late Triassic, are thought to be Late Paleozoic to the Early Triassic in age (Fig. 11) (Dong et al., 2011, 2013).

## 7 Mesozoic composite tectonics ($Mz_t$)

Here we describe two Mesozoic deformation phases evident in the LSTC, a Late Triassic ($Mz_t^1$) phase of major transpression, and a latest Triassic to Jurassic phase of extension ($Mz_t^2$). Both tectonic episodes may be affiliated with the closing and subsequent deformations of the Ganze-Litang ocean in the southwest and Mianlue ocean in the north of the LSTC, respectively (Zhang et al., 2004; Dong et al., 2011; Yan et al., 2011; Cao et al., 2015; Xu et al., in preparation).

### 7.1 The $Mz_t^1$ Tectonics

Within the LSTC, the $Mz_t^1$ tectonics has been widely described (Chen et al., 1995; Worley and Wilson, 1996; Arne et al., 1997; Harrowfield and Wilson, 2005; Roger et al., 2008; Yan et al., 2008b, 2011). This tectonic event is characterized by large-magnitude transport of nappes, metamorphism, extensive igneous activity and related sedimentary basins.

The $Mz_t^1$ assemblage of thrust faults and columnar fold and metamorphism were identified throughout the LSTC and adiacent Songpan-Ganze terrane (Bruguier et al., 1997; Zhang et al., 2004; Weislogel et al., 2006; Enkelmann et al., 2007; Yan et al., 2011; Billerot et al., 2017). The folds are upright-inclined with shapes changing from open to isoclinal depending on lithological types, NW-SE striking, shallow plunging axes and upright spaced cleavages in Songpan-Ganze terrane, while inclined, isoclinal folds with top-to-the-SSW kinematics, shallowly plunging axes and associated penetrative cleavage characterize folds within the LSTC (Worley and Wilson, 1996; Yan et al., 2011). Coeval arcuate-shape thrust faults have variable ESE- to WNW-dip direction within the LSTC. The $Mz_t^1$ within the LSTC has a fold-thrust fault system (Worley and Wilson, 1996; Jia et al., 2006). Integrated with mineral lineations on foliation, NNW- or NW-dipping fold axial plane cleavage (original), S-C fabrics and “σ”-type pressure shadows, the $Mz_t^1$ was characterized by oblique transpression with top-to-the-SSW thrusting and sinistral strike-slip faulting, which is consistent with NW- or WNW-ward underthrusting of the South China block underneath the North China block (Liu et al., 2005).

The $Mz_t^1$ metamorphism is characterized by regional greenschist rocks, local development of high-pressure blueschist facies rocks in the north and middle of the LSTC. The regional greenschist facies is represented by metamorphic mineral assemblage of chlorite + muscovite + albite + orthoclase + biotite + quartz (Liu H.et al., 2008). The blueschist facies rocks in the Bikou terrane are represented by metamorphic mineral assemblages of Calcite-Amphibole + Epidote + Chlorite + Phengite and Sodaclase-

Amphibole + Epidote + Chlorite + Phengite (Wei, 1993, 1994; Xu C.G. et al., 2018). The Barrovian metamorphic rocks in the Danba terrane have metamorphic facies from sericite- to kyanite-grade, which has estimated P-T conditions from ~3-5 kbar and ~410-530°C (biotite zone) to 5.3-8 kbar and 570-600°C (staurolite and kyanite zones) (Huang et al., 2003a). A number of the age dates include metamorphic minerals of garnet was dated at 204 Ma using Sm-Nb method, muscovite and biotite were dated at 237-220 Ma using $^{40}Ar/^{39}Ar$ method (Huang et al., 2003a, 2003b; Zhou et al., 2008; Yan et al., 2011). The metamorphic ages are equivalent within error to those of 226-215 Ma (zircon U-Pb ages) adakitic/I-type to high Ba-Sr granitic intrusions, which have relatively high $Is_r$ and low $\varepsilon_{Nd}$ values in the LSTC and the adjacent Songpan-Ganze terrane (Roger et al., 2004; Zhang et al., 2006; Xiao et al., 2007; Zhang et al., 2007; Lu et al., 2010; Yuan et al., 2010).

The $Mz_t^1$ deformation, metamorphism and magmatism reveal a tectonic event of crustal thickening, which were interpreted as a result of the South China block subducted underneath the North China block (Wei et al., 1994; Faure et al., 2001; Yan et al., 2011; Xu et al., in preparation). However, the uppermost Upper Triassic Xikang group with fine-grained flysch deposits in the Songpan-Ganze terrane, while coarse clastic rocks near the Longmenshan suggest that the LSTC was uplifted prior to the thickening of the Songpan-Ganze terrane (SBGMR, 1991; Yan et al., 2011) (Fig. 4C-F). Early Jurassic strata contain a basal conglomerate and unconformably overlie Late Triassic strata, demonstrating that $Mz_t^1$ deformation terminated at ~208 Ma (Zhang et al., 2004; Yan et al., 2008b; Yan et al., 2011) (Fig. 4).

### 7.2 The $Mz_t^2$ Tectonics

The $Mz_t^2$ Tectonics is characterized by folds, and a variable scale of ductile shear zones with penetrative foliation, mineral and stretching lineations, sheath folds, and S-C fabrics (Worley and Wilson, 1996; Yan et al., 2011; Billerot et al., 2017). The ductile shear zones around the domal complexes separate the Proterozoic metamorphic complexes from middle- to shallow- metamorphosed cover sequences in the hinterland belt of the LSTC (Figs. 2 and 6). These ductile shear zones show top-to-SE or ESE shear senses and are interpreted as thinning or removing the stratigraphic sequence by extension (Zhou et al., 2002b, 2008; Yan et al., 2003a, 2008a, 2008b, 2011; Liu et al., 2008) (Figs. 2, 6 and 11). P-T conditions of the ductile shear zones were revealed at 260-310°C and 3.9-6.2 kbar for the Bikou terrane by metamorphic mineral assemblage of Chlorite + Muscovite + Actinolite + Orthoclase + Albite + Quartz (Liu et al., 2008), 265-405°C and 3.1-4.8 kbar for the Pengguan-Xuelongbao complex by metamorphic mineral assemblage of Garnet + Biotite + Plagioclase + Muscovite + Quartz (Yan et al., 2008a), and 640-680°C and 4.8-6.3 kbar (Sillimanite + Biotite + Muscovite + Quartz + Garnet ± Ilmenite ± Plagioclase, or Hornblend + Plagioclase ± Garnet ± Clinozoisite ± Biotite ± Titanite + Quartz in sillimanite zone) to 660-720°C and 5.8-6.2 kbar (Plagioclase + K-Feldspar + Quartz + Muscovite + Biotite ± Garnet ± Sillimanite in metapelitic migmatite zone) following a clockwise P-T-t path for the Danba complex (Huang et al., 2003a). These P-T conditions are consistent with mid-crustal prograde metamorphism with variable lower greenschist facies to upper amphibolite facies metamorphism. Mineral separates were dated at 197-183 Ma ($^{40}Ar/^{39}Ar$ muscovite) in the Bikou terrane (Yan et al., 2008a, 2011), and 166-159 Ma ($^{40}Ar/^{39}Ar$ amphibole) and 168-158 Ma (SHRIMP U-Th-Pb monazite and tiantite), 177 Ma (SHRIMP zircon) for the Danba complex (Huang et al., 2003a, 2003b; Zhou et al., 2008), indicating progressive SW-ward development of the extensional tectonics.

The $Mz_t^2$ faults, which are represented by high-angle normal faults controlling the Early Jurassic half-graben basins, most likely represent a high-angle normal fault system formed at shallower structural levels (Yan et al., 2011) (Figs. 6 and 11). At this time, 211-205 Ma A-type granitic plutons intruded the northwestern Songpan-Ganze terrane (Zhang et al., 2006, 2007; Yuan et al., 2010; De Sigoyer et al., 2014). The association of normal faults and A-type granites suggests development of an extensional Songpan-Ganze turbidite basin, with regional timing constraints suggesting initiation in the northwest, progressing to the southeast (Douce and Alberto, 1997; Zhang et al., 2008; Yan et al., 2011).

Therefore, the domal complexes with ductile-brittle deformation, metamorphism, A-type granites and the Early Jurassic grabens within the hinterland belt of the LSTC might have resulted from SE-directed extensional tectonics during the late Late Triassic to the Early Jurassic, in a manner similar to that of North American Cordilleran metamorphic core complexes (c.f. Lister and Davis, 1989). The $Mz_t^2$ extensional tectonics are consistent with the collision between the Yidun arc and Songpan-Ganze terrane along the Ganze-Litang suture in a slab rollback setting (Yan et al., 2011; Yang et al., 2012).

## 8 The Cenozoic orogenic plateau superimposing ($Kz_t$)

The Cenozoic to recent LSTC overprinted the earlier $Mz_t^1$ and $Mz_t^2$ deformations and formed at the margin of a vast orogenic plateau, forming a foreland fold-thrust belt (Fig. 12). The Cenozoic tectonics of the LSTC has been widely investigated, and a number of tectonic models have been proposed (Burchfiel et al., 1995; Bai et al., 2010; Yan et al., 2011; Wang E.Q., 2012; Sun M. et al., in preparation). Three tectonic events have been recognized: (1) imbricate thrusting with SE-ward migration ($Kz_t^1$), (2) formation of the Xianshuihe sinistral strike-slip fault ($Kz_t^2$) and, (3) plateau uplift ($Kz_t^3$) (Arne et al., 1997; Richardson et al., 2008; Tan et al., 2010; Yan et al., 2011; Wang, D. et al., 2012; Cook et al., 2013; Tian et al., 2013; Wang et al., 2016; Sun et al., in preparation).

**8.1 $Kz_t^1$ imbricate thrusting**

The $Kz_t^1$ is represented by thrust motion along the Maowen and Beichuan-Yingxiu faults in the Longmenshan thrust belt, and the Muli and Yanyuan thrust faults in the Yanyuan-Muli thrust belt (Fig. 2). As described above, these faults dip to the northwest or north with dip angles of 40°-60°, and have top-to-the-SE or SSE motion (Fig. 13b) (SBGMR, 1991; Xu et al., 1992; Worley and Wilson, 1996; Yan et al., 1997, 2011; Sun et al., in preparation). Although there are extensive geochronologic constraints for the $Kz_t^1$ in the LSTC, as a whole, the age of the $Kz_t^1$ was roughly dated at 55-15 Ma with the initiation of activity of the Yanyuan-Muli thrust belt at ~55 Ma followed by ~50 Ma activity of the Longmenshan thrust belt using A/ZFT (apatite/zircon fission track), (U-Th)/He and $^{40}Ar/^{39}Ar$ methods (Richardson et al., 2008; Yan et al., 2011; Wang E.Q. et al., 2012; Sun et al., in preparation).

In the Longmenshan thrust belt, initial uplift and denudation of the Pengguan-Xuelongbao domal complex was inferred to be middle Tertiary (51-31 Ma), or perhaps the Cretaceous (70 Ma), based on zircon/apatite (U-Th)/He and biotite $^{40}Ar/^{39}Ar$ thermochronology (Arne et al., 1997; Kirby et al., 2002; Yan et al., 2011; Wang et al., 2012). The well preserved Paleocene to Eocene Minshan Formation ($E_{1-2}m$) and the

Eocene Lushan Formation ($E_2l$) in the foreland basin (i.e., the western Sichuan foreland basin), composed of coarse-grained clastic rocks, suggests activity of the southern LSTC at 55-35 Ma (Figs. 2E, 2G and 12A).

The previously mentioned imbricate thrust assemblages are composed of the Maowen fault and Beichuan-Yingxiu fault in the Longmenshan thrust belt and the Moli fault and Yanyuan fault in the Yanyuan-Muli thrust belt (SBGMR, 1991; Xu et al., 1991; Yan et al., 2011). Although the timing of initial motion for each of the faults is not well constrained, along-strike thrusting activity of SE-ward or SSE-ward in-sequence kinematics, from the Longmenshan thrust belt to the Yanyuan-Moli thrust belt, is evident from prior studies (Fig. 12A).

**8.2 $Kz_t^2$ strike-slip faults and northward extrusion**

$Kz_t^2$ is characterized by the formation of the NW-striking, sinistral-strike slip Xianshuihe fault, which cuts through and divides the LSTC into the Longmenshan thrust belt in the north and Yanyuan-Muli thrust belt in the south (Figs. 2 and 12B). This fault zone, which has mylonite and was intruded by the ~12 Ma Gongga Shan granitic plutons, was estimated to be active at ~15 Ma (Roger et al., 1995; Wang et al., 1998, 2014; Li et al., 2015a; Zhang et al., 2017). At about the same time, the Maowen and Beichuan-Yingxiu faults initiated dextral-strike slip motion, perhaps as a conjugate to the Xianshuihe fault (Enkelmann et al., 2006; Lei, 2012; Zhang et al., 2017; Sun et al., 2018b) (Fig. 12B). The conjugate strike-slip faults reveal an eastward maximum principal compressive stress, which resulted in northward extrusion of the north Songpan-Ganze terrane and southward extrusion of the south Songpan-Ganze terrane, respectively (Fig. 12B). The north and south extrusion, which are dominated by the eastward maximum principal compressive stress, are consistent with the crustal ductile channel flow (Enkelmann et al., 2006; Burchfiel et al., 2008; Bai et al., 2010; Wang et al., 2012).

**8.3 $Kz_t^3$ plateau uplift**

The $Kz_t^3$ is characterized by rapid uplift of the LSTC and formation of the foreland thrust system (Fig. 12C). A number of thermochrological results, including apatite fission track (AFT) and (U-Th)/He, reveal rapid cooling of the LSTC, Songpan-Ganze terrane and southwestern Qinling since ~5 Ma (Kirby et al., 2002; Reid et al., 2005; Enkelmann et al., 2006; Godard et al., 2009; Yan et al., 2011; Lei, 2012; Wang et al., 2012; Li et al., 2017; Sun et al., 2018a, under preparing). More than 3000 m uplift of the plateau were estimated based on AFT results and studies of the paleo- planation surface (Sun et al., in preparation). Additionally, the 2008 Wechuan 8.0 Ms and 2013 Lushan 7.0 Ms earthquakes are the results of the $Kz_t^3$ activities of the LSTC (Fig. 12C).

The foreland thrust system is composed of the frontal Guanxian-Anxian fault, several blind thrust faults, and the Longquanshan foreland uplift bounding the western Sichuan basin. (Figs. 2 and 12C). Coevally with uplift of the LSTC, the western Sichuan basin was uplifted and denudated ~4 Km based on AFT results (Richardson et al., 2008). Coupling with coeval uplift of the LSTC, formed the Pliocene lake (i.e., $N_2x$ Xigeda Formation) and deposited the Quaternary in the southwestern Sichuan foreland basin (Zhang Y.X., 2013; Wang et al., 2016; Sun et al., 2018a, in preparation (Fig. 12C).

Therefore, the present LSTC, i.e., generally called Longmenshan belt, was built by collisional orogenic affinity in-sequence imbricate thrust ($Kz_t^1$), northward extrusion ($Kz_t^2$) and internal uplift of the plateau ($Kz_t^3$). Combined with the $Kz_t^1$, $Kz_t^2$ and $Kz_t^3$, a nature of the orogenic plateau for the LSTC and Songpan-Ganze terrane could be defined (Rey et al., 2001, 2012; Vanderhaeghe, 2012).

## 9. Discussion

Although currently represented by a thrust belt along the sharp topographic gradient marking the eastern margin of the Tibetan Plateau, the Longmenshan records a protracted geologic history including Archean basement relicts ($Ar_t$), the Columbia/Nuna supercontinent ($Pt_{1t}$), Rodinia supercontinent ($Pt_{3t}$), the Paleozoic passive continent ($Pz_t$), the Mesozoic orogenic cycle ($Mz_t$) (contraction followed by extension) and the development of the Cenozoic orogenic plateau ($Kz_t$) define a complicated tectonic history of the LSTC. In the past decades, studies focus on distinguishing and accurate constraining these tectonic relics and events, which enable us to answer and respond to the five questions mentioned in the introduction, i.e., tectonic episodes, metamorphic basement, nature of the present LSTC and its affiliation with adjacent tectonic units, geological relationship between the NE-striking Longmenshan thrust belt in the north and arcuate Yanyuan-Muli thrust belt in the south, and coupling of the mountain and basin. Based on the understanding of the present tectonic framework, we discuss the tectonic episodes and their natures, and then summarize the orogenic cycles to build the present LSTC.

### 9.1 Archean basement and Columbia/Nuna supercontinental cycle

The Yudongzi gneiss group in the Bikou terrane were formed during the Archean with igneous zircon U-Pb ages of 2600-2693 Ma (Fig. 7) (Zhang et al., 2001; Zhao and Cawood, 2012; Zhou et al., 2018, in preparing). The Archean Yudongzi gneiss group has a metamorphic grade of upper amphibolite facies and is composed of TTGs with banded iron formation (BIF) and leucogranite (Zhang et al., 2001; Zhou et al., 2018). Both the age results and rock composition, which are similar to the Kongling complex in the northeast Yangtze Block (Zhang et al., 2001; Zhao and Cawood, 2012), reveal close affinity between the Bikou terrane and the Kongling complex. The rare exposures of the Yudongzi gneiss group might be a part of the enigmatic Archean crystalline basement core of the Yangtze block, and probably represents the early stages of formation of the South China craton (Ren et al., 1986a, 1986b, 2016). Thus, relics of the Archean rocks within the LSTC indicate the cratonic nature for the crystalline basement.

The Hejiayan group is exposed adjacent to the Yudongzi gneiss group and has an age of ca.1933 Ma for protolith (GRT-SBGMR, 1996; Zhang et al., 2001). These rocks are the only Paleoproterozoic metamorphic rocks identified within the LSTC and thus contain the unique record for Paleoproterozoic events ($Pt_{1t}$) (Fig. 8). The Hejiayan group includes greenschist facies rocks with protolith assemblages of island-arc basalt and ultrabasic intrusions, implying a possible Paleoproterozoic ophiolite melange (GRT-SBGMR, 1996). Although additional structural and petrological studies are needed to clarify the history of these rocks, they probably represent ophiolite melange that is coeval with the Nuna/Columbia supercontinent assembly and the associated orogenic belt ($Pt_{1t}$) in the southwestern Yangtze block (GRT-SBGMR, 1996; Dong et al., 2015; Zhou et al., 2018) (Fig. 7).

The recognition of relict Archean crystalline basement ($Ar_t$) and the Paleoproterozoic Nuna supercontinent basement ($Pt_{1t}$), not only confirm the cratonic nature of the LSTC and the Yangtze block (SBGMR, 1991; GRT-SBGMR, 1996; Zhao and Cawood, 2012), but also build a tight spatial and temporal link between the Yangtze block and Nuna supercontinent (Wang et al., 2016). Formation of the metamorphic basement dated at ca.1933 Ma represents the initial accretion of the Archean Yangtze block to the Rae craton along the LSTC during the Nuna orogeny (2320-1800 Ma) (Zhao et al., 2002; Evans and Mitchell, 2011; Zhang et al., 2012; Pisarevsky et al., 2014; Wang et al., 2016). Therefore, we suggest that the LSTC developed at the margin of the Archean Yangtze craton, which was sutured and aggregated to the Nuna supercontinent by the Paleoproterozoic orogeny (Zhao et al., 2002; Evans and Mitchell, 2011; Zhang et al., 2012; Pisarevsky et al., 2014; Wang et al., 2016) (Fig. 8).

**9.2 Rodinia supercontinental cycle**

The well exposed Neoproterozoic igneous, sedimentary and metamorphic rocks in the LSTC and Yangtze block have been widely reported. These rocks in the LSTC are mainly exposed in the core of the domal complexes, including the Bikou group in the Bikou terrane, the Jiaoziding complex, the Huangshuihe group in the Pengguan-Xuelongbao, the Baoxin and Danba complex, and the Qiasi group in the Jianglang (Taka), Changqiang and Qiasi domal complexes (Figs. 2 and 4), which show structural and petrological similarity to the Kangding complex in the western Yangtze block (Fig. 3) (Yan et al., 2002, 2008b; Zhou et al., 2002a, 2002b, 2006a, 2006b; Druschke et al., 2006; Xiao et al., 2007; Sun et al., 2008a, 2008b, 2009; Pei et al., 2009; Zhao et al., 2011, 2017).

The ophiolitic complex is represented by the Shimian ophiolite and tens of small-scale bodies of hornblende gabbro, olivine gabbro and serpentinized peridotite within the metamorphic complexes. The ophiolitic complex was dated at ~800 Ma, which is interpreted as relict oceanic slabs along a possible trench by the eastward subduction of the Neoproterozoic Mozambique ocean (Zhou et al., 2002a; Zhao et al., 2017) (Fig. 9A-C).

The Neoproterozoic intrusions, exposed mainly within the domal complexes, include adakites, mafic and granitic plutons. Adakites dated at 748-830 Ma were proposed to be a product of wet-slab melting of the subducted plate (Zhou et al., 2006b; Huang et al., 2009; Zhao and Zhou, 2007a) (Fig. 9A). The 738-812 Ma mafic intrusions and granitic plutons have geochemical and isotopic compositions of depleted lithospheric mantle and were proposed to derive from partial melting of mantle that was metasomatized by subduction-derived fluids or melts (Zhou et al., 2006b; Zhao et al., 2007a; Zhao and Zhou, 2007a; Zhu et al., 2008; Meng et al., 2015) (Fig. 9B). The 848-764 Ma granites, including tonalite, granodiorite and monzogranite, have geochemical and isotopic compositions consistent with a juvenile crustal source, derived from partial melting of amphibolities or metagreywacks in the lower crust (Zhou et al., 2002a, 2002b; Yan et al., 2008b; Liu S.W. et al., 2009b; Pei et al., 2009; Munteanu et al., 2010; Meng et al., 2015) (Fig. 9C). Therefore, the adakites, mafic and granitic intrusions of the LSTC and the western margin of the Yangtze block consistently indicate a magmatic arc, which is interpreted to be genetically connected with the eastward subduction of the Neoproterozoic Mozambique ocean (Fig. 9A-D).

The 850-700 Ma volcaniclastic turbidite sequence of the Hengdan group in the Bikou terrane was interpreted as a forearc basin, with provenance from the Bikou group volcanic rocks to the south (Druschke et al., 2006). Correspondently, the ~870 Ma Yanbian group flysch sequence in the south Kangding complex, which has characteristics of submarine fan deposits, is interlayered with arc-related lavas (Sun et al., 2007, 2008a, 2008b, 2009). Petrological, geochemical and isotopic results consistently point to a back-arc basin setting for the Yanbian group (Sun et al., 2007, 2008a, 2008b, 2009). Thus, a convergent margin, volcanic arc system has been proposed along the western margin of the Yangtze block.

The polarity of the Neoproterozoic trench-arc-basin system and geometry of the subsequent collisional orogenic belt have been reconstructed based on integration of previous studies of the ophiolitic complexes, adakitic rocks, mafic rocks, granitic intrusions and back-arc and fore-arc deposits along the LSTC and western margin of the Yangtze block (Fig. 9A-C) (Yan et al., 2002, 2008b; Zhou et al., 2002a, 2006a, 2006b; Druschke et al., 2006; Xiao et al., 2007; Sun et al., 2008, 2009; Pei et al., 2009; Zhao et al., 2011, 2017). This trench-arc-basin system has geochemical, isotopic and geochronological similarities to the northeastern Madagascar, Seychelles island and Malani in India (Tucker et al., 2001), and probably represented an Andean-type margin on the edge of the Rodinia supercontinent. We therefore correlate the western margin of the Yangtze block with the northeastern margin of the Indian Plate, both being an active arc above an eastward dipping subduction zone (Zhou et al., 2002a) (Fig. 9E).

However, a number of scientific problems, which concern the reconstruction of the Rodinia supercontinent along the LSTC, are not yet solved. For example, is there a record of inception of 725-750 Ma rifting, which corresponds to the formation of Nanhua basin within the Yangtze block, within the LSTC? Does the eastward subduction of the Mozambique ocean match with a westward subduction along the east side of the Yangtze block (Zhou et al., 2002a; Li XH et al., 2009) (Fig. 9D)? Except for an accretionary orogenic process suggested by the subduction-related trench-arc-basin system, possible collisional orogeny, orogenic plateau and post-orogeny are not yet distinguished.

### 9.3 East Paleo-Tethys Wilson cycle

Based on the Paleozoic passive continental margin of the Yangtze block, the continent breakup initiated along the northern margin of the Yangtze block represented by the ~440 Ma continental rifting, which was then transferred into the Paleozoic Mianlue ocean between the North China (North Qinling-Dabie orogenic belt, Fig. 2) and South China blocks (Li et al., 1996; Lai et al., 1998; Xu et al., 2000a, 2000b; Zhang et al., 2004; Dong et al., 2011, 2015) (Fig. 11). Although this breakup signifies the initiation of the Paleo-Tethys cycle, the LSTC marks the boundary of the Yangtze block to the western passive continental margin did not essentially change, until the formation of the possible late Permian three-armed rift system (Figs. 4D-E, 10).

The three-armed rift system proposed in this paper is based on the ELIP basalt-dominated rock assemblages and their spatial-temporal distribution. The LSTC exposes only the low-Ti type magmas, which regionally, are found only in the lower part of the basalt sequence, indicating the preservation of the initial eruptive materials and a NE-trending depositional trough or aulacogen. However, both the low-Ti basalt and the overlying high-Ti basalts, together with the coeval A-type granites, are distributed along the Kangding complex in the NS-striking Panzhihua rift (Fig. 10) (Xu et al., 2001; Shellnut and Zhou, 2007; Wang et al., 2016). Along the Ganze-Litang suture zone and its adjacent Yidun arc and Songpan-Ganze terrane, the late Permian continental basalts, together with the early Triassic oceanic affinity calc-alkaline volcanic rocks and intrusions, reconstruct a tectonic process from the late Permian continental rift to the early Triassic Ganze-Litang ocean (SBGMR, 1991; Song et al., 2004; Yang et al., 2012, 2014; Cao et al., 2015; Wang et al., 2013a, 2003b) (Figs. 5 and 10). Therefore, this three-armed rift system is composed of an aulacogen along the LSTC, a NS-trending continental rift along the

Kangding complex (Fig. 1), and an oceanic rift along the Ganze-Litang and Yidun arc. The identification of the mantle plume centre (He et al., 2003a, 2003b, 2006, 2009, 2010) and associated radial mafic dyke swarms (Li et al., 2015) of the ELIP could further refine the configuration of this three-armed rift system, although the original pattern during the late Permian to the early Triassic was not been constructed.

Subduction and closure of the Mianlue and Ganze-Litang oceans occurred almost simultaneously in the middle to late Triassic (Zhang et al., 2004; *Yan et al*., 2008b, 2011; Dong et al., 2011, 2016) (Figs. 4, 5 and 11). Although widely overprinted by the subsequently deformation, the $Mz_t^1$ within the LSTC and Songpan-Ganze terrane is well preserved with representative NW-SE or WNW-ESE striking recumbent folds and thrust faults, greenschist metamorphism and adakitic granites (Burchfiel et al., 1995; Chen et al., 1995; Worley and Wilson, 1996; Arne et al., 1997; Bruguier et al., 1997; Zhang et al., 2004; Harrowfield and Wilson, 2005; Weislogel et al., 2006; Wilson et al., 2006; Enkelmann et al., 2007; Roger et al., 2008; Yan et al., 2008b, 2011; Billerot et al., 2017). The $Mz_t^1$ fault-fold system, together with kinematic markers including mineral lineation on spaced axial planar cleavage, S-C fabrics and “σ”-type pressure shadows within local ductile shear zones, reveals top-to-the-SW thrusting with dextral strike-slip faulting (Worley and Wilson, 1996; Jia et al., 2006). Structural assemblage and kinematics of $Mz_t^1$ within the LSTC have affinity with the kinematics during northward subduction of the Mianlue oceanic plate beneath North China block, and subsequenct collision, to produce top-to-the-south thrusting (Liu et al., 2005; Yan et al., 2011) (Fig. 11). However, the $Mz_t^1$ of the LSTC may have not been significantly affected by the closure of the Ganze-Litang ocean, which has been proposed to have subducted southwestward underneath, and to have collided with, the Yidun arc (Cao et al., 2015). This implies that the Ganze-Litang ocean probably had an original WNW orientation during the middle to late Triassic (Pullen et al., 2008).

The $Mz_t^2$, which is represented by the structural assemblage of faults, recumbent folds, variable scale of ductile shear zones with penetrative foliations, stretching lineations, sheath folds, and S-C fabrics, have been recognized along the flanks of the domal complexes within the hinterland belt (Burchfiel et al., 1995; Worley and Wilson, 1996; Yan et al., 2011; Billerot et al., 2017). This deformation, which was firstly identified as faults accomplishing the omission of stratigraphy and interpreted as normal faults by Burchfiel et al. (1995), has been further described by a number of subsequent studies. The evidence includes variable thinning or omission of the stratigraphic sequence around the domal complex, ductile shear zones within the dome cores with top-to-SE or ESE kinematics, and middle to upper greenschist facies retrograde metamorphism (Zhou et al., 2002b, 2008a; Huang et al., 2003a; Yan et al., 2003a, 2008a, 2008b, 2011; Liu et al., 2008), locally preserved early Jurassic half-graben basins bound by high-angle normal fault system (Yan et al., 2011) (Figs. 2, 6 and 11), and coeval 211-205 Ma A-type granitic plutons in the western Songpan-Ganze terrane (Zhang et al., 2007; Yuan et al., 2010). We propose a history of progressive extensional tectonics, produced by roll-back subduction of the Songpan-Ganze terrane underneath the Qiangtang terrane after collision along the Ganze-Litang suture (Pullen et al., 2008; Yan et al., 2011; Yang et al., 2012). Therefore, the Paleozoic to the Mesozoic LSTC in the east Paleo-Tethys experienced plume-related continental rifting ($Pz_t^1$) in which one arm developed into an ocean ridge, producing the Ganze-Litang ocean basin ($Pz_t^2$), which was then closed by northward and southwestward subduction underneath the North China block and the Qiangtang block ($Mz_t^1$), respectively. The evolution from continental rifting, to subduction, and finally to plate collision record a complete Wilson cycle (Wilson, 1966). However, this variant of the Wilson cycle involves closure of the Mianlue and Ganze-Litang oceans by subduction in opposite directions along trenches to the north and south of the LSTC. The bidirectional subduction of the Songpan-Ganze lithosphere requires there to be a tear fault along the LSTC (De Sigoyer et al., 2014). Thus, the Paleozoic to Mesozoic LSTC has a key record for reconstructing a “bidirectional” Wilson cycle in the eastern Paleo-tethys.

### 9.4 The Cenozoic orogenic plateau superimposing ($Kz_t$)

The present LSTC, that is, what is generally called the Longmenshan belt in most literature, was finally built during the collision of the Indian and Eurasian continents by the Cenozoic superimposition of the Tibetan plateau and the Sichuan basin (Fig. 13). Much research effort has focused on the Cenozoic tectonics, including both regional and more local, detailed investigations, leading to a number of proposed models (c.f., Burchfiel et al., 1995; Bai et al., 2010; Wang E.Q., 2012; Yan et al., 2011; Sun M. et al., 2018, in preparation). Three tectonic episodes are generally recognized: imbricate thrusting with a SE-ward thrust migration ($Kz_t^1$), formation of the Xianshuihe sinistral strike-slip fault and conjugate dextral strike-slip faults of the LSTC ($Kz_t^2$), and internal plateau uplift associated with continued thrusting in the LSTC ($Kz_t^3$) (Arne et al., 1997; Richardson et al., 2008; Yan et al., 2011; Wang et al., 2012; Cook et al., 2013; Tian et al., 2013; Sun M. et al., 2018, in preparation).

The $Kz_t^1$ imbricate thrusts consist of both tectonically reactivated, northwest-dipping $Mz_t^1$ and $Mz_t^2$ thrust faults as well as foreward propagation of new thrusts in the foreland

(SBGMR, 1991; Xu et al., 1992; Worley and Wilson, 1996; Yan et al., 1997, 2011; Sun et al., 2018). This thrusting is roughly constrained between 55-15 Ma, while the initial ages were a little older in the Yanyuan-Muli thrust belt than that in the Longmenshan thrust belt, based on low-temperature thermochronology studies (Richardson et al., 2008; Yan et al., 2011; Wang E.Q. et al., 2012; Sun et al., 2017; Li et al., 2018). The initial age results are consistent with the constraints provided by development and infilling of a foreland basin by the Paleocene to Eocene Minshan Formation ($E_{1-2}m$) and the Eocene Lushan Formation ($E_2l$) in the southern segment (Figs. 2E, 2G and 12A). The sequence of activity on thrust faults, including the Maowen fault and Beichuan-Yingxiu fault, as well as the Muli fault and Yanyuan fault, together with the geometry of the fault and fold system, indicates SE-ward or SSE-ward, in-sequence kinematics, which is a far field response to India-Euroasian plate collision as suggested by previous studies (Burchfiel et al., 2008; Hubbard and Shaw, 2009; Jia et al., 2010; Jin et al., 2010; Xu et al., 2016) (Fig. 12A).

$Kz_t^2$ is characterized by the formation of the Xianshuihe sinistral strike-slip fault, and the conjugate dextral strike-slip of the LSTC. The two conjugate strike-slip faults, which were accurately dated at 15-10 Ma, resulted in the NNE-ward extrusion of the north Songpan-Ganze terrane and southward extrusion of the south Songpan-Ganze terrane (Roger et al., 1995; Wang et al., 1998, 2014; Enkelmann et al., 2006; Lei., 2012; Li et al., 2015; Zhang et al., 2017; Zhang et al., 2017; Sun et al., 2018) (Figs. 2 and 12B). Simutaneous granitic intrusion along the Xianshuihe fault, together with geophysical investigations, suggests that the initiation and movement of low viscosity crust, in the geometry of channel flow was probably produced by an eastward maximum principal compressive stress and crustal thickening (Enkelmann et al., 2006; Burchfiel et al., 2008; Bai et al., 2010; Wang et al., 2012) (Fig. 12B).

The internal uplift of the plateau $Kz_t^3$, although was recently proposed initiating since the Oligocene (Hoke, 2018; Linnemann et al., 2018), has been constrained between 5-0 Ma by FT and (U-Th)/He dating. This event is characterized by forward thrusting (Kirby et al., 2002; Reid et al., 2005; Godard et al., 2009; Yan et al., 2011, 2016; Lei, 2012; Wang et al., 2012). This tectonic eposide was believed to have resulted in more than 3000 m of plateau uplift and the corresponding Pliocene to Quaternary deposits (c.f., $N_2x$ Xigeda formation), as well as the occurrance of 2008 Wechuan 8.0 Ms, 2013 Lushan 7.0 Ms, and recently 2017 Jiuzhaigou 7.0 Ms earthquakes (Sun et al., 2018, in preparation) (Fig. 12C).

The Cenozoic development of the present LSTC, i.e., the so called Longmenshan belt, includes in-sequence imbricate thrusting ($Kz_t^1$), northward extrusion ($Kz_t^2$). Given the active faulting associated with dextral oblique shortening, this suggests that the Longmenshan itself is still undergoing crust thickening, and whether in response to shortening or lower crustal flow, the plateau itself may have now reached a critical elevation wherein the crustal cannot support any additional elevation, so that uplift is compensated for by collapse processes ($Kz_t^3$), implying a nature of the orogenic plateau (Rey et al., 2010; Vanderhaeghe, 2012). This orogenic plateau, which was previously revealed by paleomagnetic results (Chen et al., 1995; Otofuji et al., 1998; Yoshioka et al., 2003), geodetic studies (Zhang et al., 2008) and field geologic observations (Tapponnier et al., 2001), is consistent with the Cenozoic continuous and staged thickening of the eastern Tibetan Plateau and SE-ward expansion (Royden et al., 1997; Clark and Royden, 2000; Tapponnier et al., 2001; Zhang et al., 2004b; Bai et al., 2010; Wang et al., 2012, 2014), but other than the suggestion of expansion to the WNW, north of the Sichuan Basin (Enkelmann et al., 2006). Geodynamics of the southeastward expansion of the LSTC and its adjacent regions was suggested to be responsible by the continued middle to lower crustal channel flow (Burchfiel et al., 2008; Yan et al., 2009).

## 3. Conclusions

In this overview, we integrate previous studies with our recent results for the Longmenshan tectonic complex (LSTC), along the eastern margin of Tibetan plateau, and draw the following conclusions:

1. The LSTC preserves the Archean Yudongzi gneiss group, which has a genetic affinity with the Kongling group in the northern Yangtze block, and may represent part of its Archean nucleus.

2. The Paleoproterozoic Hejiayan group, which crops out adjacent to the Archean Yudongzi group, may be part of an 2000-1800 Ma orogenic belt developed during accretion to the Nuna/Columbia supercontinent.

3. The combination of Neoproterozoic tectonostratigraphic elements, including an ophiolite complex, arc-type magmatic rock assemblages and volcaniclastic, probable forearc basin deposits, suggest the presence of a Neoproterozoic trench-arc-basin system along the western margin of the Yangtze block within the LSTC. This trench-arc-basin system represents the eastward-subduction of the Neoproterozoic Mozambique ocean underneath the Yangtze block during the formation of the Rodinia supercontinent, although the Nodinian orogenic belt has not been yet distinguished.

4. A complete "bidirectional" Wilson cycle is recorded in the formation of the late Permian to the middle-late Triassic back-arc Ganze-Litang rift and ocean following the early Paleozoic Mianlue continental rift and ocean, and near simultaneous bidirectional northward and southwestward subductions and collisions. This uncommon bidirectional Wilson cycle might be attributed to the formation of the late Permian ELIP three-armed rift system in the LSTC of the eastern Paleo-Tethys.

5. We summarized three tectonic stages for the formation of present LSTC. Collisional processes along the India-Eurasian boundary lead to far field orogeny in which in-sequence imbricate thrusting at 55-15 Ma, in which Triassic south- and southeast-vergent thrusts were reactivated and new frontal thrusts developed. Extrusion at 15-5 Ma is characterized by the formation of the sinistral strike-slip Xianshuihe fault, and the initial motion of dextral strike-slip Beichuan-Yinxiu fault, and northward extrusion of the north Songpan-Ganze terrane and southward extrusion of the south Songpan-Ganze terrane. The intrusion of the 15-10 Ma Gongga granitic pluton suggests an initial crustal ductile channel flow along the Xianshuihe fault. The plateau uplift and continued shortening along the LSTC has occurred since ~5 Ma.

**Acknowledgments**

This study was supported by research grants from the NSFC (Projects 41672216, 41372212) and National Basic Research Program of China (2014CB440903). We thank Profs. Gao Jianfeng, Zhao Junhong, Wang Wei and Dr. Cao Wentao for assistance on an earlier draft and constructive comments. Graduate students, Haiying Zhang, Men Ning, Zhemin Li and Shuhang Gu, are gratefully acknowledged for assistance in the field.

## References


Ali, J. R., Lo, C.H., Thompson, G.M., Song, X.Y., 2004. Emeishan basalt Ar–Ar overprint ages define several tectonic events that affected the western Yangtze platform in the Mesozoic and Cenozoic. Journal of Asian Earth Sciences 23, 163-178.

Andersen, T.B., 1998. Extensional tectonics in the Caledonides of southern Norway, an overview. Tectonophysics 285, 333-351.

Armstrong, R. L. 1982. Cordillera metamorphic core complex from Arizona to southern Canada. Annual Review of Earth Planetary Sciences 10, 129-154.

Arne, D., Worley, B., Wilson, C., Chen, S.F., Foster, D., Zhi, L.L., Shu, G.L., Dirks, P., 1997. Differential exhumation in response to episodic thrusting along the eastern margin of the Tibetan Plateau. Tectonophysics 280, 239-256.

Bai, D.H., Unsworth, M.J., Meju, M.A., Ma, X.B., Teng, J.W., Kong, X.G., Sun, Y., Sun, J., Wang, L.F., Jiang, C.S., Zhao, C.P., Xiao, P.F., Liu, M., 2010. Crustal deformation of the eastern Tibetan plateau revealed by magnetotelluric imaging. Nature Geoscience 3, 358-362.

Billerot, A., Duchene, S., Vanderhaeghe, O., Sigoyer, J. D., 2017. Gneiss domes of the Danba metamorphic complex, Songpan Ganze, eastern Tibet. Journal of Asian Earth Sciences. Journal of Asian Earth Sciences 140, 48-74.

Bruguier, O., J. R. Lancelot., J. Malavieille., 1997. U-Pb dating on single detrital zircon granites from the Triassic Songpan-Ganze flysch (Central China); provenance and tectonic correlations, Earth Planet. Sci. Lett. 152, 217–231.

Burchfiel, B. C., Clark, B., Chen, Z. L., 2012. Tectonics of the southeastern Tibetan Plateau and its adjacent foreland. Geological Society of America, 210.

Burchfiel B. C., Royden L. H., van der Hilst R. D., Hager B. H., Chen Z., King R. W., 2008. A geological and geophysical context for the Wenchuan earthquake of 12 May 2008, Sichuan, People's Republic of China. Gsa. Today 18, 4-11.

Burchfiel, B. C., P. Molnar., Z. Zhao., K. Liang., S. Wang., J. F. Huang., and J. F. Sutter., 1989. Geology of the Ulugh Muztagh area, northern Tibet, Earth Planet. Sci. Lett. 94, 、57-70.

Burchfiel, B.C., Chen, Z., Liu, Y., Royden, L.H., 1995. Tectonic of the Longmenshan and adjacent regions. International Geology Review 37, 661–735.

Cao, W., Yan, D. P., Qiu, L., Zhang, Y., Qiu, J., 2015. Structural style and metamorphic conditions of the Jinshajiang metamorphic belt: Nature of the Paleo-Jinshajiang orogenic belt in the eastern Tibetan Plateau. Journal of Asian Earth Sciences 113, 748-765.

Chang, C., 1997. Geology and Tectonics of Qinghai-Xizang Plateau. Science Press, Beijing.

Chang, E. Z., 2000. Geology and tectonics of the Songpan-Ganze fold belt, Southwestern China. Intern. Geol. Rev. 42, 813-831.

Chen, B., Wang, K., Liu, W., Cai, Z., Zhang, Q., Peng, X., Qiu, Y., Zheng, Y., 1987. Geotectonics of the Nujiang-Lancangjiang-Jinshajiang region. Geological Publishing House, Beijing (in Chinese with English abstract).

Chen, S. F., C. J. L. Wilson., B. A. Worley., 1995. Tectonic transition from the Songpan-Ganze fold belt to the Sichuan basin, south-western China, Basin Res. 7, 235-253.

Chen, S.F., and C. J. L. Wilson., 1996. Emplacement of the Longmenshan Thrust-Nappe belt along the eastern margin of the Tibetan Plateau, J. Struct. Geol. 18, 413-430.

Clark, M.K., Royden,L.H., 2000. Topographic ooze: Building the eastern margin of Tibet by lower crustal flow. Geology 28, 703–706.

Cook, K.L., Royden, L.H., Burchfiel, B.C., Lee, Y.H., Tan, X., 2013. Constraints on Cenozoic tectonics in the southwestern Longmenshan from low-temperature thermochronology. Lithosphere 5, 393-406.

Coney, P.J., 1970. The geotectonic cycle and the new global tectonics. Geological Society of America Bulletin 81, 739–748.

Coney, P.J., 1972. Cordilleran tectonics and North American plate motions. American Journal of Science 272, 462–465.

Coney, P.J., 1980. Cordilleran metamorphic core complexes: an overview. In: Crittenden, M.D., Coney, P.J., Davis, G.H. (Eds.), Cordilleran Metamorphic Core Complexes. Geological Society of America pp. 7-34.

De Michele, M., Raucoules, D., Lasserre, C., Pathier, E., Klinger, Y., Van der Woerd, J., de Sigoyer, J., Xu, X., 2010. The Mw 7.9, 12 May 2008 Sichuan earthquake rupture measured by sub-pixel correlation of ALOS PALSAR amplitude images. Earth Planets Space 62, 875–879.

De Sigoyer J., Vanderhaeghe O., Duchêne S., Billerot A., 2014. Generation and emplacement of Triassic granitoids within the Songpan Ganze accretionary-orogenic wedge in a context of slab retreat accommodated by tear faulting, Eastern Tibetan plateau, China. Journal of Asian Sciences 88, 192-216.

Deng, Y., Chen, Y., Wang, P., Essa, K. S., Xu, T., Liang, X., 2016. Magmatic underplating beneath the Emeishan large igneous province (South China) revealed by the COMGRA-ELIP experiment. Tectonophysics 672-673, 16-23.

Dewey, J. F., Shackleton, R.M., Chang, C.F., Sun, Y.Y., 1988. The tectonic evolution of the Tibetan Plateau, Philos. Trans. R. Soc. London, Ser. A. 327, 379-413.

Dewey, J.F., 1988. Extensional collapse of orogens. Tectonics 7, 1123–1139.

Dilek, Y., Furnes, H., Shallo, M., 2008. Geochemistry of the Jurassic Mirdita Ophiolite (Albania) and the MORB to SSZ evolution of a marginal basin oceanic crust. Lithos 100, 174–209.

Dirks, P.H.G.M., Wilson C.J.L., Chen S.F., Luo Z.L., Liu S.G., 1994. Tectonic evolution of the NE margin of Qinghai-Tibet Plateau: evidences from the central Longmen Montains, Sichuan province, China. Journal of eastern Earth sciences 9, 181-192.

Dong, Y.P., Liu, X.M., Li, W., Yang, Z., Sun, S.S., Cheng, B., Zhang, F.F., Zhang, X.N., He, D.F., Zhang, G.W., 2015. Mesozoic intracontinental orogeny in the Qinling Mountains, central China. Gondwana Research 30, 144-158.

Dong, Y.P., Liu, X.M., Neubauer, F., Zhang, G.W., Tao, N., Zhang, Y.G., Zhang, X.N., Li, W., 2013. Timing of Paleozoic amalgamation between the North China and South China Blocks: evidence from detrital zircon U–Pb ages. Tectonophysics 586, 173–191.

Dong, Y.P., Zhang, G.W., Neubauer, F., Liu, X.M., Genser, J., Hauzenberger, C., 2011. Tectonic evolution of the Qinling orogen, China: review and synthesis. Journal of Asian Earth Sciences 41, 213–237.

Dong, Y.P., Zhang, G.W., Zhao, X., Yao, A.P., Liu, X.M., 2004. Geochemistry of the subduction-related magmatic rocks in the Dahong Mountains, northern Hubei Province: constraint on the existence and subduction of the eastern Mianlue oceanic basin. Science in China (Series D) 47, 366–377.

Dong, Y.P., Santosh, M., 2016. Tectonic architecture and multiple orogeny of the Qinling Orogenic Belt, Central China. Gondwana Research 29, 1-40.

Douce, P., Alberto, E., 1997. Generation of metaluminous A-type granites by low-pressure melting of calc-alkaline granitoids. Geology 25, 743.

Druschke, P., Hanson, A. D., Yan, Q., Wang, Z., Wang, T., 2006. Stratigraphic and U-Pb SHRIMP detrital zircon evidence for a Neoproterozoic continental arc, central China: Rodinia implications. Journal of Geology 114, 627-636.

Eglington, B.M., Pehrsson, S.J., Ansdell, K.M., Lescuyer, J.L., Quirt, D., Milesi, J.P., Brown, P., 2013. A domain-based digital summary of the evolution of the Palaeoproterozoic of North America and Greenland and associated unconformity-related uranium mineralization. Precambrian Research 232, 4–26.

Enkelmann, E., Ratschbacher, L., Jonckheere, R., Nestler, R., Fleischer, M., Gloaguen, R., 2006. Cenozoic exhumation and deformation of northeastern Tibet and the Qinling: Is Tibetan lower crustal flow diverging around the Sichuan Basin? Geological Society of America Bulletin 118, 651-671.

Enkelmann, E., A. Weislogel., L. Ratschbacher., E. Eide., A. Renno., J. Wooden., 2007. How was the Triassic Songpan-Ganzi basin filled? A provenance study, Tectonics 26, 640-641.

Evans, D.A.D., Mitchell, R.N., 2011. Assembly and breakup of the core of Paleoproterozoic Mesoproterozoic supercontinent Nuna. Geology 39, 443–446.

Faure, M., Lin, W., Le Breton, N., 2001. Where is the North China–South China block boundary in eastern China. Geology 29, 119–122.

Feng, Q.L., Du, Y.S., Yin, H.F., Sheng, J.H., Xu, J.F., 1996. Carboniferous radiolaria fauna firstly discovered in Mian–Lue ophiolitic melange belt of south Qinling Mountains. Science in China (Series D) 39, 87–91.

GBGMR (Gansu Bureau of Geology and Mineral Resources)., 1989. Regional geology of Gansu Province: Beijing, China, 690 pp., Geol. Publ. House, Beijing (in Chinese with English abstract).

Godard, V., R. Pik., J. Lave´., R. Cattin., B. Tibari., J. de Sigoyer., M. Pubellier., J. Zhu., 2009. Late Cenozoic evolution of the central Longmenshan, eastern Tibet: Insight from (U-Th)/He thermochronometry. Tectonics 28, TC5009.

Harrowfield, M.J., Wilson, C.J.L., 2005, Indosinian deformation of the Songpan Garze Fold Belt, northeast Tibetan Plateau: Journal of Structural Geology 27, 101-117.

He, B., Xu, Y.G., Campbell, I., 2009. Comment on: 'Re- evaluating plume-induced uplift in the Emeishan large igneous province' by I.U. Ukstins Peate and S.E. Bryan: Nature Geoscience v. 2, p. 531–532.

HBGMR (Hubei Bureau of Geology and Mineral Resources)., 1990. Regional geology of Hubei province, Geol. Publ. House, Beijing, China. pp. 1-645(in Chinese with English abstract).

He, B., Xu, Y. G., Guan, J. P., Zhong, Y. T., 2010. Paleokarst on the top of the Maokou Formation: Further evidence for domal crustal uplift prior to the Emeishan flood volcanism. Lithos 119, 1-9.

He, B., Xu, Y. G., S.L, C., Xiao, L., Wang, Y., 2003a. Sedimentary evidence for a rapid, kilometer-scale crustal doming prior to the eruption of the Emeishan flood basalts. Earth Planetary Science Letters 213, 391-405.

He, B., Xu, Y., Xiao, L., Wang, K., Sha, S., 2003b. Generation and spatial distribution of the Emeishan large igneous province: New evidence from stratigraphic records. Acta Geologica Sinica.

He, B., Xu, Y., Wang, Y., Luo, Z., 2006. Sedimentation and lithofacies paleogeography in southwes- tern China before and after the Emeishan flood volcanism: New insights into surface response to mantle plume activity. Journal of Geology 114, 117-132.

Hoke, G.D., 2018. Geochronology transforms our view of how Tibet's southeast margin evolved. Geology 46, 95-96

Hou, Z., Wang, L., Zaw, K., Mo, X., Wang, M., Li, D., Pan, G., 2003. Post-collisional crustal extension setting and VHMS mineralization in the Jinshajiang orogenic belt, southwestern China. Ore Geology Reviews 22, 177–199.

Huang, M. H., I. S. Buick., L. W. Hou., 2003a. Tectonometamorphic evolution of the Eastern Tibet plateau: evidence from the central Songpan-Ganze orogenic belt, western China. Journal of Petrology 44, 255-278.

Huang, M.H., Maas, R., Buick, I. S., Williams, I., 2003b. Crustal response to continental collisions between the Tibet, Indian, South China and North China blocks: geochronological constraints from the Songpan-Garze Orogenic Belt, Western China. Journal of Metamorphic Geology 21, 223-240.

Huang, T. K., 1947. On the major tectonic forms of China. Journal of Geology 55.

Huang, X.L., Xu, Y.G., Lan, J.B., Yang, Q.J., Luo, Z.Y., 2009. Neoproterozoic adakitic rocks from Mopanshan in the western Yangtze Craton: partial melts of a thickened lower crust. Lithos 112, 367–381.

Huang, Z.K., Li, H.C., 2001. 1:500 000 digital geological map and geometadata. Geology in China 28, 43-47.

Hubbard, J. and J. H. Shaw., 2009. Uplift of the Longmenshan and Tibetan plateau, and the 2008 Wenchuan (M=7.9) earthquake. Nature 458, 194-197.

Lü, J., Yao, H., Kirby, E., 2008. A geological and geophysical context for the Wenchuan earthquake of 12 May 2008, Sichuan, People's Republic of China, GSA Today 18, 4-11.

Ji, X. Z., Yang, L. Q., Santosh, M., Li, N., Zhang, C., Zhang, Z. C., 2016. Detrital zircon geochronology of Devonian quartzite from tectonic melange in the MianlueSuture Zone, Central China: provenance and tectonic implications. International Geology Review 1-18.

Jia, D., G. Q. Wei, Z. X. Chen, B. L. Li, Q. Zen, and G. Yang., 2006. Longmenshan fold-thrust belt and its relation to the western Sichuan basin in central China: New insights from hydrocarbon exploration, AAPG Bull. 90, 1425-1447.

Jia, D., Y. Li, A. Lin, M. Wang, W. Chen, X. Wu, Z. Ren, Y. Zhao, L. Luo., 2010. Structural model of 2008 M w 7.9 Wenchuan earthquake in the rejuvenated Longmenshan thrust belt, China. Tectonophysics 491, 174-184.

Jian, P., Liu, D., Kröner, A., Zhang, Q., Wang, Y., Sun, X., Zhang, W., 2009. Devonian to Permian plate tectonic cycle of the Paleo-Tethys Orogen in southwest China (II): Insights from zircon ages of ophiolites, arc/back-arc assemblages and within-plate igneous rocks and generation of the Emeishan CFB province. Lithos 113, 767-784.

Jin, W. Z., L. J. Tan., K. M. Yang., G. M. Wan., Z. Z. Lu., and Y. X. Yu., 2007. Deformation and zonation of the Longmenshan fold and thrust zone in the western Sichuan basin. Acta Geol Sinica 81, 1072-1080 (in Chinese with English abstract).

Jin, W. Z., L. J. Tang., K. M. Yang., G. M. Wan., Z. Z. Lu., Y. X. Yu., 2010. Structural Styles of Longmen Mountain Thrust Belt, SW China. Journal of Earth Sciences 21, 19-31.

Jolivet, M., Roger, F., Paquette, J. L., 2015.Mesozoic-Cenozoic evolution of the Danba dome (Songpan Garzê, East Tibet) as inferred from LA-ICP-MS U-Pb and fission track data. Journal of Asian Earth Science 102, 180- 204.

Jolivet, L., Faccenna, C., 2000. Meditterranean extension and the Africa-Eurasia collision. Tectonics 19, 1095–1106.

Kirby, E., Reiners, P. W., Krol, M. A., Whipple, K. X., Hodges, K. V., Farley, K. A., Chen, Z., 2002. Late Cenozoic evolution of the eastern margin of the Tibetan Plateau: Inferences from 40Ar/39Ar and (U - Th)/He thermochronology. Tectonics 21, 1-1.

Kusky, T.M., Wang, L., Dilek, Y., Robinson, P., Peng, S.B., Huang, X., 2011. Application of the modern ophiolite concept in China with special reference to Precambrian ophiolites. Science China Earth Science 54, 1–27.

Lai, S.C., Yang, Y.C., 1997. Petrology and geochemistry features of the metamorphic volcanic rocks in the Mianxian–Lueyang suture zone, southern Qinling. Acta Petrologica Sinica 13, 563–573 (in Chinese with English abstract).

Lai, S.C., Zhang, G.W., Yang, R.Y., 2000. Identification of the island-arc magmatic zone in the Lianghe–Raofeng–Wuliba area, south Qinling and its tectonic significance. Science in China (Series D) 43, 69–79.

Lai, S.C., Zhang, G.W., Pei, X.Z., Yang, H.F., 2004. Geochemistry of the ophiolite and oceanic island basalt in the Kangxian-Pipasi-Nanping tectonic melange zone, south Qinling and their tectonic significance. Science in China (Series D) 47, 128–137.

Lai, S.C., Li, Y.F., Qin, J.F., 2007. Geochemistry and LA-ICP-MS zircon U–Pb dating of the Dongjiahe ophiolite complex from the western Bikou terrane. Science in China (Series D) 50, 305–313.

Lai, S.C., Zhang, G.W., Yang, Y.C., Chen, J.Y., 1998. Geochemistry of the ophiolite and island arc volcanic rock in the Mianxian -Lueyang suture zone, southern Qinling and their tectonic significances. Geochemica 27, 283–292.

Lei, Y., 2012. Meso-Cenozoic Tectonic Events Recorded by Apatite Fission Track in the Northern Longmen-Micang Mountains. Acta Geologica Sinica-English Edition 86, 153-165.

Li, H., Zhang, Y., Zhang, C., Dong, S., Zhu, F., 2015. Middle Jurassic syn-kinematic magmatism, anatexis and metamorphism in the Zheduo-Gonggar massif, implication for the deformation of the Xianshuihe fault zone, East Tibet. Journal of Asian Earth Sciences 107, 35-52.

Li, H., Zhang, Z., Ernst, R., Lü, L., Santosh, M., Zhang, D., Cheng, Z., 2015. Giant radiating mafic dyke swarm of the Emeishan Large Igneous Province: Identifying the mantle plume centre. Terra Nova 27, 247-257.

Li, H., Zhang, Z., Santosh, M., Linsu, L. Ü., Han, L., Liu, W., 2016. Late Permian basalts in the northwestern margin of the Emeishan large igneous province: implications for the origin of the Songpan-Ganzi terrane. Lithos 256–257, 75-87.

Li, J., Liu, C.L., Zheng, Y., Xiong, X., 2017. Rupture Process of the Ms 7.0 Lushan Earthquake Determined by Joint Inversion of Local Static GPS Records, Strong Motion Data, and Teleseismograms. Journal of Earth Science 28, 404-410.

Li, J., Wang, Z., Zhao, M., 1999. 40Ar/39Ar thermochronological constraints on the timing of collisional orogeny in the Mianlue collisional belt, southern Qinling Mountains, Acta Geol. Sinica 73, 208–215.

Li, M.K., Zhang, S.X., Zhang, C.Y., Zhang, Y., 2015. Fault Slip Model of 2013 Lushan Earthquake Retrieved Based on GPS Coseismic Displacements. Journal of Earth Science 26, 537–547.

Li, S. G., W. D. Sun, G. W. Zhang, J. Y. Chen, and Y. C. Yang., 1996. Chronology and geochemistry of metavolcanic rocks from Heigouxia Valley in the Mianlue tectonic zone, South Qinling - evidence for a Paleozoic oceanic basin and its close time, Sci. China, Ser. D, 39, 300–310.

Li, S.Z., Kusky, T.M., Wang, L., Lai, S.C., Liu, X.C., Dong, S.W., Zhao, G.W., 2007. Collision leading to multiple-stage large-scale extrusion in the Qinling orogen: insights from the Mianlue suture. Gondwana Research 12, 121–143.

Li, X.H., Li, W.X., Li, Z.X., Lo, C.H., Wang, J., Ye, M.F., Yang, Y.H., 2009. Amalgamation between the Yangtze and Cathaysia Blocks in South China: constraints from SHRIMP U–Pb zircon ages, geochemistry and Nd–Hf isotopes of the Shuangxiwu volcanic rocks. Precambrian Research 174, 117–128.

Li, X.H., Zhao, J.X., McCulloch, M. T., Zhou, G.Q., Xing, F.M., 1997. Geochemical and Sm-Nd isotopic study of Neoproterozoicophiolites from southeastern China: petrogenesis and tectonic implications. Precambrian Research 81, 129-144.

Li, X.T., Yan, D.P., Qiu, L., 2018. Early Cretaceous post-collisional collapse of the Yidun terrane: geochronological and geochemical constraints from calc-alkaline to alkaline basalts in Xiqiu area, southwest China. Journal of Earth Science 29, 57-77.

Li, Z.X., Li, X.H., Kinny, P.D., Wang, J., Zhang, S., Zhou, H., 2003. Geochronology of Neoproterozoic syn-rift magmatism in the Yangtze Craton, South China and correlationswith other continents: evidence for amantle superplume that broke up Rodinia. Precambrian Research 122, 85–109.

Li, Z.X., Zhang, L., Powell, C.M., 1995. South China in Rodinia: part of the missing link between Australia–East Antarctica and Laurentia? Geology 23, 407–410.

Lister, G. S., Davis, G.A., 1989. The origin of metamorphic core complexes and detachment faults formed during tertiary continental extension in the northern Colorado River region, USA. Journal of Structural geology 11, 65–94.

Linnemann, U., Su, T., Kunzmann, L., Spicer, R.A., Ding, W.-N., Spicer, T.E.V., Zieger, J., Hofmann, M., Moraweck, K., Gärtner, A., Gerdes, A., Marko, L., Zhang, S.-T., Li, S.-F., Tang, H., Huang, J., Mulch, A., Mosbrugger, V., Zhou, Z.‐ K., 2018. New U-Pb dates show a Paleogene origin for the modern Asian biodiversity hot spots. Geology 46, 3–6.

Liu, H., D. P. Yan., G. Q. Wei., 2008. Deformation and metamorphic sequence of Bikou terrane in the northwest margin of Yangtze plate: implications for extension collapse and transition of Songpan-Ganze orogenic belt. Acta Geol. Sinica 82, 464－474 (in Chinese with English abstract).

Liu, S.F., Steel, R., Zhang, G.W., 2005. Mesozoic sedimentary basin development and tectonic implication, northern Yangtze Block, eastern China: record of continent–continent collision. Journal of Asian Earth Sciences 25, 9–27.

Liu, S.W., Yang, K., Li, Q.G., Wang, Z.Q., Yan, Q.R., 2009a. Petrogenesis of the Neoproterozoic Baoxing complex and its constrait on the tectonic environment in the western margin of Yangtze Craton. Earth Science Frontiers 16, 107–118.

Liu, S.W., Yan, Q.R., Li, Q.G., Wang, Z.Q., 2009b. Petrogenesis of granitoid rocks in the Kangding complex, western margin of the Yangtze Craton and its tectonic significance. Acta Petrologica Sinica 25, 1883–1896 (in Chinese with English abstract).

Lo, C. H., Chung, S. L., Lee, T. Y., Wu, G., 2002. Age of the Emeishan flood magmatism and relations to Permian–Triassic boundary events. Earth Planetary Science Letters 198, 449–458.

Lu, S., D. P. Yan., Y. Wang., J. F. Gao., L. Qi., 2010. Geochemical and geochronological constraints on Mashan and Mupi plutons in the South Qinling orogenic belt: implications for tectonic nature of the Bikou terrane. Acta Petrol. Sinica 26, 1889-1901 (in Chinese with English abstract).

Mattauer, M., J. Malavieille, S. Calassou, J. Lancelot, F. Roger, Z. W. Hao, Z. Q. Xu, and L. W. Hou., 1992. The Songpan-Ganze Triassic belt of west Sichuan and eastern Tibet-a decollement fold belt on passive margin. Comptes Rendus de I' Academie des Sci. Paris, II, 314, 619–626.

Meng, E., Liu, F.L., Du, L.L., Liu, P.H., Liu, J.H., 2015. Petrogenesis and tectonic significance of the Baoxing granitic and mafic intrusions, southwestern China: evidence from zircon U–Pb dating and Lu–Hf isotopes, and whole-rock geochemistry. Gondwana Research 28, 800–815.

Meng, Q. R., G. W. Zhang., 2000. Geologic framework and tectonic evolution of the Qinling orogen, central China, Tectonophysics 323, 183–196.

Meng, Q.R., E. Wang., J. M. Hu., 2005. Mesozoic sedimentary evolution of the northwest Sichuan basin: implication for continued clockwise rotation of the South China block, GSA Bull. 117, 396–410.

Mo, X., Deng, J., Lu, F., 1994. Volcanism and the evolution of Tethys in Sanjiang area, southwestern China. Journal of Southeast Asian Earth Sciences 9, 325–333.

Mo, X.X., Lu, F.X., Sheng, S.Y., 1993. Sanjiang Tethyan volcanism and related mineralization. Geological Publishing House, Beijing.

Munteanu, M., Wilson, A., Yao, Y., Harris, C., Chunnett, G., Luo, Y.N., 2010. The Tongde dioritic pluton (Sichuan, SWChina) and its geotectonic setting: regional implications of a local-scale study. Gondwana Research 184, 55–65.

Nie, S., A., Yin, D. B. Rowley, and Y. Jin., 1994. Exhumation of the Dabie Shan ultra-high-pressure rocks and accumulation of the Songpan Ganze flysch sequence, central China, Geology 22, 999–1002.

Otofuji, Y., Liu, Y.Y., Yokoyama, M., Tamai, M., Yin, J.Y., 1998. Tectonic deformation of the southwestern part of the Yangtze craton inferred from paleomagnetism. Earth and Planetary Science Letter 156, 47-60.

Parsons, T., C. Ji., E. Kirby., 2008. Stress changes from the 2008 Wenchuan earthquake and increased hazard in the Sichuan basin, Nature 454, 509–510.

Pehrsson, S.J., Eglington, B.M., Evans, D.A.D., Huston, D., Reddy, S.M., 2015. Metal-logeny and its link to orogenic style during the Nuna supercontinent cycle. Geol. Soc. (Lond.) Spec. Publ.424.

Pei, X.Z., Ding, S.P., Zhang, G.W., Liu, H.B., Li, Z.C., Li, W.Y., Liu, Z.Q., Meng, Y., 2007. Zircons LA-ICP-MS U–Pb dating of Neoproterozoic granitoid gneisses in the north margin of West Qinling and geological implication. Acta Geologica Sinica 81, 772–786 (in Chinese with English abstract).

Pei, X.Z., Li, Z.C., Ding, S.P., Li, R.B., Feng, J.Y., Sun, Y., Zhang, Y.F., Liu, Z.Q., 2009. Neoproterozoic Jiaoziding peraluminous granite in the Northwestern margin of Yangtze block: zircon SHRIMP U–Pb age and geochemistry and their tectonic significance. Earth Science Frontiers 16, 231–249.

Pisarevsky, S.A., Elming, S.A., Pesonen, L., Li, Z.X., 2014. Mesoproterozoic paleogeography: Supercontinent and beyond. Precambrian research 244, 207-225.

Pullen, A., P. Kapp., G. Gehrels., J. D. Vervoot., L. Ding., 2008. Triassic continental subduction in central Tibet and Mediterranean-style closure of the Paleo-Tethys ocean, Geology 36, 351-354.

Qian, T., Liu, S., Wang, Z., Li, W., Chen, X., 2016. A detrital record of continent-continent collision in the Early-Middle Jurassic foreland sequence in the northern Yangtze foreland basin, South China. Journal of Asian Earth Sciences.

Qin, K.L., Zou, X.H., He, S.P., 1990. Sequence, time and division of the Bikou group in the junction of Shanxi, Sichuan and Gansu provinces. Journal of Xian Geological Institute 30, 1-61.

Qin, K.L., Jin, H.J., Zhao, D.H., 1994. Tectonic evolution and mineralization in Bikou ancient island arc belt. Henan Geology 12, 304–317 (in Chinese with English abstract).

Rao, R., J. Xu., Y. Chen., D. Zou., 1987. The Triassic System of the Qianghai-Xizang Plateau, 239 pp., Geol. Publ. House, Beijing.

Ratschbacher, L., Hacker, B.R., Calvert, A., Webb, L.E., Grimmer, J.C., McWilliams, M.O., Ireland, T., Dong, S.W., Hu, J.M., 2003. Tectonics of the Qinling (Central China):

tectonostratigraphy, geochronology, and deformation history. Tectonophysics 366, 1–53.

Reid, A.J., Fowler, A.P., Phillips, D., Wilson, C.J.L., 2005. Thermochronology of the Yidun Arc, central eastern Tibetan Plateau: constraints from 40Ar/39Ar K-feldspar and apatite fission track data. Journal of Asian Earth Sciences 25, 915-935.

Reid, A., Wilson, C.J.L., Shun, L., Pearson, N., Belousova, E., 2007. Mesozoic plutons of the Yidun arc, SW China/U/Pb geochronology and Hf isotopic signature. Ore Geology Reviews 31, 88–106.

Ren, J.S., Zhao, L., Qinqin, X. U., Zhu, J., 2016. Global Tectonic Position and Geodynamic System of China. Acta Geologica Sinica 90, 2100-2108.

Ren, J.S., Zhang, Z.K., Niu, B.G., Liu, Z.G., 1986a. On the Qinling Orogenic Belt-integration of the Sino-Korean and Yangtze Blocks, Qinling Orogenic Belt. Northwest University Press, Xi'an, pp. 99–110 (in Chinese with English abstract).

Ren, J.S., Chen, T.Y., Liu, Z.G., Niu, B.G., Liu, F.R., 1986b. Some problems on the tectonics of South China. Chinese Science Bulletin 31, 751-754.

Rey, P., Vanderhaeghe, O., Teyssier, C., 2001. Gravitational collapse of the continental crust: definition, regimes and modes. Tectonophysics 342, 435-449.

Rey, P., Teyssier, C., Kruckenberg, S., Whitney, D., 2012. Viscous collision in channel explains double domes in metamorphic core complexes. Geology 39, 387-390.

Rey, P., Teyssier, C., Whitney, D.L., 2010. Limit of channel flow in orogenic plateaux. Lithosphere 2, 328-332.

Richardson, N.J., Densmore, A.L., Seward, D., Fowler, A., Wipf, M., Ellis, M.A., Yong, L., Zhang, Y., 2008. Extraordinary denudation in the Sichuan Basin: Insights from low temperature thermochronology adjacent to the eastern margin of the Tibetan Plateau, Journal of Geophysical Research 113, B04409, doi:10.1029/2006JB004739.

Roger, F., Calassou, S., Lancelot, J., Malavieille, J., Mattauer, M., Xu, Z., 1995. Miocene emplacement and deformation of the Kongashan granite (Xianshuihe fault zone, west Sichuan, China): geodynamic implications. Earth Planetary Science Letters 130, 201-216.

Roger, F., Jolivet, M., Malavieille, J., 2010. The tectonic evolution of the Songpan Garzê (North Tibet) and adjacent areas from Proterozoic to Present: a synthesis. Journal of Asian Earth Sciences 39, 254-269.

Roger, F., Jolivet, M., Malavieille, J., 2008. Tectonic evolution of the Triassic fold belts of Tibet. Comptes Rendus Geoscience 340, 180-189.

Roger, F., Malavieille, J., Leloup, H., Calassou, S., Xu, Z., 2004. Timing of granite emplacement and cooling in the Songpan-Garze Fold Belt (eastern Tibetan Plateau) with tectonic implications. Journal of Asian Earth Sciences 39, 254-269.

Royden, Leigh, H., 1997. Surface deformation and lower crustal flow in eastern Tibet. Science 276, 788-790.

SBGMR (Shaanxi Bureau of Geology and Mineral Resources)., 1989. Regional geology of Shan'xi Province: Beijing, China, 689 pp., Geol. Publ. House, Beijing (in Chinese with English abstract).

SBGMR (Sichuan Bureau of Geology and Mineral Resources)., 1991. Regional geology of Sichuan Province: Beijing, China, 680 pp., Geol. Publ. House, Beijing (in Chinese with English abstract).

She, Z., Ma, C., Mason, R., Li, J., Wang, G., Lei, Y., 2006. Provenance of the Triassic Songpan-Ganzi flysch, west China. Chemical Geology 231, 159-175.

Shellnutt, J. G., Zhou, M. F., 2007. Permian peralkaline, peraluminous and metaluminous A-type granites in the Panxi district, SW China: Their relationship to the Emeishan mantle plume. Chemical Geology 243, 286-316.

Shi, F., He, H., Densmore, A. L., Li, A., Yang, X., Xu, X., 2016. Active tectonics of the Ganzi-Yushu fault in the southeastern Tibetan Plateau. Tectonophysics 676, 112-124.

Song, X. Y., Zhou, M. F., Cao, Z. M., Robinson, P. T., 2004. Late permian rifting of the South China Craton caused by the Emeishan mantle plume? Journal of the Geological Society 161, 773-781.

Sun, C.M., Vuagnat, M., 1992. Proterozoic ophiolites from Yanbian and Shimian (Sichuan Province, China) - petrography, geochemistry, petrogenesis, and geotectonic environment. Schweizerische Mineralogische Und Petrographische Mitteilungen. 72, 389-413

Sun, M., Yan, D.P., Zhu, L.T. Mu, H.X., Zhang, Y.X., Yin, A., 2018. Northeastward transpression of the Cenozoic Longmenshan thrust belt in eastern Tibet Plateau revealed by fission-track thermochronology. In preparation.

Sun, M., Yin, A., Yan, D., Ren, H., Mu, H., Zhu, L., Qiu, L., 2018. Role of pre-existing structures in controlling the Cenozoic tectonic evolution of the eastern Tibetan plateau: New insights from analogue experiments. Earth and Planetary Science Letters 491, 207-215.

Sun, W.H., Zhou, M.F., Zhao, J.H., 2007. Geochemistry and tectonic significance of basaltic lavas in the Neoproterozoic Yanhian Group, Southern Sichuan Province, Southwest China. International Geology Review 49, 554-571.

Sun, W.H., Zhou, M. F., Yan, D. P., Li, J. W., Ma, Y., 2008a. Petrology, geochemistry and Zircon U-Pb geochronology of turbidites from the Neoproterozoic Yanbian Group in the Yangtze Block, SW China: Implications for provenance and tectonic setting. Annual 72.

Sun, W. H., Zhou, M. F., Yan, D. P., Li, J. W., Ma, Y. X., 2008b. Provenance and tectonic setting of the Neoproterozoic Yanbian Group, western Yangtze Block (SW China). Precambrian Research 167, 213-236.

Sun, W.H., M. F. Zhou., J. F. Gao., Y. H. Yang., X. F. Zhao., J. H. Zhao., 2009. Detrital zircon U–Pb geochronological and Lu–Hf isotopic constraints on the Precambrian magmatic and crustal evolution of the western Yangtze Block, SW China. Precambrian Research 172, 99-126.

Tan, X. B., Xu, X. W., Lee, Y. H., Chen, G. H., Wan, J. L., 2010. Apatite fission track evidence for rapid uplift of the Gongga Mountain and discussion of its mechanism. Chinese Journal of Geophysics 53, 1859-1867.

Tapponnier, P., Xu, Z.Q., Roger, F., Meyer, B., Arnaud, N., Wittlinger, G., Yang, 2011. Oblique Stepwise Rise and Growth of the Tibet Plateau. Science 294, 1671-1677

The Geological Research Team of Shaanxi Bureau of Geology and Mineral Resources (GRT-SBGMR), 1996. 1:50000 geological maps of Daanzeng, Hejiayan, Dajiaba and Lueyang. Unpublished geological maps and reports.

Tian, Y., Kohn, B. P., Gleadow, A. J. W., Hu, S., 2013. Constructing the Longmenshan eastern Tibetan Plateau margin: Insights from low-temperature thermochronology. Tectonics 32, 576–592.

Tucker, R. D., Ashwal, L. D., Torsvik, T. H., 2001. U–Pb geochronology of Seychelles granitoids: a Neoproterozoic continental arc fragment. Earth Planetary Science Letters 187, 27-38.

Vanderhaeghe, O., 1999. Pervasive melt migration from migmatites to leucogranite in the Shuswap metamorphic core complex, Canada: control of regional deformation. Tectonophysics 312, 35-55.

Vanderhaeghe, O., 2012. The thermal mechanical evolution of crustal orogenic belts at convergent plate boundaries: A reappraisal of the orogenic cycle. Journal of Geodynamics 56–57, 124-145.

Wang, B.-Q., Zhou, M.-F., Li, J.-W., Yan, D.-P., 2011. Late Triassic porphyritic intrusions and associated volcanic rocks from the Shangri-La region, Yidun terrane, Eastern Tibetan Plateau: Adakitic magmatism and porphyry copper mineralization. Lithos 127, 24–38.

Wang, B. Q., Wang, W., Chen, W. T., Gao, J. F., Zhao, X. F., Yan, D. P., 2013a. Constraints of detrital zircon U-Pb ages and Hf isotopes on the provenance of the TriassicYidun Group and tectonic evolution of the Yidun Terrane, Eastern Tibet. Sedimentary Geology 289, 74-98.

Wang, B. Q., Zhou, M. F., Chen, W. T., Gao, J. F., Yan, D. P., 2013b. Petrogenesis and tectonic implications of the Triassic volcanic rocks in the northern Yidun Terrane, Eastern Tibet. Lithos 175, 285-301.

Wang, D., Shu, L.S., 2012. Late Mesozoic basin and range tectonics and related magmatism in Southeast China. Geoscience Frontiers 3, 109-124.

Wang, E.C., Burchfiel, B.C., 2000, Late Cenozoic to Holocene deformation in southwestern Sichuan and adjacent Yunnan, China, and its role in formation of the southeastern part of the Tibetan Plateau. Geological Society of America Bulletin 112, 413-423.

Wang, E., Kirby, E., Furlong, K. P., Soest, M. V., Xu, G., Shi, X., 2012. Two-phase growth of high topography in eastern Tibet during the Cenozoic. Nature Geoscience 5, 640-645.

Wang, E., Meng, K., Su, Z., Meng, Q., Chu, J. J., Chen, Z., 2014. Block rotation: Tectonic response of the Sichuan basin to the southeastward growth of the Tibetan Plateau along the Xianshuihe-Xiaojiang fault. Tectonics 33, 421-426.

Wang, E.C., Burchfiel, B.C., Royden, L.H., 1998, Late Cenozoic Xianshuihe-Xiaojiang, Red River, and Dali fault systems of southwestern Sichuan and central Yunnan, China. Geological Society of America-Special Paper 327, 6-39.

Wang, Y., Luo, Z., Wu, P., Chen, L., Hao, J., 2014. A new interpretation of the sedimentary environment before and during eruption of the Emeishan LIP, Southwest China. International Geology Review 56, 1295-1313.

Wang, W., Cawood, P.A., Zhou, M.F., Zhao, J.H., 2016. Paleoproterozoic magmatic and metamorphic events link Yangtze to northwest Laurentia in the Nuna supercontinent. Earth and Planetary Science Letters 433, 269-279.

Wang, W.F., Zhu, C.H., Zhang, X.J., et al., 2016. Genetic Types and Geological Significances of Transverse Faults at Longmenshan Fault Zone. Earth Science 41, 718-728.

Wei, C.J., 1993. Epidote and its petrological implication in the Bikou group, south Qinling orogenic belt. Journal of Petrology and Mineralogy 12, 332-340 (in Chinese with English abstract).

Wei, C.J., 1994. Metamorphism and its significanceof the Bikou group in the junction region of Sha'nxi and Sichuan Provinces. Acta Geologica Sinica 68, 241-254 (in Chinese with English abstrract).

Weislogel, A.L., 2008. Tectonostratigraphic and geochronologic constraints on evolution of the northeast Paleotethys from the Songpan-Ganzi complex, central China. Tectonophysics 451, 331-345.

Weislogel, A. L., S. A. Graham., E. Z. Chang., J. L. Wooden., G. E. Gehrels., 2010. Detrital zircon provenance from three turbidite depocenters of the Middle-Upper Triassic Songpan-Ganzi complex, central China: Record of collisional tectonics, erosional exhumation, and sediment production, GSA Bull. 122, 2041-2062.

Weislogel, A. L., Graham, S. A., Chang, E. Z., Wooden, J. L., Gehrels, G. E., Yang, H., 2006. Detrital zircon provenance of the Late Triassic Songpan-Ganzi complex: Sedimentary record of collision of the North and South China blocks, Geology 34, 97-100.

Weller, O. M., St-Onge, M. R., Waters, D. J., Rayner, N., Searle, M. P., Chung, S. L., 2013. Quantifying Barrovian metamorphism in the Danba Structural Culmination of eastern Tibet. Journal of Metamorphic Geology 31, 909–935.

Wilson, P. J. T., 1966. Did the Atlantic close and then re-open?. Nature 211, 676-681

Wilson, Christopher, J. L., Harrowfield, M.J., Reid, A.J., 2006. Brittle modification of Triassic architecture in eastern Tibet: implications for the construction of the Cenozoic plateau. Journal of Asian Earth Sciences 27, 341-357.

Whattam, S.A., Stern, R.J., 2011. The 'subduction initiation rule': a key for linking ophiolites, intra-oceanic forearcs, and subduction initiation. Contrib. Miner. Petrol. 162, 1031–1045.

Worley, B. A., Wilson, C. J. L., 1996. Deformation partitioning and foliation reactivation during transpressional orogenesis, an example from central Longmenshan, China. Journal of Structural Geology 18, 395-411.

Xiao, L., He, Q., Pirajno, F., Ni, P.Z., Du, J.X., Wei, Q.R., 2008. Possible correlation between a mantle plume and the evolution of Paleo-Tethys Jinshajiang Ocean: Evidence from a volcanic rifted margin in the Xiaru-Tuoding area, Yunnan, SW China. Lithos 100, 112-126.

Xiao, L., Zhang, H.F., Ni, P.Z., Xiang, H., Liu, X.M., 2007. LA-ICP-MS U–Pb zircon geochronology of early Neoproterozoic mafic-intermediate intrusions from NW margin of the Yangtze Block, South China: implication for tectonic evolution. Precambrian Research 154, 221–235.

Xu, C.G., Yan, D.P., Zhou, M.F., Wells, M.L., Qiu, L., Wang, J.B., Tang, X.L., 2018. Blueschist facies rocks from the northwestern margin of the Yangtze Block, South China: implications for Neoproterozoic subduction. In preparing.

Xu, J.F., Wang, Q., Yu, X.Y., 2000a. Geochemistry of high-Mg andesites and adakitic andesite from the Sanchazi block of the Mian-Lue ophiolitic melange in the Qinling

Mountains, central China: evidence of partial melting of the subducted Paleo-Tethyan crust. Geochemical Journal 34, 359–377.

Xu, J.F., Yu, X.Y., Li, X.H., Zhang, B.R., Hang, Y.W., 2000b. Geochemistry of the Anzishan ophiolitic complex in the Mian–Lue belt of Qinling Orogen: evidence and implication of the Palaeo-ocean crust. Acta Geologica Sinica 74, 39–50 (in Chinese with English abstract).

Xu, J. F., B. R. Zhang, and Y. W. Han., 2008. Geochemistry of the Mian-Lue ophiolites in the Qinhng Mountains, central China: constraints on the evolution of the Qinling orogenic belt and collision of the North and South China Cratons. J. Asian Earth Sci. 32, 336-347.

Xu, Y.G., Chung, S. L., Jahn, B. M., Wu, G., 2001. Petrologic and geochemical constraints on the petrogenesis of Permian–Triassic Emeishan flood basalts in southwestern China. Lithos 58, 145-168.

Xu, Z. Q., Ji, S. C., Li, H. B., Hou, L. W., Fu, X. F. Cai, Z. F., 2008. Uplift of the Longmenshan range and the Wenchuan earthquake. Episodes 31, 291-301.

Xu, Z.Q., Hou, L., Wang, Z., 1992. Orogenic processes of the Songpan Garze orogenic belt of China. Geological Publishing House, Beijing, 190 pp.

Yan, D.P., Song, H.L., Fu, Z.R., Tian, J.Y., 1997. Metamorphic core complexes in the western margin of Yangtze craton. Beijing: Geological in press, 1997, 165 pp (in Chinese with English abstract).

Yan, D. P., Zhou, M. F., Song, H. L., Malpas, J., 2002. Where was South China located in the reconstruction of Rodinia? Earth Science Frontiers 9, 249-256.

Yan, D.P., M.F. Zhou, G.Q. Wei, H. Liu, T. Z. Dong, W. C. Zhang, and Z. L. Jin., 2008a. Collapse of the Songpan-Ganze Orogenic belt resulted by a Mesozoic middle-crustal ductile channel flow: evidences from deformation and metamorphism within the Sinian-Paleozoic strata in the hinterland of Longmenshan foreland thrust belt. Earth Sci. Frontiers 15, 186-198.

Yan, D.P., Zhou, M.F., Wei, G.Q., Gao, J.F., Liu, S.F., Xu, P., Shi, X.Y., 2008b. The Pengguan tectonic dome of Longmen Mountains, Sichuan Province: Mesozoic denudation of a Neoproterozoic magmatic arc-basin system. Science in China Series D: Earth Sciences 5, 1545-1559.

Yan, D. P., Zhou, M. F., Song, H., Fu, Z., 2003a. Structural style and tectonic signi¢cance of the Jianglang metamorphic core complex, eastern margin of the Tibetan Plateau, China. Journal of Structural Geology 25, 765-779.

Yan, D.P., M.F. Zhou., H. Song., X.W. Wang., J. Malpas., 2003b. Origin and tectonic significance of a Mesozoic multi-layer over-thrust system within the Yangtze Block (South China). Tectonophysics 361, 239-254.

Yan, D.P., B. Zhang., M.F. Zhou., G.Q. Wei., H. L. Song., S. F. Liu., 2009. Constraints on the depth, geometry and kinematics of blind detachment faults provided by fault propagation folds: an example from the Mesozoic fold belt of South China, J. Struct. Geol. 31, 150-162.

Yan, D.P., M.F. Zhou, G.Q. Wei, J. F. Gao, S. F. Liu, P. Xu, and X. Y. Shi., 2008a. The Pengguan tectonic dome of Longmen Mountains, Sichuan Province: Mesozoic denudation of a Neoproterozoic magmatic arc-basin system. Sci. China-Ser. D. 51, 1545-1559.

Yan, D.P., M.F. Zhou., S.B. Li., G.Q. Wei., 2011. Structural and geochronological constraints on the Mesozoic-Cenozoic tectonic evolution of the Longmenshan thrust belt, eastern Tibetan Plateau. Tectonics 30, 81-7.

Yan, D.P., Xu, Y.B., Dong, Z.B., Qiu, L., Zhang, S., Wells, M., 2016. Fault-related fold styles and progressions in fold-thrust belts: insights from sandbox modeling. Journal of Geophysical Research-Solid Earth 121, n/a-n/a.

Yan, D.P., Zhou, M.F., Wang, C.Y., Xia, BN., 2006. Structural and geochronological constraints on the tectonic evolution of the Dulong-Song Chay tectonic dome in Yunnan province, SW China. Journal of Asian Earth Sciences 28, 332-353.

Yan, Q.R., Wang, Z.Q., Yan, Z., Xiang, Z.J., Chen, J.L., Wang, T., 2007. SHRIMP analyses for ophiolitic–mafic blocks in the Kangxian–Mianxian section of the Mianxian–Lueyang melange: their geological implications. Geological Review 53, 755–764 (in Chinese with English abstract).

Yang, C., Dong, Y.P., Liang, W.T., Li, W., Yang, Z., Zha, X.F., Chen, Q., 2013. Characteristics of magnetic fabric and its significance in Kangxian segment of Mianlue tectonic zone. Progress in Geophysics 28, 214–223 (in Chinese with English abstract).

Yang, T. N., Ding, Y., Zhang, H. R., Fan, J. W., Liang, M. J., Wang, X. H., 2014. Two-phase subduction and subsequent collision defines the Paleotethyan tectonics of the southeastern Tibetan Plateau: Evidence from zircon U-Pb dating, geochemistry, and structural geology of the Sanjiang orogenic belt, southwest China. Geological Society of America Bulletin 126, 1654-1682.

Yang, T.N., Hou, Z.Q., Wang, Y., Zhang, H.R., Wang, Z.L., 2012. Late Paleozoic to Early Mesozoic tectonic evolution of northeast Tibet: Evidence from the Triassic composite western Jinsha-Garze-Litang suture. Tectonics 31, TC4004.

Yang, T.N., Zhang, H.R., Liu, Y.X., Wang, Z.L., Song, Y.C., Yang, Z.S., Tian, S.H., Xie, H.Q., Hou, K.J., 2011. Permo-Triassic arc magmatism in central Tibet: Evidence from zircon U-Pb geochronology, Hf isotopes, rare earth elements, and bulk geochemistry. Chemical Geology 284, 270-282.

Yin, A., S. Nie., 1993. An indentation model for North and South China collision and the development of the Tanlu and Honam fault systems, eastern Asia, Tectonics 12, 801-813.

Yin, A., T. M. Harrison., 2000. Geologic evolution of the Himalayan-Tibetan orogen, Annual Rev. Earth Planet. Sci. 28, 211-280.

Yong, L., P. A. Allen., A. L. Densmore., X. Qiang., 2003. Evolution of the Longmenshan Foreland basin (Western Sichuan, China) during the Late Triassic Indosinian orogeny, Basin Res. 15, 117-138.

Yoshioka, S., Liu, Y.Y., Sato, K., Inokuchi, H., Su, L., Zaman, H., Otofuji, Y., 2003. Paleomagnetic evidence for post-Cretaceous internal deformation of the Chuan Dian Fragment in the Yangtze block: a consequence of indentation of India into Asia. Tectonophysics 376, 61-74

Yuan, C., M.F. Zhou., M. Sun., Y. J. Zhao., S. Wilde., X. P. Long., D.P. Yan., 2010. Triassic granitoids in the eastern Songpan Ganzi Fold Belt, SW China: Magmatic response to geodynamics of the deep lithosphere, Earth Planet. Sci. Lett. 290, 481-492.

Zhang, N., Cao, Y., Liao, Y., Zhang, H., Hu, D., Zhang, R., Wang, L., 1998. Geology and Metallogeny in the Ganzi-Litang Rift Zone. Geological Publishing House, Beijing.

Zhang, C.L., Gao, S., Yuan, H.L., Zhang, G.W., Yan, Y.X., Luo, J.L., Luo, J.H., 2007. Sr–Nd–Pb isotopes of the Early Paleozoicmafic–ultramafic dykes and basalts fromSouth Qinling belt and their implications for mantle composition. Science in China Series D: Earth Sciences 50, 1293–1301.

Zhang, G. W., Y. P. Dong, S. C. Lai, A. L. Guo, Q. R. Meng, S. F. Liu, S. Y. Cheng, A. P. Yao, Z. Q. Zhang, X. Z. Pei, and S. Z. Li, 2004. Mianlue tectonic zone and Mianlue suture zone on southern margin of Qinling-Dabie orogenic belt, Sci. China series D. 47, 300-316.

Zhang, H. F., L. Zhang., N. Harris., L. L. Jin., H. Yuan., 2006. U–Pb zircon ages, geochemical and isotopic compositions of granitoids in Songpan-Garze fold belt, eastern Tibetan Plateau: constraints on petrogenesis and tectonic evolution of the basement, Contrib. Mineral Petrol 152, 75-88.

Zhang, H. F., R. Parrish., L. Zhang., W. C. Xua., H. L. Yuan., S. Gao., Q. G. Crowley., 2007. A-type granite and adakitic magmatism association in Songpan-Garze fold belt, eastern Tibetan Plateau: Implication for lithospheric delamination. Lithos 97, 323-335.

Zhang, K. J., B. Li., Q. G. Wei., J. X. Cai., Y. X. Zhang., 2008. Proximal provenance of the western Songpan-Ganzi turbidite complex (Late Triassic, eastern Tibetan plateau): Implications for the tectonic amalgamation of China. Sediment. Geol. 208, 36-44.

Zhang, P., Zhou, Z., Xu, C., Zhang, Q., 2008. Geochemistry of Pengguan complex in the Longmenshan region, Western Sichuan province, SW China: Petrogenesis and tectonic implications. Geotectonica et Metallogenia 32, 105-116.

Zhang, S.H., Li, Z.X., Evans, D.A.D., Wu, H.C., Li, H.Y., Dong, J., 2012. Pre-Rodinia supercontinent Nuna shaping up: a global synthesis with new paleomagnetic results from North China. Earth and Planetary Science Letters 353–354, 145–155.

Zhang, Y. Z., Replumaz, A., Leloup, P. H., Wang, G. C., Bernet, M., Peter, V. D. B., 2017. Cooling history of the Gongga batholith: Implications for the Xianshuihe Fault and Miocene kinematics of SE Tibet. Earth Planetary Science Letters 465, 1-15.

Zhang, Y.X., 2013. The Nature of the Xigeda Ancestral Basin from Pliocene to EarlyPleistocene in Panxi area，Sichuan Province. Master Degree thesis of China University of Geosciences, Beijing, 77pp (in Chinese with English abstract).

Zhang, Z.Q., Tang, S.H., Zhang, G.W., Yang, Y.C., Wang, J.H., 2005. Ages of metamorphic mafic–andesitic volcanic rock blocks and tectonic evolution complexity of Mianxian–Lueyang ophiolitic melange belt. Acta Geologica Sinica 79, 531–539 (in Chinese with English abstract).

Zhang, Z.Q., Zhang, G.W., Tong, S.H., 2001. Metamorphic ages of the Yudongzi group and the Archean basement of the Qinling orogenic belt. Geologica Sinica Acta 75, 189-204.

Zhang, Z.Q., Zhang, G.W., Tang, S.H., Wang, J.H., Xu, J.F., Yang, Y.C., 2002. Age of Anzishan granulites in the Mianxian-Lueyang suture zone of Qinling orogen: with a discussion of the timing of final assembly of Yangtze and north China craton blocks. Chinese Science Bulletin 47, 1925–1929.

Zhao, G.C., Cawood, P.A., 2012. Precambrian geology of China. Precambrian Research 222-223, 13-54.

Zhao, G.C., Cawood, P.A., Wilde, S.A., Sun, M., 2002. Review of global 2.1–1.8 Ga orogens: implications for a pre-Rodinia supercontinent. Earth-Science Reviews 59, 125–162.

Zhao, G.C., Li, S.Z., Sun, M., Wilde, S.A., 2011. Assembly, accretion, and break-up of the Palaeo-Mesoproterozoic Columbia supercontinent: record in the North China Craton revisited. International Geology Review 53, 1331–1356.

Zhao, J.H., Zhou, M.F., 2007a. Geochemistry of Neoproterozoic mafic intrusions in the Panzhihua district (Sichuan Province, SW China): implications for subduction related metasomatism in the upper mantle. Precambrian Research 152, 27–47.

Zhao, J.H., Zhou, M.F., 2007b. Neoproterozoic adakitic plutons and arc magmatism along the western margin of the Yangtze Block, South China. Journal of Geology 115, 675-689.

Zhao, J.H., Zhou, M.F., Yan, D.P., Zheng, J.P., Li, J.W., 2011. Reappraisal of the ages of Neoproterozoic strata in South China: No connection with the Grenvillian orogeny. Geology 39, 299-302.

Zhao, J.H., Zhou, M.F., 2008. Neoproterozoic adakitic plutons in the northernmargin of the Yangtze Block, China: partial melting of a thickened lower crust and implications for secular crustal evolution. Lithos 104, 231–248.

Zhao, J.H., Zhou, M.F., 2009a. Secular evolution of the Neoproterozoic lithospheric mantle underneath the northern margin of the Yangtze Block, South China. Lithos 107, 152–168.

Zhao, J.H., Zhou, M.F., 2009b. Melting of newly formed mafic crust for the formation of Neoproterozoic I-type granite in the Hannan Region, South China. Journal of Geology 117, 54–70.

Zhao, J.H., Zhou, M.F., Zheng, J.P., 2010a. Metasomatic mantle source and crustal contamination for the formation of the Neoproterozoic mafic dike swarm in the northern Yangtze Block, South China. Lithos 115, 177–189.

Zhao, J.H., Zhou, M.F., Zheng, J.P., Fang, S.M., 2010b. Neoproterozoic crustal growth and reworking of the Northwestern Yangtze Block: constraints from the Xixiang dioritic intrusion, South China. Lithos 120, 439–452.

Zhao, J.H., Zhou, M.F., Zheng, J.P., Griffin, W.L., 2013a. Neoproterozoic tonalite and trondhjemite in the Huangling complex, South China: crustal growth and reworking in a continental arc environment. American Journal of Science 313, 540–583.

Zhao, J.H., Zhou, M.F., Zheng, J.P., 2013b. Neoproterozoic high-K granites produced by melting of newly formed mafic crust in the Huangling region, South China. Precambrian Research 233, 93–107.

Zhao, J.H., Asimow, P.D., Zhou, M.F., Zhang, J., Yan, D.P., Zheng, J.P., 2017. An Andean-type arc system in Rodinia constrained by the Neoproterozoic Shimian ophiolite in South China. Precambrian Research 296, 93-111.

Zhao, J.X., McCulloch, M.T., Korsch, R.J., 1994. Characterisation of a plume-related ~ 800 Ma magmatic event and its implications for basin formation in central-southern Australia. Earth and Planetary Science Letters 121, 349–367.

Zhao, X. F., Zhou, M. F., Hitzman, M. W., Li, J. W., Bennett, M., Meighan, C., 2012. Late Paleoproterozoic to Early Mesoproterozoic Tangdan Sedimentary Rock-Hosted

Strata-bound Copper Deposit, Yunnan Province, Southwest China. Economic Geology 107, 357-375.

Zhao, X.X., Coe, R., 1987. Palaeomagnetic constraints on the collision and rotation of North and South China. Nature 327, 141–144.

Zheng, Y.F., Zhao, Z.F., Wu, Y.B., Zhang, S.B., Liu, X., Wu, F.Y., 2006. Zircon U–Pb age, Hf and O isotope constraints on protolith origin of ultrahigh-pressure eclogite and gneiss in the Dabie orogen. Chemical Geology 231, 135–158.

Zheng, Y., Li, H., Sun, Z., Wang, H., Zhang, J., Li, C., 2016. New geochronology constraints on timing and depth of the ancient earthquakes along the Longmenshan fault belt, eastern Tibet. Tectonics 35.

Zhou, D., S. A. Graham., 1996. The Songpan-Ganzi complex of the western Qinling Shan as a Triassic remnant ocean basin, in The Tectonic Evolution of Asia, edited by Yin, A., and T. M. Harrison, pp. 281-299, Cambridge University Press, New York.

Zhou, M. F., Zhao, T. P., Malpas, J., Sun, M., 2000. Crustal-contaminated komatiitic basalts in southern China: products of Proterozoic mantle plume underneath the Yangtze Block. Precambrian Research 103, 175-189.

Zhou, M.-F., D.P. Yan., A.K. Kennedy., Y.Q. Li., J. Ding., 2002a. SHRIMP zircon geochronological and geochemical evidence for Neo-proterozoic arc-related magmatism along the western margin of the Yangtze Block, South China. Earth Planetary Science Letters 196, 51-67.

Zhou, M.F., Kennedy, A.K., Sun, M., Malpas, J., Lesher, C.M., 2002b. Neoproterozoic arcrelated mafic intrusions along the northern margin of South China: implications for the accretion of Rodinia. Journal of Geology 110, 611–618.

Zhou, M.F., D.P. Yan, C. L. Wang, L. Qi, and A. Kennedy., 2006a. Subduction-related origin of the 750 Ma Xuelongbao adakitic complex (Sichuan Province, China): Implications for the tectonic setting of the giant Neoproterozoic magmatic event in South China. Earth Planetary Science Letters 248, 271-285.

Zhou, M.F., Ma, Y.X., Yan, D.P., Xia, X.P., Zhao, J.H., Sun, M., 2006b. The Yanbian Terrane (Southern Sichuan Province, SW China): a Neoproterozoic arc assemblage in the western margin of the Yangtze Block. Precambrian Research 144, 19–38.

Zhou, M.F., D.P. Yan., P. M. Vasconcelos., J. W. Li., R. Z. Hu., 2008. Structural and geochronological constraints on the tectono-thermal evolution of the Danba domal terrane, eastern margin of the Tibetan plateau. Journal of Asian Earth Sciences 33, 414–427.

Zhou, Y., Yan, D.P., Xu, C.G., Zhou, M.F., 2018. Age and petrological constraints for the Archean Yudongzi group in the northeast Longmenshan tectonic belt. In preparation.

Zhu, L.M., Zhang, G.W., Chen, Y.J., Ding, Z.J., Guo, B., Wang, F., Lee, B., 2011. Zircon U–Pb ages and geochemistry of the Wenquan Mo-bearing granitioids in West Qinling, China: constraints on the geodynamic setting for the newly discovered Wenquan Mo deposit. Ore Geology Reviews 39, 46–62.

Zhu, W.G., Zhong, H., Li, X.H., Deng, H.L., He, D.F., Wu, K.W., Bai, Z.J., 2008. SHRIMP zircon U–Pb geochronology, elemental, and Nd isotopic geochemistry of the Neoproterozoic mafic dykes in the Yanbian area, SW China. Precambrian Research 164, 66–85.

**Figure captions:**

Fig. 1 Geological map of the Longmenshan Tectonic Complex (LSTC)and its adjacent Songpan-Ganze terrane, western Sichuan Basin, and SW-Qinling orogenic belt in the northeast margin of the Tibet Plateau (Edited base on Huang and Li, 2001). Inset map indicates tectonic location of the geological map.

Fig. 2 Division for the tectonic units of the LSTC and its adjacent regions. Only first-order tectonic units are divided except third-order tectonic units for the LSTC.

Fig. 3 Simplified geological map showing the outcrop of basement complexes, including the metamorphic Archean and Proterozoic rocks. Insert map shows the rock types in Ab-An-Or triangular projection (Zhao and Zhou, 2007b; Zhao and Zhou, 2008).

Fig. 4 Stratigraphic correlation diagram includes synthesis columnar in: A. South Qinling Orogenic belt, B. Bikou terrane, C. Songpan-Ganze terrane, D. Longmenshan thrust belt-Hinterland belt, E. Yanyuan-Muli thrust belt, F. Longmenshan thrust belt-Foreland belt, and G. Western Yantze Block (Synthesized edited after GBGMR, 1989; SBGMR, 1989; SBGMR, 1991; and related 1:200 000 regional geological maps).

Fig. 5 Schematic model for the tectonic evolution of Ganze-Litang suture zone and adjacent area under current E–W direction, showing the formation and closing of the Ganze-Litang ocean (Modified based on Cao et al., 2015).

Fig. 6. Geological section transects the middle part of the Longmenshan thrust belt. (A) Strip geological map of a belt from Xuecheng to Bailuchang; (B) the corresponding geological section, which transects the Songpan - Ganze terrane, Longmenshan thrust belt and Sichuan Basin; (C) Seismic profile with Structural interpretation of the foreland thrust belt and Sichuan Basin; (D) Summarized the geochromological constraints for the Beichuan-Yinxiu faults. Location of (A)-(B) is shown in Fig. 1, and location of (D) is shown in (A). (A), (B) and (D) are from Yan et al. (2011) and (C) is from Zheng et al. (2016).

Fig. 7 Simplified geological map showing Yudongzi and Hejiayan groups (edited based on GRT-SBGMR, 1996 and Zhou et al., in preparation).

Fig.8 Schematic reconstructions showing position of the Yangtze Block within the configuration of Columbia/Nuna supercontinent (Eglington et al., 2013; Pehrsson et al., 2015; Wang W., 2016).

Fig.9 Proposed schematic models for Neoproteroozic reconstructions. A-C: Neoproterozoic subduction beneath the western margin of the Yangtze block, showing the formation of adakitic plutons, gabbros and arc-like granites along the western margin of the Yangtze block during the Neoproterozoic from 860 to 740 Ma (Zhao and Zhou, 2007a, 2007b; Zhao and Zhou, 2008). D: A proposed Neoproterozoic tectonic reconstruction of the Yangtze block by Zhou et al. (2002a); E: a possible reconstruction of the Yangtze block/South China block in the Rodinia supercontinent (Yan et al., 2002).

Fig.10 Distribution of the ELIP basalts and a possible late Permian three-armed rift system.

Fig. 11 Schematic model for the Wilson cycle of the A'nymaqen-Mianlue suture zone (modified after Dong et al., 2011).

Fig. 12 Tectonic model showing the Cenozoic three-stage tectonic evolution of the LSTC and its adjacent area (Sun et al., 2018, in preparation).

**Table:**

Table 1 Tectonic divisions of the LSTC and its adjacent regions

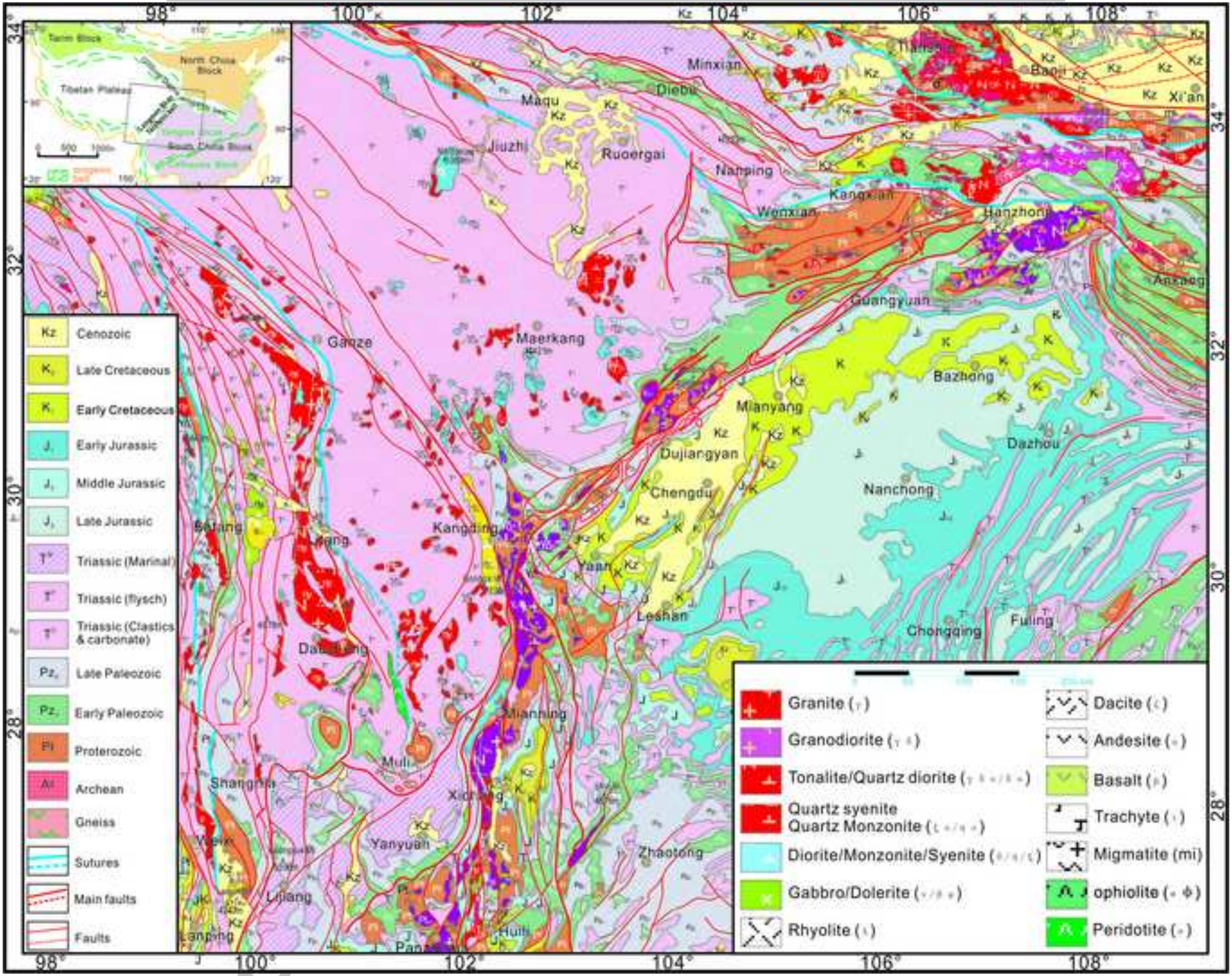
Tarim Block
North China Block
Tibetan Plateau
South China Block
Kz Cenozoic
K2 Late Cretaceous
K1 Early Cretaceous
J1 Early Jurassic
J2 Middle Jurassic
J3 Late Jurassic
Triassic (Marine)
Triassic (flysch)
Triassic (Clastics & carbonate)
Pz2 Late Paleozoic
Pz1 Early Paleozoic
Pt Proterozoic
Ar Archean
Gneiss
Sutures
Main faults
Faults
Granite
Granodiorite
Tonalite/Quartz diorite
Quartz syenite
Quartz Monzonite
Diorite/Monzonite/Syenite
Gabbro/Dolerite
Rhyolite
Dacite
Andesite
Basalt
Trachyte
Migmatite (mi)
ophiolite
Peridotite
Minxian
Tianshui
Baoji
Xi'an
Maqu
Diebu
Jiuzhi
Ruoergai
Nanping
Kangxian
Wenxian
Hanzhong
Ankang
Guangyuan
Ganze
Maerkang
Bazhong
Mianyang
Dujiangyan
Dazhou
Chengdu
Nanchong
Kangding
Batang
Litang
Yaan
Leshan
Chongqing
Fuling
Daocheng
Mianning
Muli
Shangrila
Xichang
Yanyuan
Zhaotong
Weixi
Lijiang
Lanping
Huili
98°
100°
102°
104°
106°
108°
28°
30°
32°
34°

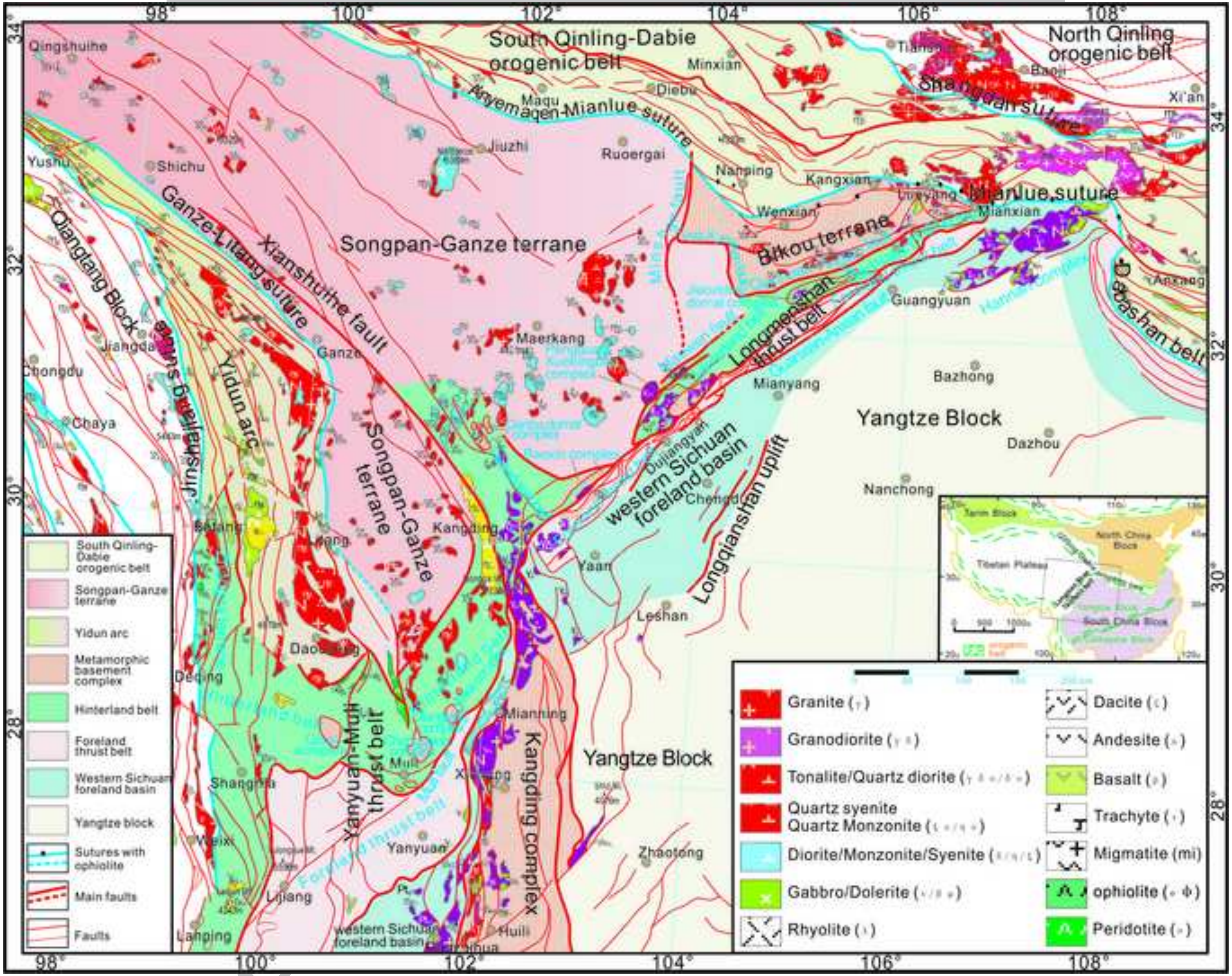
South Qinling-Dabie orogenic belt
North Qinling orogenic belt
Anyemaqen-Mianlue suture
Shangdan suture
Mianlue suture
Songpan-Ganze terrane
Bikou terrane
Ganze-Litang suture
Xianshuihe fault
Qiangtang Block
Jinshajiang suture
Yidun arc
Longmenshan thrust belt
Yangtze Block
western Sichuan foreland basin
Longqianshan uplift
Yanyuan-Muli thrust belt
Kangding complex
Dabashan belt
Qingshuihe
Yushu
Shichu
Jiuzhi
Ruoergai
Maqu
Diebu
Minxian
Tianshui
Baoji
Xi'an
Nanping
Kangxian
Wenxian
Lueyang
Mianxian
Ankang
Guangyuan
Maerkang
Ganze
Jiangda
Chongdu
Chaya
Batang
Litang
Kangding
Yaan
Dujiangyan
Chengdu
Mianyang
Bazhong
Dazhou
Nanchong
Leshan
Daocheng
Deqing
Muli
Mianning
Xichang
Shangrila
Weixi
Lijiang
Yanyuan
Lanping
Huili
Zhaotong
South Qinling-Dabie orogenic belt
Songpan-Ganze terrane
Yidun arc
Metamorphic basement complex
Hinterland belt
Foreland thrust belt
Western Sichuan foreland basin
Yangtze block
Sutures with ophiolite
Main faults
Faults
Granite
Granodiorite
Tonalite/Quartz diorite
Quartz syenite
Quartz Monzonite
Diorite/Monzonite/Syenite
Gabbro/Dolerite
Rhyolite
Dacite
Andesite
Basalt
Trachyte
Migmatite (mi)
ophiolite
Peridotite
Tarim Block
North China Block
Tibetan Plateau
South China Block
98°
100°
102°
104°
106°
108°
34°
32°
30°
28°

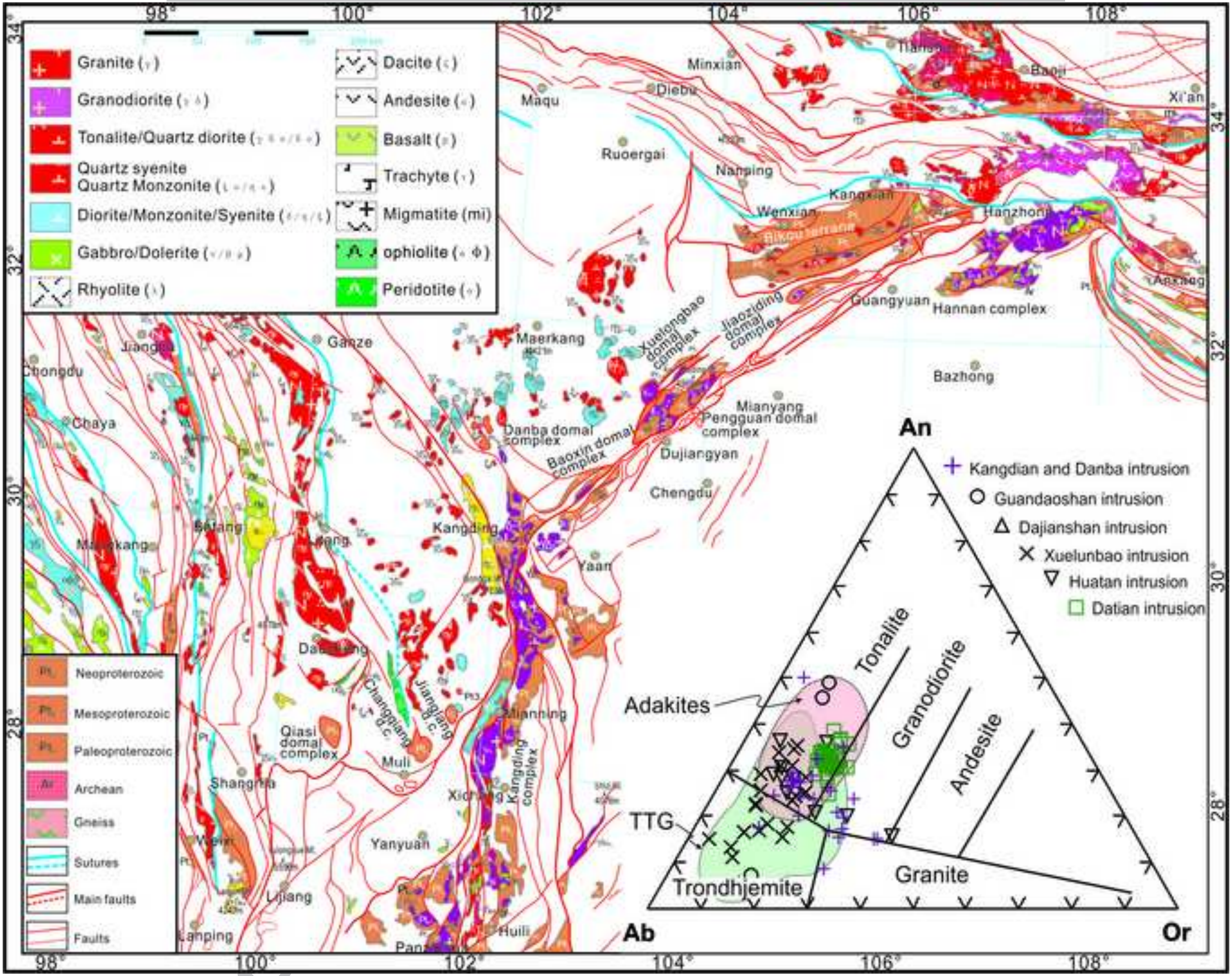

Granite
Granodiorite
Tonalite/Quartz diorite
Quartz syenite
Quartz Monzonite
Diorite/Monzonite/Syenite
Gabbro/Dolerite
Rhyolite
Dacite
Andesite
Basalt
Trachyte
Migmatite (mi)
ophiolite
Peridotite
Neoproterozoic
Mesoproterozoic
Paleoproterozoic
Archean
Gneiss
Sutures
Main faults
Faults
98°
100°
102°
104°
106°
108°
34°
32°
30°
28°
Minxian
Tianshui
Baoji
Xi'an
Maqu
Diebu
Ruoergai
Nanping
Kangxian
Wenxian
Bikou terrane
Hanzhong
Ankang
Guangyuan
Hannan complex
Bazhong
Ganze
Jiangda
Chongdu
Chaya
Maerkang
Xuelongbao domal complex
Jiaoziding domal complex
Mianyang
Pengguan domal complex
Danba domal complex
Baoxin domal complex
Dujiangyan
Chengdu
Kangding
Yaan
Batang
Litang
Markang
Daocheng
Changgiang d.c
Jianglang d.c
Qiasi domal complex
Muli
Mianning
Shangrila
Xichang
Kangding complex
Yanyuan
Weixi
Lijiang
Lanping
Huili
Pan
An
Ab
Or
Kangdian and Danba intrusion
Guandaoshan intrusion
Dajianshan intrusion
Xuelunbao intrusion
Huatan intrusion
Datian intrusion
Tonalite
Granodiorite
Andesite
Adakites
TTG
Trondhjemite
Granite

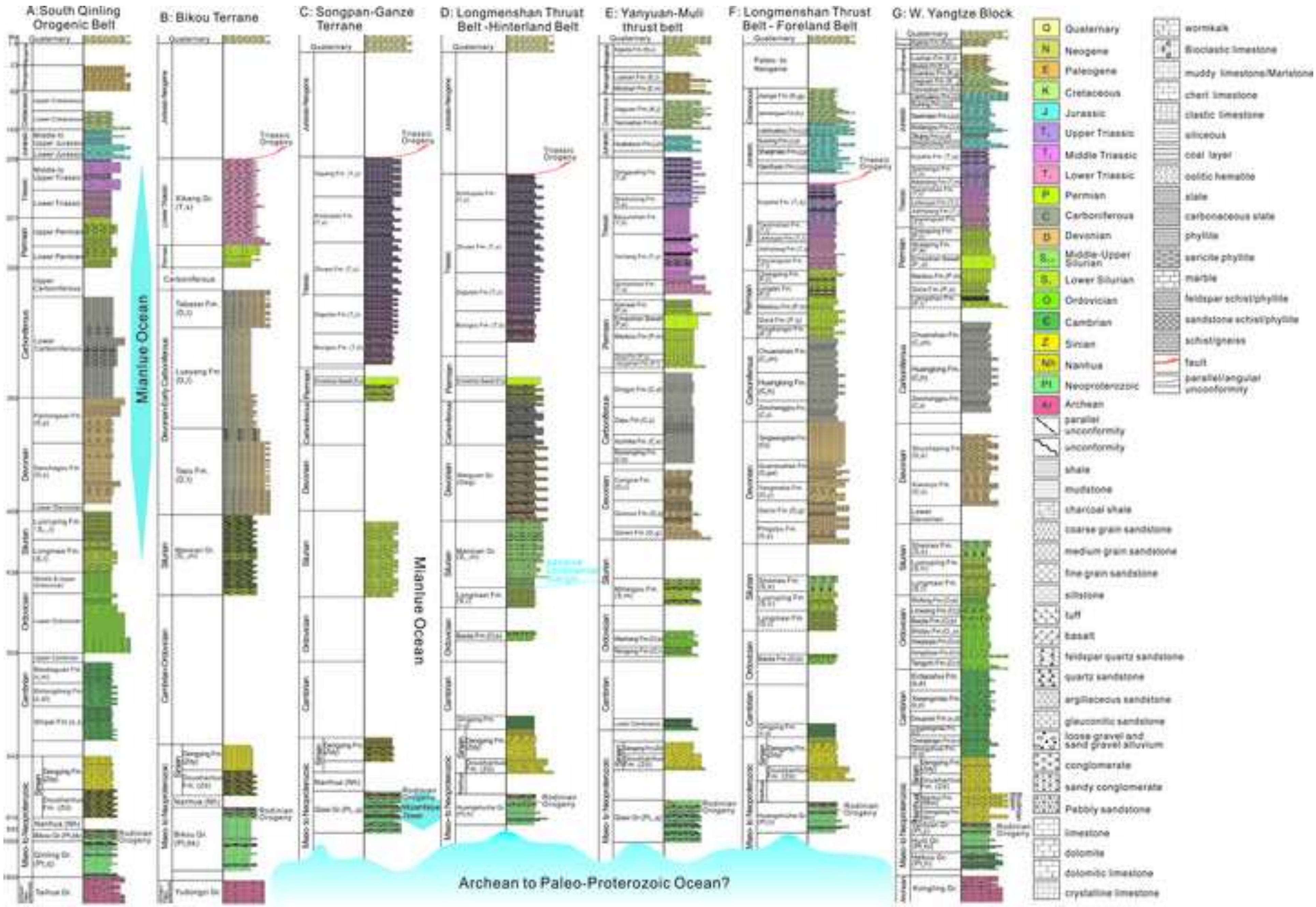
A:South Qinling Orogenic Belt
B: Bikou Terrane
C: Songpan-Ganze Terrane
D: Longmenshan Thrust Belt -Hinterland Belt
E: Yanyuan-Muli thrust belt
F: Longmenshan Thrust Belt - Foreland Belt
G: W. Yangtze Block
Mianlue Ocean
Mianlue Ocean
Triassic Orogeny
Rodinian Orogeny
Archean to Paleo-Proterozoic Ocean?
Quaternary
Neogene
Paleogene
Cretaceous
Jurassic
Upper Triassic
Middle Triassic
Lower Triassic
Permian
Carboniferous
Devonian
Middle-Upper Silurian
Lower Silurian
Ordovician
Cambrian
Sinian
Nanhua
Neoproterozoic
Archean
parallel unconformity
unconformity
shale
mudstone
charcoal shale
coarse grain sandstone
medium grain sandstone
fine grain sandstone
siltstone
tuff
basalt
feldspar quartz sandstone
quartz sandstone
argillaceous sandstone
glauconitic sandstone
loose gravel and sand gravel alluvium
conglomerate
sandy conglomerate
Pebbly sandstone
limestone
dolomite
dolomitic limestone
crystalline limestone
wormkalk
Bioclastic limestone
muddy limestone/Marlstone
chert limestone
clastic limestone
siliceous
coal layer
oolitic hematite
slate
carbonaceous slate
phyllite
sericite phyllite
marble
feldspar schist/phyllite
sandstone schist/phyllite
schist/gneiss
fault
parallel/angular unconformity

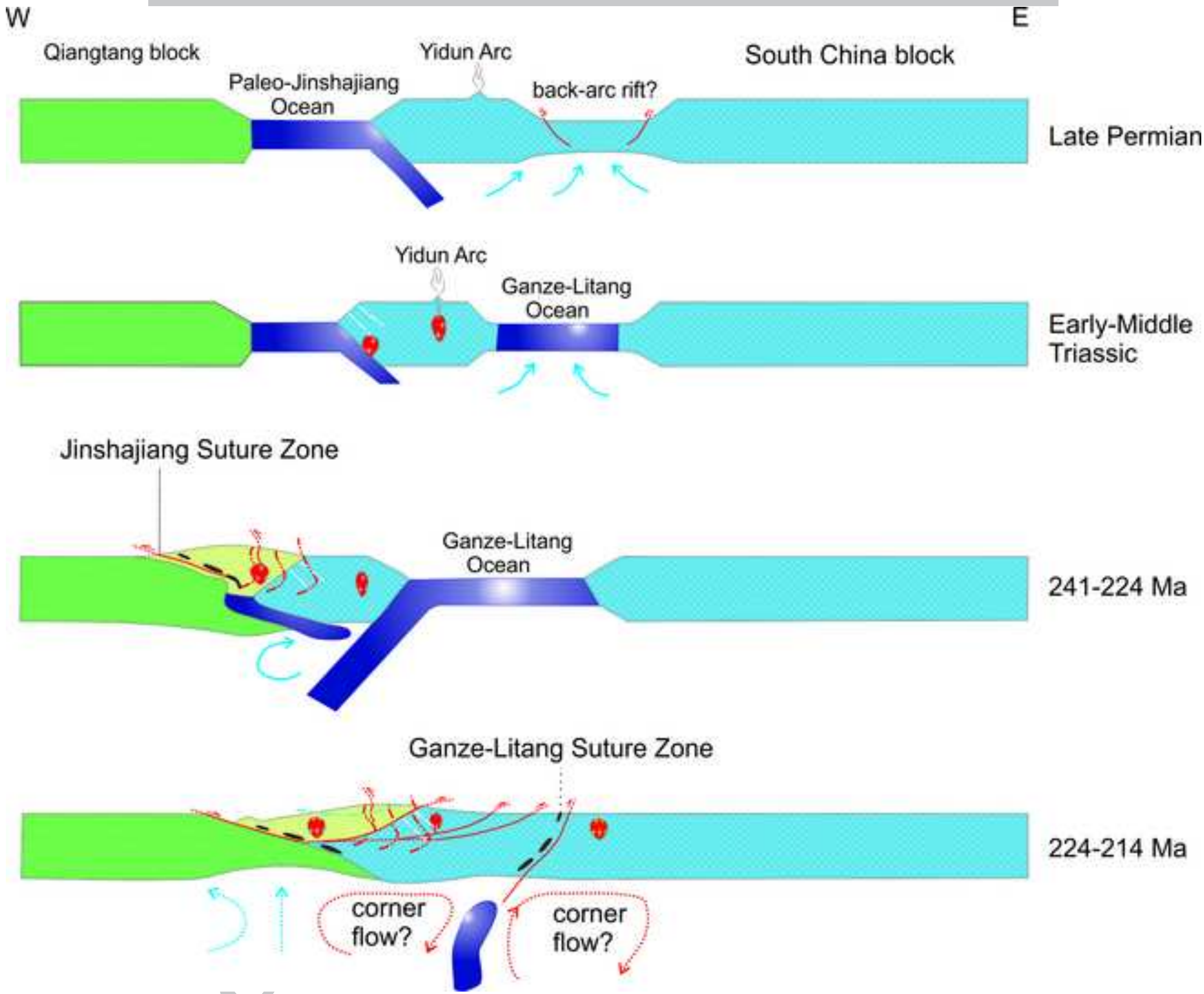
W
E
Qiangtang block
Yidun Arc
South China block
Paleo-Jinshajiang
Ocean
back-arc rift?
Late Permian
Yidun Arc
Ganze-Litang
Ocean
Early-Middle
Triassic
Jinshajiang Suture Zone
Ganze-Litang
Ocean
241-224 Ma
Ganze-Litang Suture Zone
224-214 Ma
corner
flow?
corner
flow?

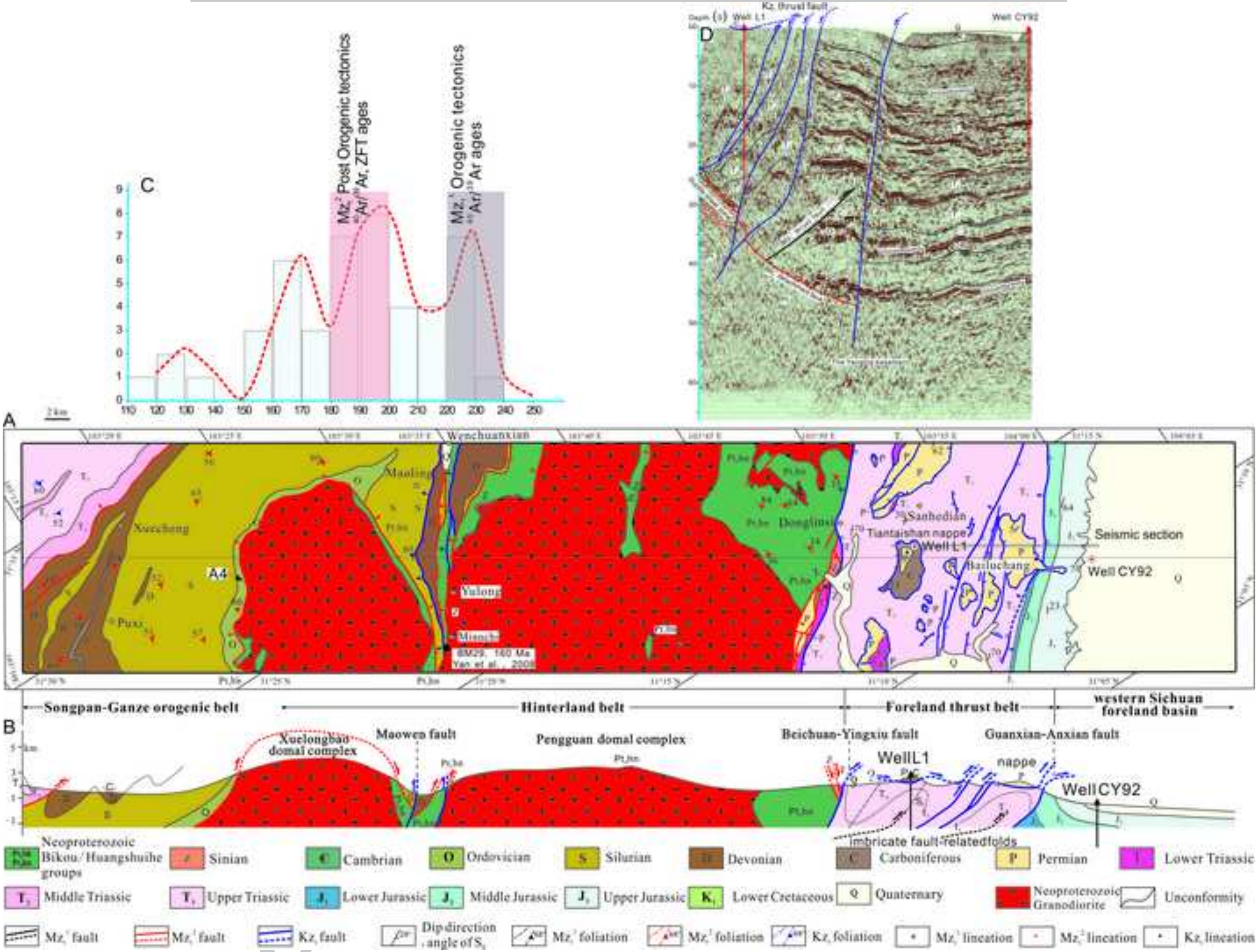

C
Mz₂ Post Orogenic tectonics ⁴⁰Ar/³⁹Ar, ZFT ages
Mz₁ Orogenic tectonics ⁴⁰Ar/³⁹Ar ages
D
Kz thrust fault
Well L1
Well CY92
A
Wenchuanxian
Xuecheng
Puxi
A4
Maoling
Yulong
Minchi
Donglinsi
Sanhedian
Tiantaishan nappe
Well L1
Bailuchang
Seismic section
Well CY92
Songpan-Ganze orogenic belt
Hinterland belt
Foreland thrust belt
western Sichuan foreland basin
B
Xuelongbao domal complex
Maowen fault
Pengguan domal complex
Beichuan-Yingxiu fault
Guanxian-Anxian fault
Well L1
nappe
Well CY92
imbricate fault-related folds
Neoproterozoic Bikou/Huangshuihe groups
Sinian
Cambrian
Ordovician
Silurian
Devonian
Carboniferous
Permian
Lower Triassic
Middle Triassic
Upper Triassic
Lower Jurassic
Middle Jurassic
Upper Jurassic
Lower Cretaceous
Quaternary
Neoproterozoic Granodiorite
Unconformity
Mz₁ fault
Mz₂ fault
Kz fault
Dip direction angle of S₀
Mz₁ foliation
Mz₂ foliation
Kz foliation
Mz₁ lineation
Mz₂ lineation
Kz lineation

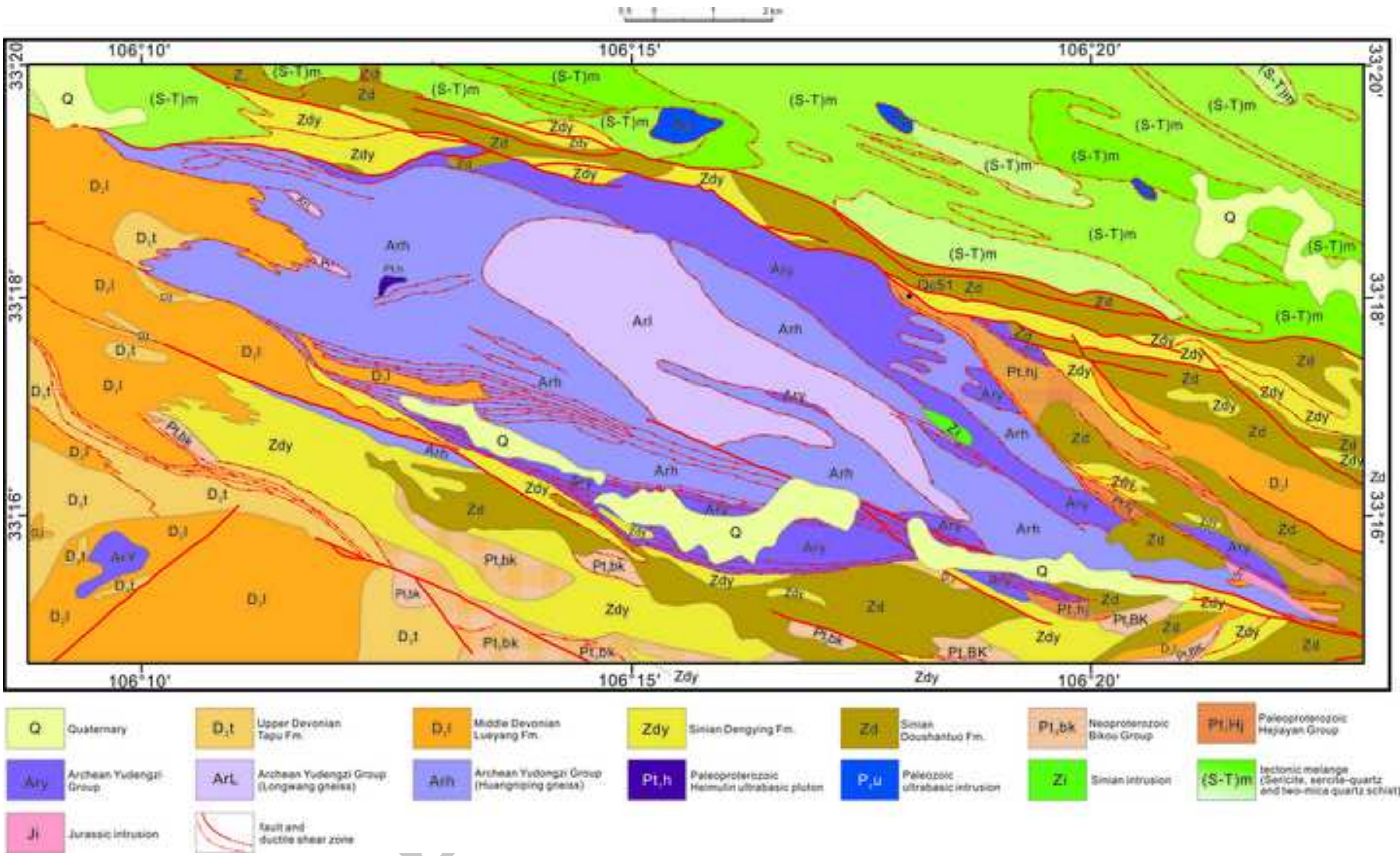
106°10'
106°15'
106°20'
33°20'
33°18'
33°16'
Q
Quaternary
D3t
Upper Devonian Tapu Fm.
D2l
Middle Devonian Lueyang Fm.
Zdy
Sinian Dengying Fm.
Zd
Sinian Doushantuo Fm.
Pt3bk
Neoproterozoic Bikou Group
Pt1Hj
Paleoproterozoic Hejiayan Group
Ary
Archean Yudengzi Group
ArL
Archean Yudengzi Group (Longwang gneiss)
Arh
Archean Yudongzi Group (Huangniping gneiss)
Pt1h
Paleoproterozoic Heimulin ultrabasic pluton
P1u
Paleozoic ultrabasic intrusion
Zi
Sinian intrusion
(S-T)m
tectonic melange (Sericite, sercite-quartz and two-mica quartz schist)
Ji
Jurassic intrusion
fault and ductile shear zone

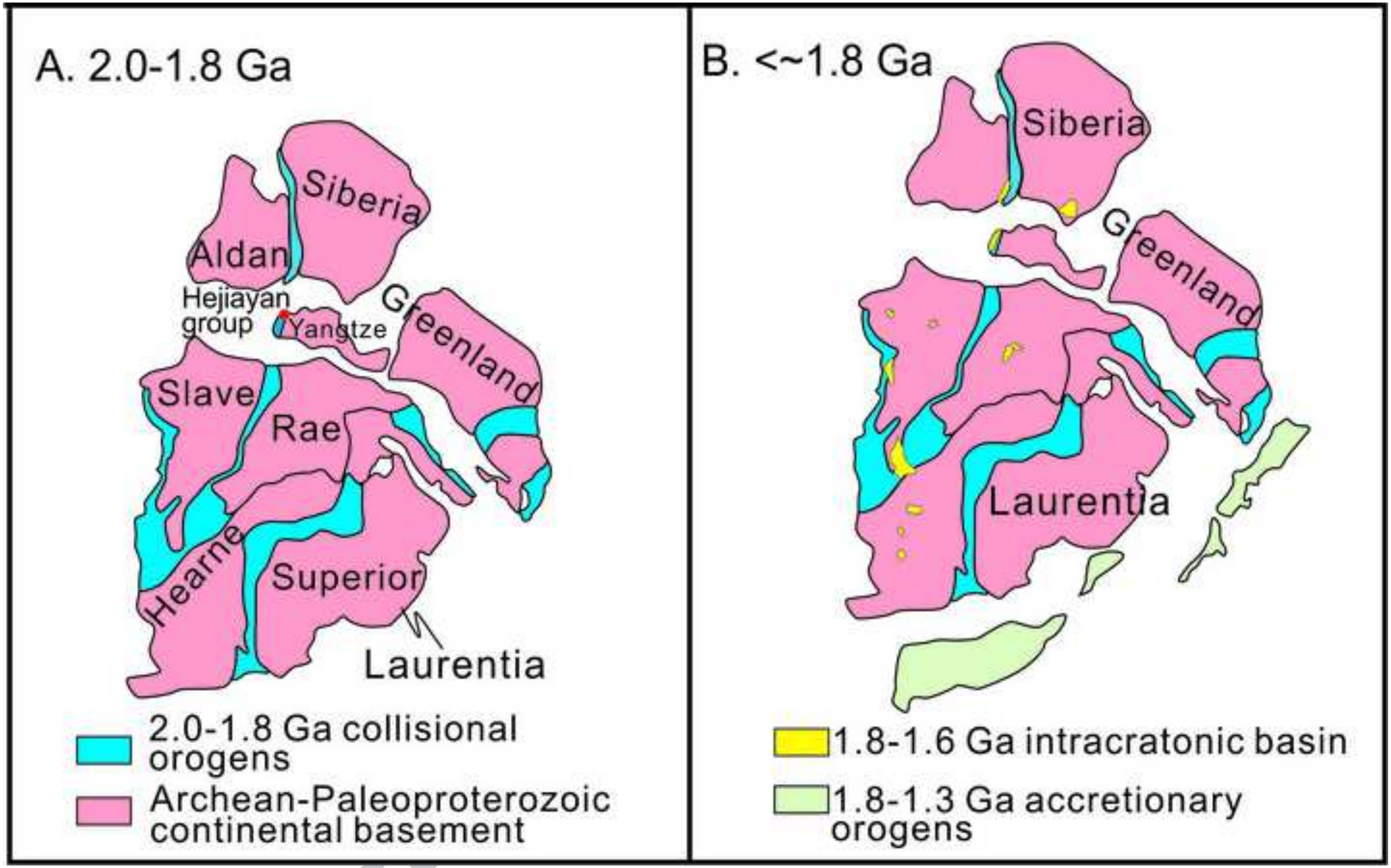
A. 2.0-1.8 Ga
Siberia
Aldan
Hejiayan group
Yangtze
Greenland
Slave
Rae
Hearne
Superior
Laurentia
2.0-1.8 Ga collisional orogens
Archean-Paleoproterozoic continental basement
B. <~1.8 Ga
Siberia
Greenland
Laurentia
1.8-1.6 Ga intracratonic basin
1.8-1.3 Ga accretionary orogens

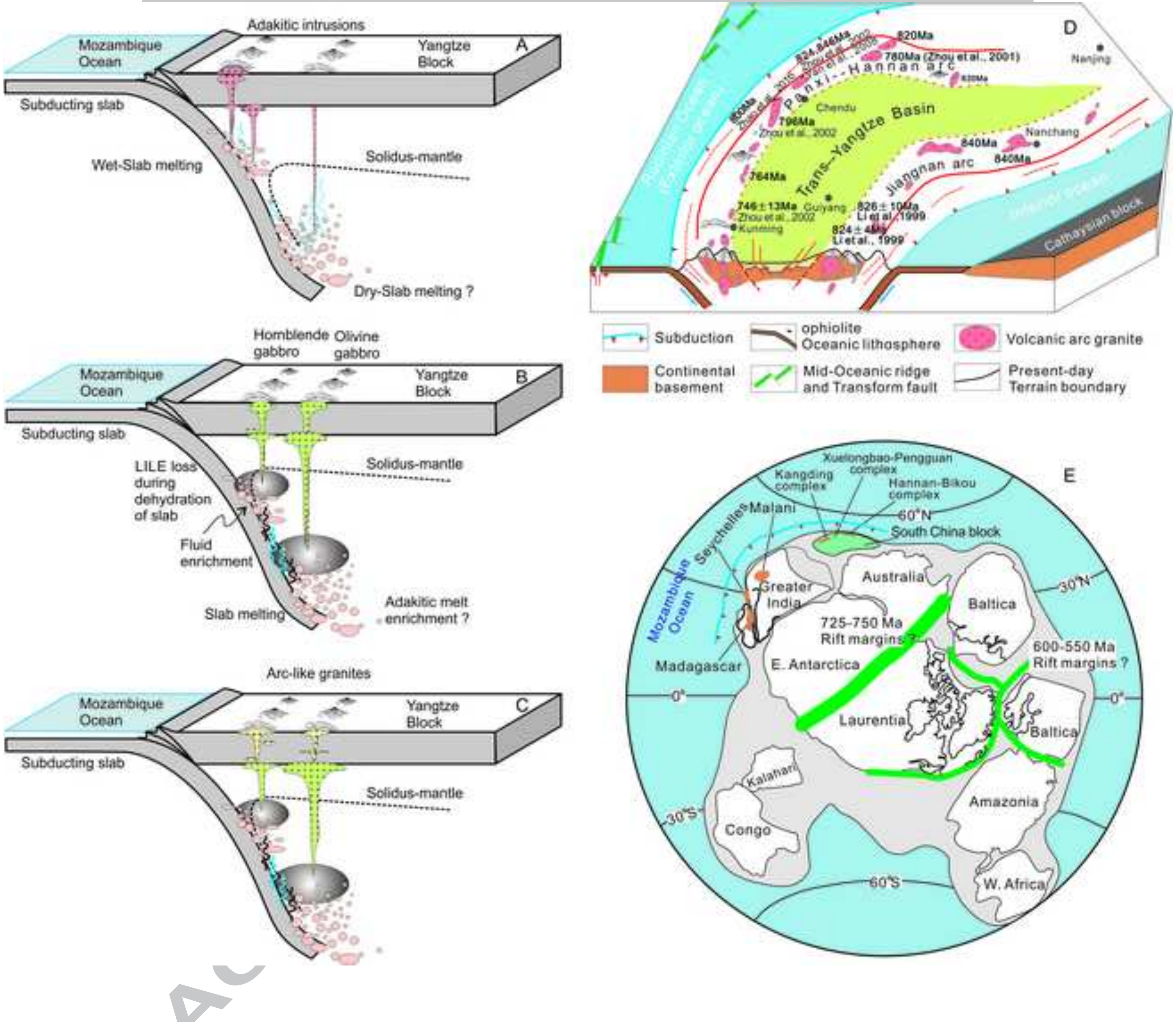
Adakitic intrusions
Mozambique Ocean
Yangtze Block
A
Subducting slab
Wet-Slab melting
Solidus-mantle
Dry-Slab melting ?
Hornblende gabbro
Olivine gabbro
B
LILE loss during dehydration of slab
Fluid enrichment
Slab melting
Adakitic melt enrichment ?
Arc-like granites
C
D
820Ma
780Ma (Zhou et al., 2001)
Nanjing
Chendu
Trans-Yangtze Basin
796Ma
Zhou et al., 2002
Nanchang
840Ma
840Ma
Jiangnan arc
764Ma
746±13Ma
Zhou et al., 2002
Guiyang
826±10Ma
Li et al., 1999
824±4Ma
Li et al., 1999
Kunming
Cathaysian block
Subduction
ophiolite
Oceanic lithosphere
Volcanic arc granite
Continental basement
Mid-Oceanic ridge and Transform fault
Present-day Terrain boundary
E
Xuelongbao-Pengguan complex
Kangding complex
Hannan-Bikou complex
60°N
South China block
Seychelles
Malani
Mozambique Ocean
Greater India
Australia
Baltica
30°N
725-750 Ma Rift margins ?
600-550 Ma Rift margins ?
Madagascar
E. Antarctica
0°
Laurentia
Baltica
Kalahari
30°S
Congo
Amazonia
60°S
W. Africa

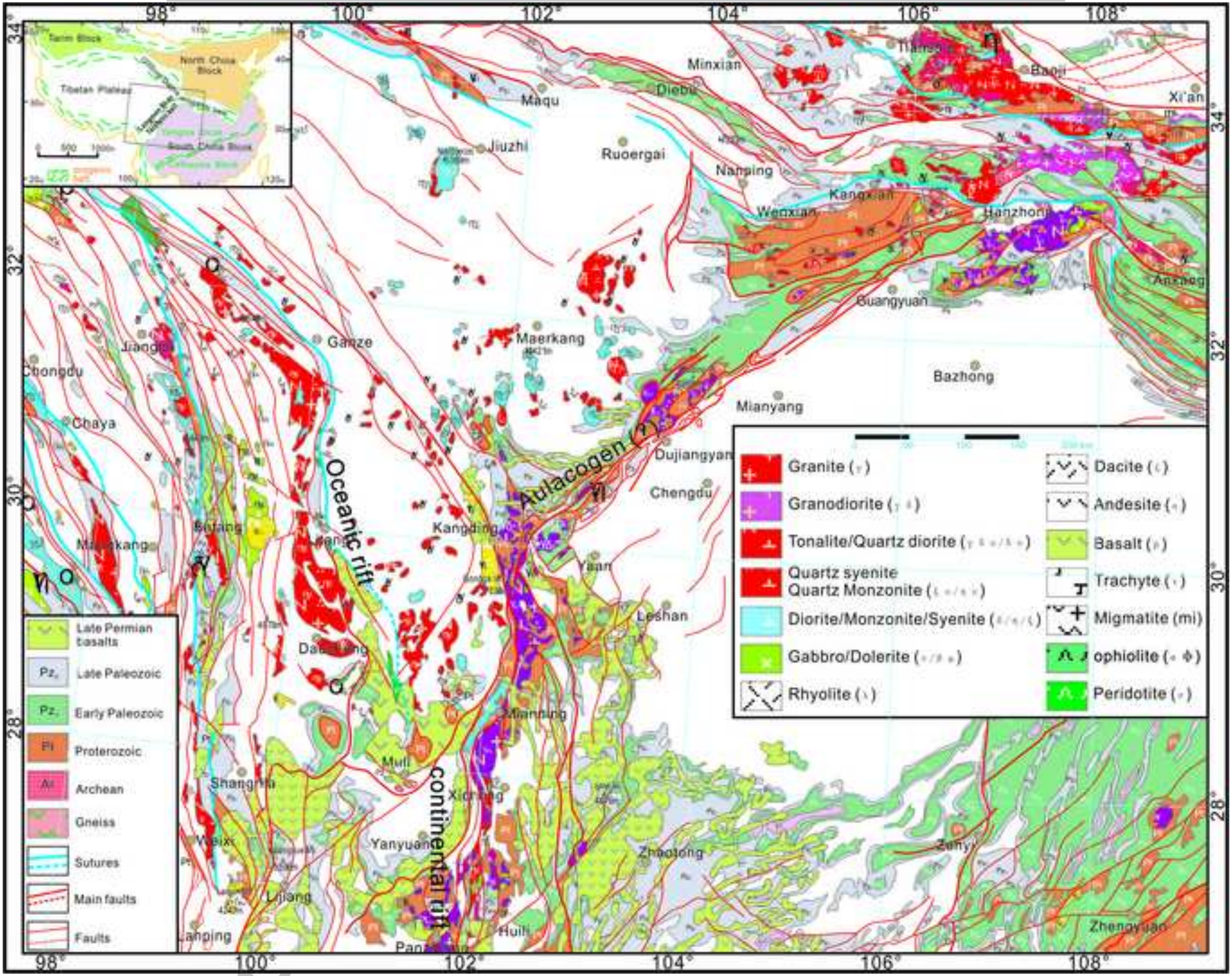
Minxian
Tianshui
Baoji
Xi'an
Maqu
Diebu
Jiuzhi
Ruoergai
Nanping
Kangxian
Wenxian
Hanzhong
Ankang
Guangyuan
Ganze
Maerkang
Jiangda
Chongdu
Chaya
Mianyang
Bazhong
Dujiangyan
Chengdu
Aulacogen (?)
Oceanic rift
Kangding
Yaan
Leshan
Batang
Daocheng
Mianning
Muli
Xichang
continental rift
Yanyuan
Zhaotong
Zunyi
Zhenyuan
Shangrila
Weixi
Lijiang
Lanping
Panzhihua
Huili
Granite
Granodiorite
Tonalite/Quartz diorite
Quartz syenite
Quartz Monzonite
Diorite/Monzonite/Syenite
Gabbro/Dolerite
Rhyolite
Dacite
Andesite
Basalt
Trachyte
Migmatite (mi)
ophiolite
Peridotite
Late Permian basalts
Late Paleozoic
Early Paleozoic
Proterozoic
Archean
Gneiss
Sutures
Main faults
Faults
Tarim Block
North China Block
Tibetan Plateau
South China Block
98°
100°
102°
104°
106°
108°
28°
30°
32°
34°

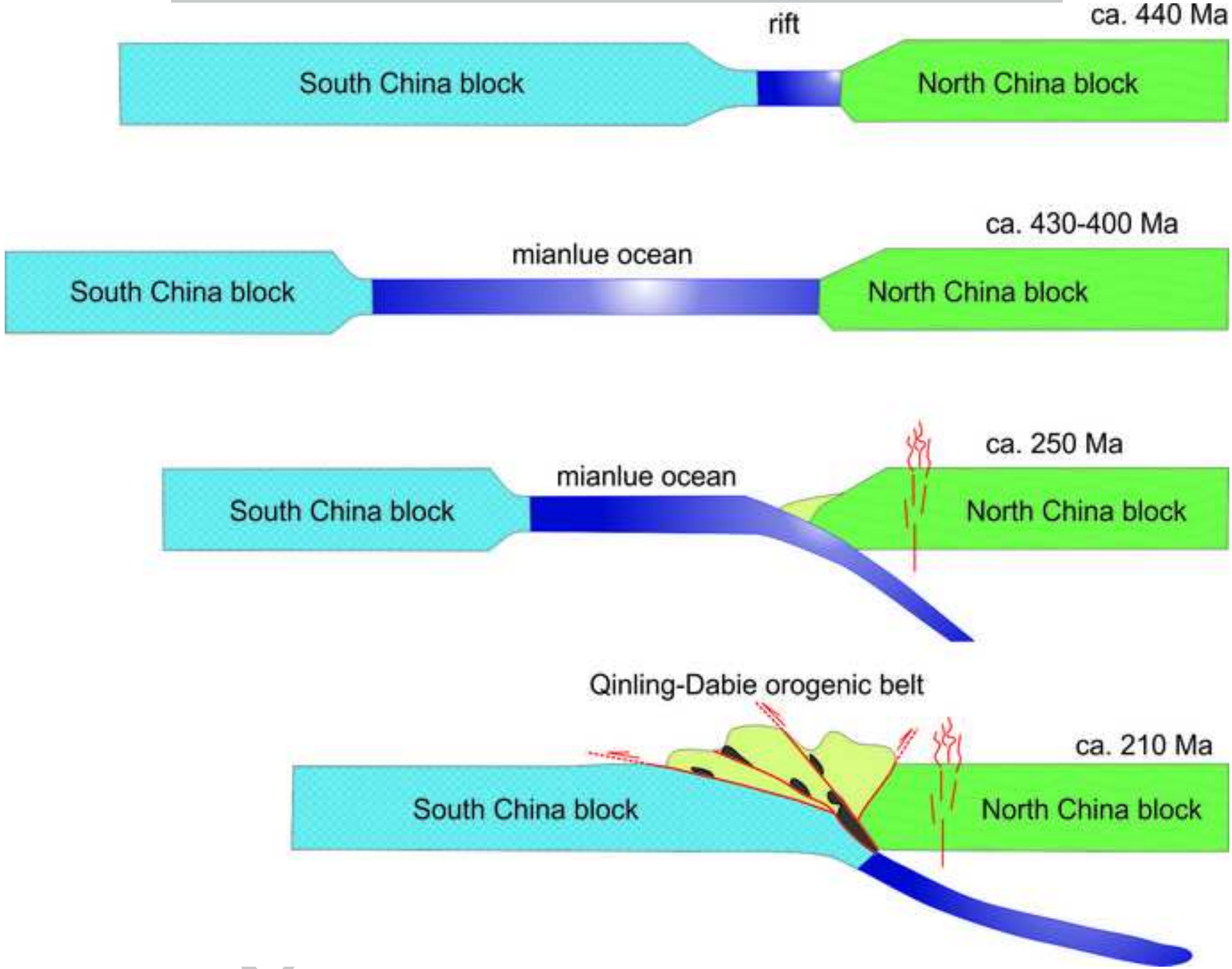

rift
ca. 440 Ma
South China block
North China block
ca. 430-400 Ma
mianlue ocean
South China block
North China block
ca. 250 Ma
mianlue ocean
South China block
North China block
Qinling-Dabie orogenic belt
ca. 210 Ma
South China block
North China block

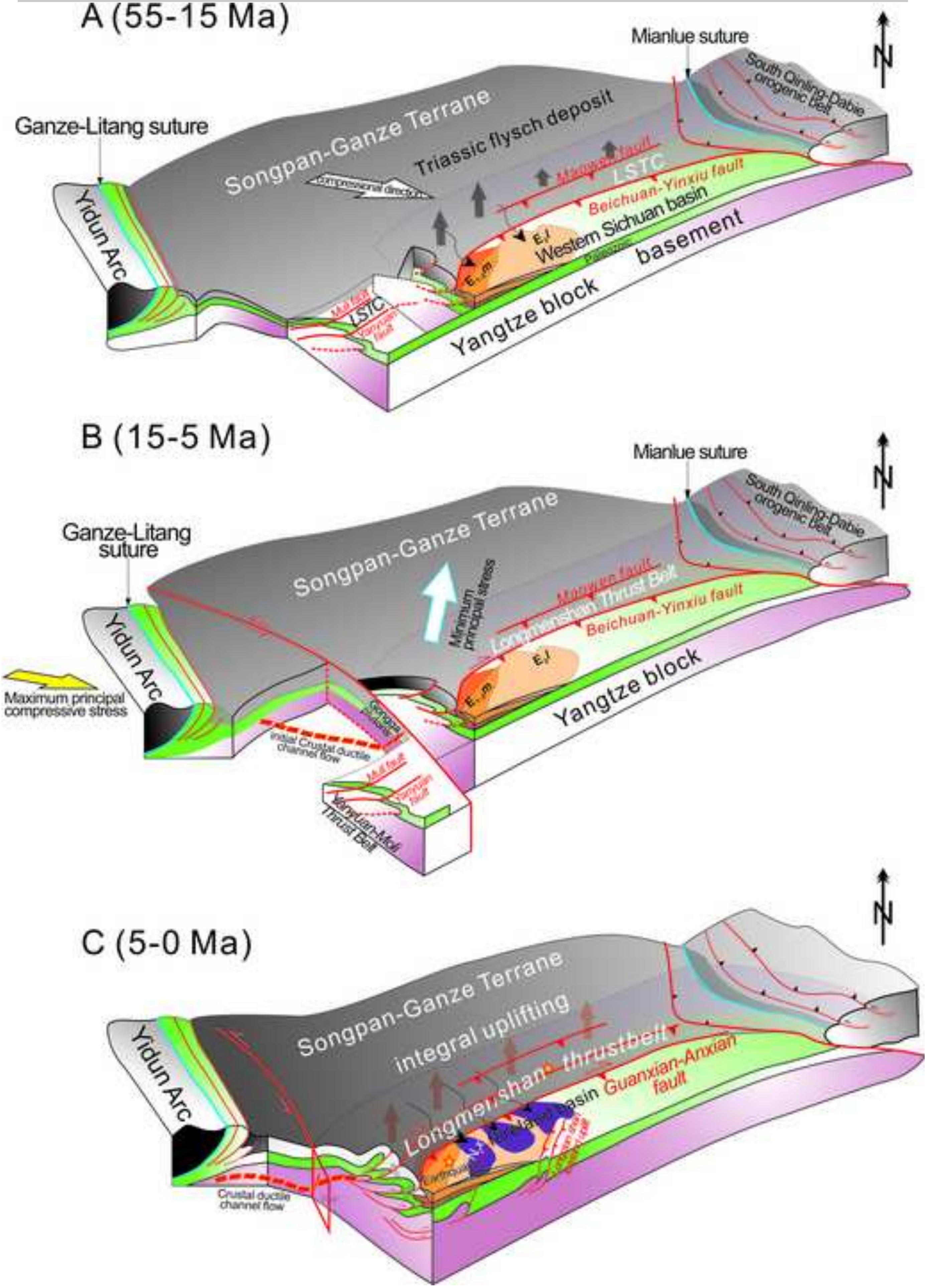
A (55-15 Ma)
Mianlue suture
South Qinling-Dabie orogenic belt
Ganze-Litang suture
Songpan-Ganze Terrane
Triassic flysch deposit
LSTC
Beichuan-Yinxiu fault
Western Sichuan basin
basement
Yidun Arc
Yangtze block
LSTC
B (15-5 Ma)
Mianlue suture
South Qinling-Dabie orogenic belt
Ganze-Litang suture
Songpan-Ganze Terrane
Minimum principal stress
Longmenshan Thrust Belt
Beichuan-Yinxiu fault
Yidun Arc
Maximum principal compressive stress
Yangtze block
Yanyuan-Muli Thrust Belt
C (5-0 Ma)
Songpan-Ganze Terrane
integral uplifting
Yidun Arc
Longmenshan thrustbelt
Guanxian-Anxian fault
Crustal ductile channel flow

Table 1 Tectonic division of the LSTC and its adjacent regions

| | First-order tectonic unit | Secondary-order tectonic unit | Third-order tectonic unit |
|---|---|---|---|
| 1 | Qinling-Dabie orogenic belt | | |
| 2 | Bikou terrane | | |
| 3 | Songpan-Ganze terrane | | |
| 4 | Yidun arc | | |
| 5 | Western Yangtze block | | |
| 6 | Longmenshan tectonic complex | Longmenshan thrust belt | Hinterland belt |
| | | | Foreland thrust belt |
| | | Yanyuan-Muli thrust belt | Hinterland belt |
| | | | Foreland thrust belt |

# Highlights

1. The Longmenshan Tectonic Complex experienced at least 6 regional tectonic events

2. Reconstruction reveals a Rodinian trench-arc-basin system

3. The Longmenshan Tectonic Complex was bounded by Paleozoic passive continental margin and Yangtze Craton

4. A Paleotethys orogenic belt was superposed by a Neotethys orogenic Plateau

Graphical abstract

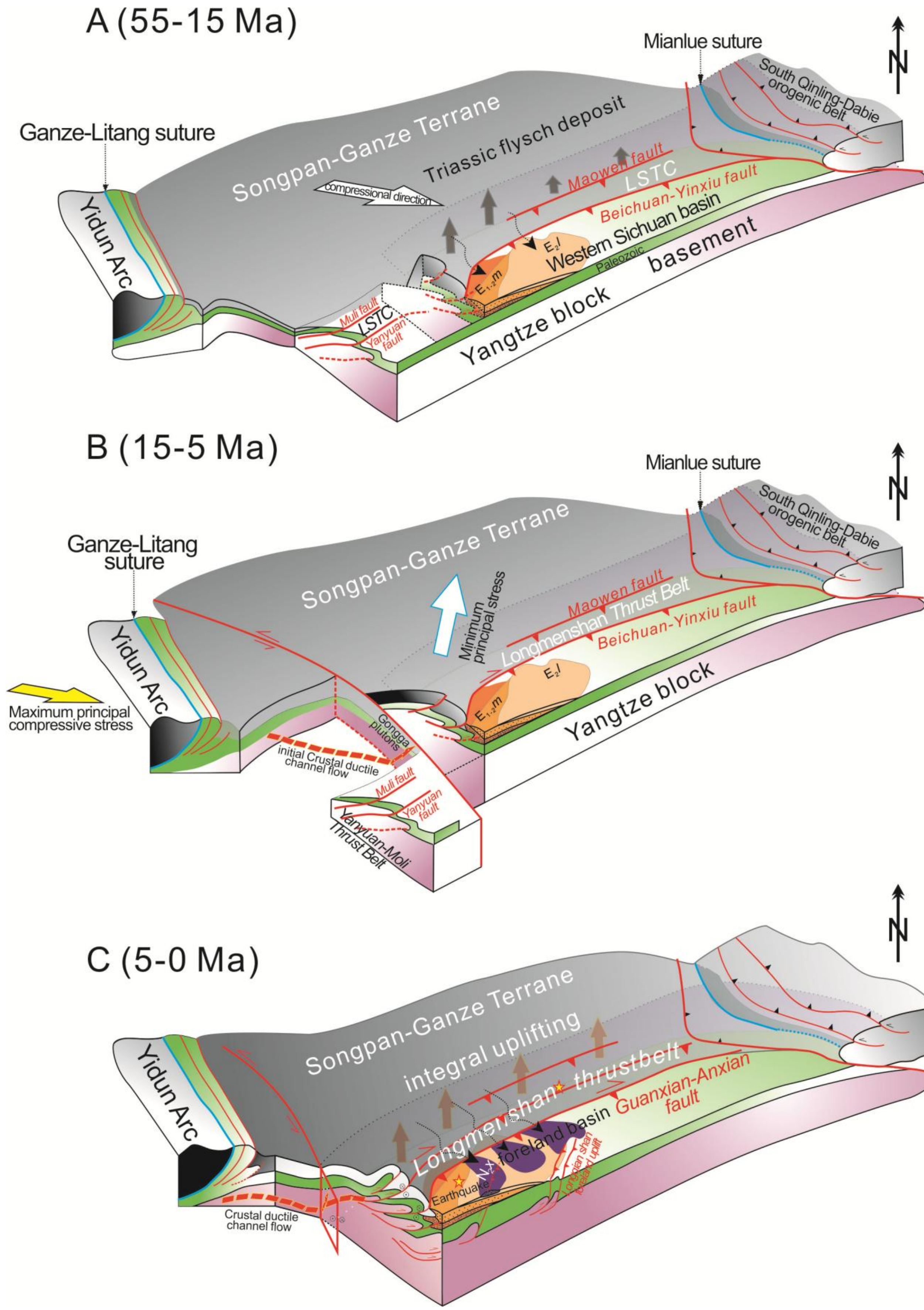
A (55-15 Ma)
Mianlue suture
South Qinling-Dabie orogenic belt
N
Ganze-Litang suture
Songpan-Ganze Terrane
Triassic flysch deposit
compressional direction
Maowen fault
LSTC
Beichuan-Yinxiu fault
Western Sichuan basin
basement
Paleozoic
Yidun Arc
Muli fault
LSTC
Yanyuan fault
Yangtze block
B (15-5 Ma)
Mianlue suture
South Qinling-Dabie orogenic belt
N
Ganze-Litang suture
Songpan-Ganze Terrane
Minimum principal stress
Maowen fault
Longmenshan Thrust Belt
Beichuan-Yinxiu fault
Yidun Arc
Yangtze block
Maximum principal compressive stress
Gongga plutons
initial Crustal ductile channel flow
Muli fault
Yanyuan fault
Yanyuan-Moli Thrust Belt
C (5-0 Ma)
N
Songpan-Ganze Terrane
integral uplifting
Longmenshan thrustbelt
Guanxian-Anxian fault
Longmenshan foreland basin
Yidun Arc
Earthquake
Crustal ductile channel flow